

UC Berkeley

UC Berkeley Electronic Theses and Dissertations

Title

Human-centric Indoor Air Quality

Permalink

<https://escholarship.org/uc/item/1sx9r75s>

Author

Vannucci, Matthew

Publication Date

2018

Peer reviewed|Thesis/dissertation

Human-centric Indoor Air Quality

By

Matthew Vannucci

A dissertation submitted in partial satisfaction of the

requirements for the degree of

Doctor of Philosophy

in

Engineering – Civil and Environmental Engineering

in the

Graduate Division

of the

University of California, Berkeley

Committee in charge:

Professor Robert Harley, Chair

Professor Stefano Schiavon

Professor Arpad Horvath

Spring 2018

Human-centric Indoor Air Quality

Copyright © 2018 by

Matthew Vannucci

Abstract

Human-centric Indoor Air Quality

by

Matthew Vannucci

Doctor of Philosophy in Civil and Environmental Engineering

University of California, Berkeley

Professor Robert Harley, Chair

People are a direct source of bioeffluent pollutants, mechanical air mixing, and heat, all of which lead to the formation of a unique perihuman microenvironment, and in certain environments also affect the room conditions. For indoor air quality (IAQ) research and professional work it is desirable to utilize the simplest possible conceptual model that captures the majority of the occupant exposure. In this dissertation a general process is put forth to determine how many zones an indoor space needs to be divided into, and how to model the pollutant transport within each zone simply. Exploring near-person pollutant sources, pollutant mixing in thermally stratified spaces, and optimizing CO₂ demand control sensor placement in a displacement ventilation system are illustrated using a series of laboratory experiments. A short example is also presented at the end to illustrate how this process might inform professional IAQ diagnostics work, and communicate the results to a non-expert client.

Personal care products (PCP) might be a significant source of ultrafine particle exposure for users owing to the reaction of ozone with terpene ingredients. The near-person emissions associated with PCP may contribute to exposures that would not be properly accounted for with indoor microenvironmental measurements. To better understand this issue, screening experiments were conducted with 91 PCP to detect the occurrence of ultrafine particle production from exposure to common indoor levels of ozone (23 ± 2 ppb). Twelve products generated measurable particle emissions; quantification experiments were performed for these to determine total particle production and peak particle production rate. A high-resolution, small volume reaction chamber was used with a heated sample plate to simulate conditions found in the human thermal plume. Ten of the quantified PCP exhibited total emissions of less than 10^9 particles, suggesting that they may not be significant sources of total ultrafine particle exposure as other common sources of particles indoor have emissions 1–4 orders of magnitude higher. Two samples, a tea tree oil-based scalp treatment and a white lavender body lotion, exhibited relatively elevated peak particle emission rates, $6.2 \times 10^7 \text{ min}^{-1}$ and

$2.0 \times 10^7 \text{ min}^{-1}$, respectively. The use of such products in the presence of significant ozone levels might materially influence personal exposure to ultrafine particles.

The pollutant mixing time in an indoor environment may be a good characteristic for researchers to differentiate when it is appropriate to use the well-mixed assumption in exposure models and investigations. For a certain amount of time, episodic emissions of pollutants in an indoor environment will create spatial heterogeneities that are significant when compared to the mean concentration. There have only been a small number of studies that directly measure the amount of time it takes a pulse emission to become well-mixed in a typical indoor environment. To add to this body of knowledge, a series of mixing time experiments were conducted in a $1.2 \text{ m} \times 1.2 \text{ m} \times 1.2 \text{ m}$ chamber. A vertical temperature gradient was established by symmetrically heating the ceiling and cooling the floor, a pulse release of neutrally buoyant mixture of CO_2 and He was used as a tracer gas, and six CO_2 sensors were used to measure when the relative standard deviation fell below 20%. Under isothermal conditions the mixing time varied between 40 and 100 minutes, the large variability suggesting that the mixing conditions were unstable. Under stratified conditions the variability was lower, indicating more stable conditions, and the mixing time was reduced to 38 to 52 min for a 0.5 to 3.0 $^\circ\text{C}/\text{m}$ stratification. The presence of a heated object also had a strong effect on increasing the mixing within the chamber, a 5 W heated object reduced the mixing time from 40–60 min to 12 min. A heated wall has less effect on mixing than a freestanding object, and the position of the heated object may have a small effect as well.

There are no guidelines on where to locate the CO_2 sensor in rooms ventilated by demand control (DC) displacement ventilation (DV). Locating the CO_2 sensor at the breathing height may be incorrect in such rooms because wall locations at the breathing height may be subject to enough spatial variability in concentration that the measurement will not be representative of the mean breathing height concentration. A full-sized chamber experiment was conducted with heated manikins that had a steady release of pure CO_2 in the breathing zone to simulate an office environment. Vertical lines of temperature and CO_2 sensors were placed in the center of the room and at two different wall locations to measure the horizontal concentration variability at different heights. 1, 3, and 5 manikins were used under low and high stratification conditions, and the chamber was allowed to stabilize overnight to obtain steady state conditions. Significant CO_2 horizontal variability of the order of 50–150 ppm was found between 1.1–1.7 m, while there was low temperature horizontal variability at all heights. These results suggest that the current practice of placing CO_2 DC sensors in a DV system at breathing height be changed to placing them at the ceiling or the return grille instead to reduce the likelihood that local variations in CO_2 misrepresent the room conditions. The possibility of developing a correction factor to relate the ceiling CO_2 level to the mean breathing height level was explored as well.

Dedicated to the public universities, which have given me an excellent education debt free

Contents

Abstract	1
Dedication	i
Contents	iii
Acknowledgments	vii
1 Introduction	1
1.1 Indoor pollutant exposure	2
1.2 Microenvironments	4
1.3 Overview of dissertation	5
2 Ultrafine Particle Production from the Ozonolysis of Personal Care Prod-	

ucts	7
2.1 Introduction	7
2.2 Methods	9
2.2.1 Apparatus	9
2.2.2 Product Selection	10
2.2.3 Screening Survey	11
2.2.4 Quantification Survey	11
2.2.5 Data Analysis	12
2.3 Results	13
2.3.1 Quantifying Particle Emissions from Specific Products	18
2.3.2 UFP Emissions from Selected Personal Care Products	18
2.3.3 Estimating Exposure Consequences	20
3 Pollutant Mixing Time in a Thermally Stratified Chamber	23
3.1 Introduction	23

3.2	Methods	25
3.2.1	Apparatus	25
3.2.2	Experimental procedure	26
3.3	Results and Discussion	29
3.4	Conclusion	33
4	Optimal Placement of CO₂ Sensors for a Displacement Ventilation System	35
4.1	Introduction	35
4.2	Methods	37
4.2.1	Experimental setup	37
4.2.2	Experimental procedure	39
4.3	Results and Discussion	41
4.4	Conclusion	49
5	Conclusion	51
5.1	Summary of Major Findings	51

5.2	Recommendations for Future Research	54
5.2.1	Contextualizing indoor sources by their microenvironmental conditions	54
5.2.2	Improving control in a DCDV system	54
5.2.3	Implications for IAQ engineers	55
	References	59
	Appendix	69
A.1	Supplemental methods and results for Chapter 2	69
A.1.1	Supplemental methods	69
A.1.2	Results of all quantification runs	73
A.2	Supplemental methods for Chapter 3	76
A.3	Supplemental methods and results for Chapter 4	81
A.3.1	Supplemental Methods	81
A.3.2	Supplemental Results	82
A.4	Example technical report for IAQ diagnosis	83

Acknowledgments

I would like to thank Professor Robert Harley for his invaluable support guiding me to finish my Ph.D., and for his advice throughout my time at U.C. Berkeley. With his kind attention and generous nature he brings together all of the members of the air quality group as a family, and I appreciate his encouragement toward civic mindedness. I am also grateful for the research mentorship I received from Professor William Nazaroff, who gave me an excellent introduction to the indoor air quality field, and Professor Stefano Schiavon, whose ability to bring scientific knowledge of the built environment into industry I hope to be able to emulate. I also want to thank the faculty members who served on my dissertation and qualifying exam committees, including Professor Arpad Horvath, and Professor Thomas McKone.

I'm also indebted to all the colleagues that I have had the pleasure of working with, in particular Paul Raftery, Fred Bauman, Jovan Pantelic, Shichao Liu, Seema Bhangar, and Donghyun Rim. I am especially grateful for all the help I received from Yilin Tian and Dusan Licina, whose advice was essential in completing my second project. I'd also like to thank my officemates Lucas Bastien and Chelsea Preble, as well as my undergraduate research assistants Ada Shaw and Vineet Nair for their help.

I would never have been able to do any scientific work without the dedication and kindness of the staff in the Civil and Environment Engineering Dept., and Center for the Built Environment. I don't know of any CEE graduate student who is not deeply grateful for Shelley Okimoto, and I am thankful for all the practical help that I received over the years from Paul Haller, Li-Ci Lau, and Jeff Higginbotham.

Chapter 1

Introduction

Creating a flexible conceptual model of indoor air quality (IAQ) that is as simple as possible, while capturing the bulk of the occupant exposure is desirable for both IAQ researchers, and professional engineers consulting with individual clients. With the invention of highly sophisticated computer models, and the advent of inexpensive, internet-of-things sensors, the production of data is becoming increasingly cheap and abundant. The role of the expert then becomes the selective use of these data tools to maximize the amount of practical knowledge gained. The goal of this dissertation is to propose a process to develop a simple model of occupant exposure for a particular indoor space or type of ventilation system. Furthermore this model should suggest steps that can be done to estimate the exposure in laboratory experiments and field measurements. The scope of this dissertation will be kept narrowly on thermally stratified environments with a small number of occupants, and no other sources of mixing besides thermal plumes. Occupant exposure will be measured as the concentration of a pollutant of concern in the occupant breathing zone. This approach will be used to attempt to better inform current industrial practices, and provide an example of how the results of this method can be communicated to a non-expert client.

1.1. Indoor pollutant exposure

Exposure science is a relatively recent scientific field concerned with whether and how humans come into contact with toxicants in the environment. In a general sense exposure science is concerned with the entire system connecting pollutant releases to human health effects: pollutant source, environmental concentration, exposure, intake, dose, and finally health effects (Lioy, 2010). Practically studies in exposure are mainly concerned with measuring the environmental concentrations that are relevant to actual exposure. The use of exposure science is to better inform risk prevention by source and pathway identification. Exposure itself acts as a conceptual bridge linking the concentration of a pollutant found in an environment to the amount of pollutant that a human comes into contact with. In the context of air pollutants, while there is increasing evidence that dermal exposure is a significant pathway, inhalation exposure is still the most important pathway for pollution intake. When considering inhalation exposure, the first National Research Committee on Exposure settled on a consensus definition for constitutes exposure:

$$E = \int_{t_0}^{t_1} C(t)dt \tag{1.1}$$

where $C(t)$ is the pollutant concentration in the environment surrounding a person, and t_0 to t_1 is the exposure period. For inhalation exposure $C(t)$ is the concentration within the human breathing zone, which is an approximately 0.5 L sphere underneath the nose or in front of the mouth, and is the physical location that an occupant's breath draws the air from. The location, timing, and activities of humans are therefore central to exposure studies, and wide-scale activity pattern studies are essential for other researchers to be able to use (Klepeis *et al.*, 2001).

Exposure to indoor pollutants is a significant health concern, and there are moral incentives to understanding how to improve indoor conditions. The average American spends around 90% of their time indoors, so it is important to understand how indoor air quality differs from the outdoors condition (Godwin and Batterman, 2007; Leech *et al.*, 2002). When indoor pollutant sources are an issue, identifying the source and removing it is the best solution. In 2012 there were an estimated 7 million deaths from air pollution in general, and 4.3 million deaths attributable to indoor pollution sources (Lim *et al.*, 2013; Lelieveld *et al.*, 2015). Most of these deaths occur in the population of 3 billion worldwide who live in residences where cooking and heating comes from the open combustion solid fuels, which is a highly emitting source of many damaging pollutants. The most efficacious action that can be taken to improve the health effects of IAQ in these residences is to remove the solid fuel

stoves and replace them with more modern alternatives that are substantially less polluting, such as natural gas or induction stove tops (Ezzati and Kammen, 2002). Even in modern homes that do not have the same magnitude of indoor pollutant sources, IAQ issues can often arise from the presence of singular high emission sources. In a *in situ* study conducted in California, two of the houses had stoves with unvented pilot lights, which alone were responsible for 12% and 16% of the occupants particle number exposure (Bhangar *et al.*, 2011). Whenever possible, improving IAQ conditions through the identification and removal of pollutant sources is preferable.

For some emission sources, especially in the case of bioeffluent pollutants emitted by the occupants themselves, source removal is impossible and IAQ improvements can be achieved through altering ventilation conditions. There are well documented health benefits to increased per person ventilation, for a good review of the spectrum of health effects associated with ventilation see Seppänen and Fisk (2004); Seppänen *et al.* (1999). Per person ventilation rates used in the ASHRAE standards range from 3.5–8.5 L/s·person for offices at average occupancy, and 2.5 L/s·person + 0.3 L/s·m² for residential units (ASHRAE, 2016b). There is abundant evidence that there are significant health advantages to higher per person ventilation rates (Sundell *et al.*, 2011; Norbäck and Nordström, 2008). In a survey of 3720 employees in 40 different buildings, Milton *et al.* (2000) found consistent increase in sick leave with decreasing ventilation rates that is independent of general indoor environmental quality complaints. An attributable risk of 35% is associated with lower than recommended per person ventilation rates, and the study suggests a savings of \$400 per employee for increasing the ventilation rate above recommended levels (Milton *et al.*, 2000). Higher ventilation rates are also associated with increased productivity, fewer IAQ complaints, and an overall 1.7% increase in performance for a doubling of the per person ventilation rate (Wargocki *et al.*, 2000).

There is no physical reason why the direct action of providing additional fresh air has health benefits, as an occupant whose breathing zone is 100% fresh air during inhalation should see no difference in how much air flows through that space. The health benefits derive from the fact that the additional fresh air lowers the amount of pollutants from indoor sources, especially exhalations and bioeffluents from the various occupants. CO₂ is a good proxy for bioeffluents, and has been used as an indicator of indoor air quality where occupants are the main source of pollution (Persily, 1997). Similar to increased ventilation rates, lower CO₂ concentration exposure have been associated with increased health benefits and productivity (Seppänen *et al.*, 1999). CO₂ concentrations above 1000 ppm have been associated with 10-20% increase in student absence (Shendell *et al.*, 2004). There is some evidence that CO₂ itself may lead to decreased cognitive performance, specifically with higher order executive functions, (Satish *et al.*, 2012; Allen *et al.*, 2016), though other studies do not find this effect (Zhang *et al.*, 2017). Different ventilation systems will provide outdoor air to occupants at different levels of efficiency. In an ideal mixed ventilation system the pollutant concentra-

tion is inversely proportional to the ventilation rate, while other systems like displacement ventilation are more efficient at removing air contaminants (He *et al.*, 2005). Changing from a mixed ventilation system to a more efficient displacement ventilation system has been associated with better health outcomes and perceived air quality (Norbäck *et al.*, 2011).

1.2. Microenvironments

The term microenvironment is well understood by researchers in the IAQ field; however, a formal definition has not been explicitly formulated. For the purposes of this dissertation a microenvironment is a spatial and temporal space within a room that has a distinct exposure to the rest of the room. Microenvironments can be thought of as having strong central tendencies, but fuzzy boundaries. It is often difficult to define strict spatial boundaries or disentangle when a microenvironment is a temporal phenomenon versus a spatial phenomenon, but empirically there is strong evidence that microenvironments in the indoor environment have significant exposure effects (Klepeis *et al.*, 2001). In households that use indoor solid fuel combustion for cooking and heating in Kenya it is estimated that exposure would be underestimated by 3-71% depending on the occupant's demographics (Ezzati *et al.*, 2000). Personal measurements show an increased particulate matter concentration and other VOC's over bulk air indoor measurements (Ferro *et al.*, 2004; Ozkaynak *et al.*, 1996; Allen *et al.*, 2007). Being able to identify the existence of microenvironments is a key skill for IAQ practitioners to have to ensure that their measurements are representative of occupant exposure.

In the indoor environment without strong mixing sources the volume near the human body, known as the perihuman zone, can be its own microenvironment with an increased pollutant exposure. In part the increased exposure is probably a temporal phenomena, as occupant activity can cause episodic emissions to occur within the perihuman zone (Ozkaynak *et al.*, 1996; Ferro *et al.*, 2004; Licina *et al.*, 2017). The thermal plume caused by the human body being a heat source in a relatively quiescent air mass also has the effect of concentrating emissions that occur close to the body (Vannucci and Nazaroff, 2017; Licina *et al.*, 2015; Rim and Novoselac, 2010, 2009; Corsi *et al.*, 2007). Estimating the concentration within the perihuman space from sensors placed in the indoor environment is non-trivial, and highly dependent on the type of pollutants, room conditions, and ventilation conditions.

It is possible to model an indoor space with microenvironments as a set of nested compartment, such as measuring the concentration within the perihuman zone separately from the room concentration and coupling the two (Licina *et al.*, 2017). If one can model the room as a system of linear equations, then there are a wealth of techniques and theories from other

disciplines that can be easily applied to IAQ (Evans, 1996). At a basic level it is necessary to understand the building ventilation characteristics, occupancy patterns, and pollutant dynamics to build an adequate exposure model (Nazaroff, 2008). To use such a model in a practical sense, it is also necessary to make logical sensor placement decisions. Generally IAQ researchers simply place sensors in the center of a room or near occupants, between 1.0-1.2 m high Mahyuddin and Awbi (2012). This sensor placement works well when a room is essentially well-mixed, which is problematic when we are considering ventilation systems that are designed to generate pollutant concentration gradients, and when occupants are in close proximity to emission sources (Furtaw *et al.*, 1996; Chenari *et al.*, 2016; Acevedo-Bolton *et al.*, 2012). In this dissertation we will treat the perihuman zone as a well mixed, flow-through reactor, and will consider thermally stratified room conditions that are both unventilated and ventilated by displacement ventilation systems.

1.3. Overview of dissertation

The simplest model of an occupied indoor environment is a well-mixed, time-invariant box where the occupant is separately a source and a receptor. The only quantities necessary to characterize the exposure in this space are then: volume, ventilation rate, number of occupants, emission rate per occupant, non-occupant emission rates, and pollutant loss rate. Complexity is achieved spatially with additional compartments to model microenvironments, and identifying when there is different vertical and horizontal behaviors. Time is taken into account to identify the significance of particular events and as the characteristic time for transport mechanisms. As a principle we would like to use models that are governed by the minimum number of dimensions at the coarsest resolution, slowly take into consideration additional dimensions, and design these models to be parameterized by the minimum number of measurements. A general process for accounting for the effects of microenvironments in an indoor space is proposed below. This process is designed to identify significant microenvironments within a occupied space, describe the relationships coupling the system, determine measurable parameters, and communicate the findings to an audience of non-experts.

1. **Describe** the space as a function of room characteristics, air distribution, ventilation rate and control strategies.
2. **Identify** relevant microenvironments, significant pollutant sources, and any occupant IAQ complaints.
3. **Estimate** exposure to pollutant sources to determine the simplest appropriate model
4. **Describe** the pollutant transport within and between the compartments
5. **Parameterize** the system variables to a set of measurable conditions

6. **Experiment** with field measurements and laboratory studies
7. **Summarize** the knowledge gained by the process to obtain the maximum impact with the intended audience

The remaining chapters in this dissertation use IAQ research techniques to explore different aspects of the proposed process using chamber experiments. A potential perihuman source of ultrafine particles is explored by a flow-through reactor with conditions similar to the human thermal plume in Chapter 2. This chapter illustrates one method to perform Step 2, and determine whether a perihuman compartment is necessary for estimating ultrafine particle exposure. Chapter 3 is an example of determining mixing characteristics, specified in Step 4, for a thermally stratified zone. A sealed chamber is used to measure the effect of thermal stratification and other heat sources on the time it takes a pulse release of CO₂ to become well-mixed. Chapter 4 utilizes this process to better inform sensor placement guidelines for demand control, displacement ventilation systems. A series of full-scale chamber experiments was performed to determine if breathing height wall sensors truly have a 1-to-1 relationship to breathing zone CO₂ concentration, as is assumed in current industrial practice. An example of how to summarize the results of an IAQ diagnosis of a particular building for a non-expert client is also presented.

Chapter 2

Ultrafine Particle Production from the Ozonolysis of Personal Care Products

Reproduced in part with permission from Vannucci, M. P.; Nazaroff, W. W. 2017. Ultrafine particle production from the ozonolysis of personal care products. *Environmental Science & Technology*, 51 (21) 12737–12744. Copyright 2017 American Chemical Society.

2.1. Introduction

Characterizing indoor sources of airborne particle emissions is important for accurately estimating exposures and, when necessary, for informing control strategies. Exposure to ultrafine particles (UFP) has been linked with increased morbidity and mortality (Knol *et al.*, 2009; Ostro *et al.*, 2015). Indoor sources of UFP may contribute substantially to a person's total exposure (Wallace and Ott, 2011). In the presence of significant indoor UFP sources, indoor concentrations do not correlate well with outdoor concentrations (Bhangar *et al.*, 2011; Singer *et al.*, 2017). He *et al.* (He *et al.*, 2004) found that activities like frying, using a toaster oven, or using a candle- heated oil evaporator could increase particle number (PN) concentrations by more than a factor of 5 above background levels. When present, emissions from unvented pilot lights on cooking appliances have been shown to contribute as much as

20% of PN concentrations in households (Bhangar *et al.*, 2011).

Ozonolysis of terpenes is a common indoor source of ultrafine particles and ozone-terpene reaction products have been linked with adverse human health effects (Weschler and Shields, 1999; Morawska *et al.*, 2001; Rohr, 2013; Hallquist *et al.*, 2009). Terpenes are found in common fragrances such as citrus, lavender, and pine. Many cleaning products and air fresheners contain terpenes and their use has been shown to result in increased concentrations of fine particles (Sarwar *et al.*, 2004). Terpene-based cleaning products, in particular, have been studied for UFP emissions from ozonolysis under a variety of conditions (Coleman *et al.*, 2008; Huang *et al.*, 2011; Nørgaard *et al.*, 2014).

Organic chemicals including terpenes that can react with ozone may be incorporated into personal care products (PCP) that people apply to their bodies. Corsi *et al.* (Corsi *et al.*, 2007) introduced the concept of the personal reactive cloud, drawing attention to the potential reactive chemistry that may occur in the perihuman space when chemical emissions from people combine with reactive agents in indoor air such as ozone. Such reactions might disproportionately affect human exposure because of proximity to the breathing zone. Assuming a well-mixed environment has been shown to systemically underestimate particle exposure in field measurements when compared to personal concentration measurements (Rodes *et al.*, 2010; Ozkaynak *et al.*, 1996; Ferro *et al.*, 2004). Computation fluid dynamic models and heated manikin studies have shown that breathing zone particle concentrations are strongly affected by the source position and thermal plume characteristics (Rim and Novoselac, 2010; Licina *et al.*, 2015; Li *et al.*, 2013; Salmanzadeh *et al.*, 2012; Rim *et al.*, 2009).

In relation to its potential importance, little research has been reported on ultrafine particle emissions from products used on or near humans. Lemon- and orange-scented coloring markers, as well as D-limonene emitted from peeling oranges have been shown to produce particles as a consequence of ozonolysis (Fung *et al.*, 2014; Vartiainen *et al.*, 2006). Personal care products (PCP) are another potential source of reactive chemicals that could produce ultrafine particles owing to ozonolysis. The direct application of PCPs to the human surface places them within the human thermal plume, and the variety of chemicals used in their formulation provides a spectrum of potential reactive species. Many PCPs are fragranced, often lacking chemical-specific labels; some fragrances in household products have been linked to indoor air quality concerns (Steinemann, 2009; Uhde and Schulz, 2015).

Very few personal care products have been tested for particle production under ozonolysis. Liu *et al.* (Liu *et al.*, 2014) measured particle emission from the ozonolysis of natural oil-based mosquito repellents as a function of applied dosage, and found significant overall emissions. Some essential oils have been shown to increase levels of known secondary organic aerosol

(SOA) precursors and to produce particles under ozonolysis (Su *et al.*, 2007; Huang *et al.*, 2012). Hsu *et al.* (Hsu *et al.*, 2012) reported significant particle production in chamber tests of essential oils that were used for massages as well as identifying in situ increases in particle number concentration in spa air. Given the widespread and diverse uses of fragrances in personal care products, along with existing knowledge that some fragrances can react with ozone to produce ultrafine particles, it is worthwhile to consider more carefully the scope and significance of particle production generated by ozonolysis of personal care products. The goals of the research reported here are (a) to broadly survey common PCPs to determine the frequency of particle production during ozonolysis, and (b) to quantify emissions in cases in which screening experiments indicate a potential for substantial particle production.

2.2. Methods

2.2.1. Apparatus

This study was conducted using a small, purpose-built reaction chamber (see Figure 2.1). The chamber was a PTFE-lined, cylindrical steel pipe with a volume of 10.8 L (15 cm diameter \times 61 cm length, Marspec Technical Products). Inlet air was provided by the laboratory air supply, dehumidified using a desiccant and treated with a two-stage filter (Parker Hannifin Corporation) to remove particles and ozone. The air stream was then split into two branches, one directed to a gas bubbler with deionized water for humidification and the other to an ozone generator (UVP, Pen-Ray). The streams were recombined in a 2-L mixing bottle, where relative humidity was measured (HW Group, Humid-1 Wire) before sending the combined flow to the chamber. Inlet air was sampled for ozone (Model 205, 2B Tech) immediately before entering the reaction chamber. A water-based condensation particle counter (1120 WCPC, MSP Corp.) sampled from the outlet of the chamber to measure particle concentrations; excess outlet gas was vented. The WCPC has a lower particle size limit of 12 nm for hydrophobic particles, 8 nm for hydrophilic particles, and an upper concentration limit for quantification of 60 000 cm^{-3} . The chamber was cleaned before each experimental run by wiping the interior surfaces with methanol and quenching the chamber with high concentrations of ozone produced by a corona discharge ozone generator (Ozone Solutions, HP-500) to reduce surface-bound reactive compounds. A purpose-designed sample holder was suspended in the center of the chamber by tabs that rested on the curved wall, allowing for airflow around the holder. This sample holder was made of two stainless steel plates sandwiched around a heating element and thermocouple (Omega Engineering Inc.) and sealed using Teflon (see appendix Figure A.1.1). The top of the sample holder had a recess coated in thermal putty to facilitate utilization of disposable aluminum foil sample trays that were maintained at a slightly elevated temperature to approximate the thermal environment of the skin surface.

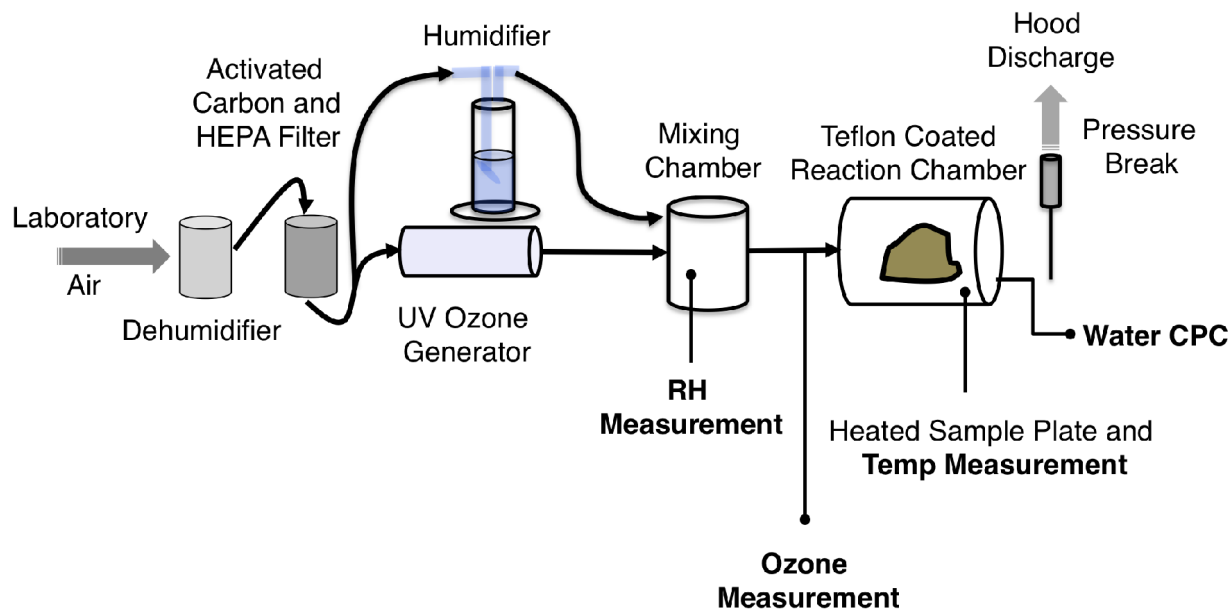


Figure 2.1: Schematic for chamber setup used in this study. Boldfaced labels indicate sampling points for each measurement taken.

2.2.2. Product Selection

Altogether, 91 products were sampled for particle production under ozonolysis. All products were purchased within a year of the survey, mostly from a popular multinational retailer. Roughly half of the products were chosen from widely available and popular brands, with preference given to product lines that include multiple fragrances, preparations, or specialty ingredients. Other products were chosen to broaden the scope of items tested (e.g., to include products with herbal infusions) or because of a listed fragrance that was suspected to contain terpenes. Pine scents are uncommon in personal care products, so targeted fragrances tended to be lavender (potentially containing linalool, a terpene alcohol) or citrus (potentially containing D-limonene).

Three product categories—body and face lotions, deodorants, and sunscreens—were chosen for broader screening. The range of products within each category included at least one complete product line, along with other common brands and some specialty products. Due to the range of available fragrances for body and face lotions as well as deodorants, these two categories had the highest number of products tested in the initial survey. There were also seven product categories that had three or fewer tested products. Products in these categories represented popular formulations, and products with suspected terpene-based fragrances were chosen whenever possible.

2.2.3. Screening Survey

Screening experiments were conducted to identify personal care products that exhibited any detectable particle generation when exposed to ozone. The screening survey was conducted by applying a quantity of the product to the unheated sample plate. This quantity was intended to be generous, yet representative of a single application for personal use. After application, the plate was sealed in the chamber and purged at 14 L min^{-1} for 5 min. Ozone was then introduced, and the flow rate reduced to 2.8 L min^{-1} . Inlet conditions were room temperature air ($\sim 25 \text{ }^\circ\text{C}$), relative humidity near 50%, and ozone concentration in the range 20–35 ppb. The experiment ran for a minimum of 20 min, and the existence of a particle production event, or lack thereof, was noted based on any detectable increase in PN concentration. No replicate experiments were conducted to confirm the results of the screening survey.

2.2.4. Quantification Survey

The second phase of the study was designed to characterize particle generation events for those personal care products that exhibited particle production with exposure to ozone in the screening experiments. For each sample tested in this phase, an aluminum foil vessel of area 180 cm^2 was prepared with a template. A consistent sample mass, $1.5 \pm 0.1 \text{ g}$, was applied to the template. (An exception applied in the case of facial scrubs, which could not be spread thinly; $3.1 \pm 0.1 \text{ g}$ was applied for these samples.) The sample mass was measured by weighing the aluminum vessel directly before the sample was spread, and subtracting the amount of sample left on the spatula used to spread it. Loretz et al. (Loretz *et al.*, 2005, 2006) assessed exposure of 360 adult women to various personal care products, and the sample quantity used here is consistent in magnitude with average daily uses from that study. Specifically, the reported mean usage per application of perfumes, solid deodorants, face creams, facial cleansers, and body lotions, were, respectively, 0.3, 0.6, 1.2, 2.6, and 4.4 g. After spreading the sample onto the aluminum foil vessel, the vessel was placed on the preheated sample plate and pressed into the thermal putty for good thermal contact immediately before being loaded into the reaction chamber.

Electrical power was applied at a constant rate to the sample plate’s heating element to maintain the plate surface temperature to an appropriate value for exposed skin. The measured temperature was $30.8 \pm 1.3 \text{ }^\circ\text{C}$ under steady state conditions in normal experimental conditions. The power applied, selected through trial and error, was 56 W/m^2 , which is comparable to 1.0 metabolic equivalent ($1.0 \text{ MET} = 58.2 \text{ W/m}^2$). Other chamber conditions during these quantification experiments were designed to be consistent for typical

indoor conditions. Inlet ozone was 23 ± 2 ppb, and air temperature in the chamber was 25.3 ± 1.1 °C. Increased humidity has been implicated in increasing particle formation and growth,(Jonsson *et al.*, 2008) so a moderately elevated relative humidity of $69 \pm 3\%$ was used in these experiments. Sample preparation was carefully timed; each sample was exposed to laboratory air for a consistent period prior to measurement so as to reduce uncontrolled reactant loss and ozone deposition. All samples were removed from their container, weighed, applied to the preheated sample plate and sealed in the purging chamber over a period of 7.0 min. (Periodic sampling showed the laboratory ozone concentration to vary in the range 5–30 ppb.) Once the chamber was sealed it was purged with filtered air at 14 L min^{-1} for 5 min. After purging, ozone injection was initiated, and the airflow was reduced to $2.76 \pm 0.04 \text{ L min}^{-1}$, corresponding to a chamber air-exchange rate of $15.6 \pm 0.2 \text{ h}^{-1}$. Experimental runs continued for at least 1 h, and the termination time was selected to ensure that significant particle production could no longer be observed. At the end of each run, the chamber was cleaned and purged in the same fashion as for the screening experiments. Two replicate quantification experiments were conducted for all samples except for P1 and P2, which each had three quantification experiments.

2.2.5. Data Analysis

At the beginning of each measurement day, ozone loss by reaction in the chamber with the sample plate was measured. The average first-order ozone loss coefficient in the chamber was 0.13 min^{-1} . The background particle concentration with the sample plate installed and with ozone on was measured at the beginning of the day and was always less than 1.0 cm^{-3} . With this low background, the minimum detectable particle emission rate was 56 min^{-1} .

Assuming a well-mixed reaction chamber, the particle emission rate was determined based the following material-balance equation:

$$\frac{dC}{dt} = \frac{E}{V} - AER \times C \quad (2.1)$$

Here C is the measured concentration. The effects of inlet particle concentration, particle losses owing to deposition and also to coagulation are used to estimate uncertainty, but are not included in the material balance equation for C . A full treatment of the emission rate, including the inlet concentration and loss terms, is presented in the Appendix. An assumption of monodispersed aerosol at the diameter of maximum loss was used to estimate the magnitude of the effect of these other terms. Using mean flow velocity in the chamber, the influence of the neglected terms was consistently smaller than 1% in contributing to the estimated total particle emissions. Uncertainty in C for the purposes of calculating the error reported in Table 2.2 was estimated using the inlet velocity as an upper bound for the flow velocity inside of the chamber, as this approach maximizes the estimated losses from

chamber air due to deposition.

To reduce signal noise in the emission profile, the concentration data with 1 s resolution were binned into 1 min intervals to calculate the total particle emissions and the maximum emission rate. The emission rate, E , was estimated by rearranging eq 2.1 as follows:

$$E = V \times \left(AER \times C + \frac{dC}{dt} \right) \quad (2.2)$$

Total particle emission was calculated as the time-integral of E over the duration of the particle production event. The particle production event was defined to be ongoing when the chamber particle concentration exceeded the larger of (a) 1% of the peak number concentration or (b) 1 cm^{-3} . The average particle production was calculated as the ratio of the total particle emission to the duration of the event. The peak particle emission rate was defined as the largest 1 min particle emission rate. Event duration was determined by the time between the two crossings of the appropriate threshold.

2.3. Results

Table 2.1 reports the aggregate results from the screening survey of personal care products. Twenty of the 91 screened personal care products exhibited a detectable particle emission event and were included in the quantification experiments. During the second phase experiments, 12 of the 20 tested products exhibited quantifiable emissions. Five of these 12 showed mixed results in replicate experiments, meaning that a product had a detectable particle production event in only one of two experimental runs. Differences in particle production between the screening survey and the quantification experiments could be a consequence of the application of heating to the sample plate, which would encourage increased volatilization during the initial 5 min purge. The sample plate was left unheated in the screening survey. The chamber apparatus is capable of measuring low cumulative particle production, and many of the detected particle production events were small relative to those that would produce discernible signals in field studies. With appropriately low ozone concentrations (for indoor exposure conditions) and small quantities of applied products, it is possible that nucleated particles were close in size to the minimum detection limit of the WCPC. If so, then outcomes could be sensitive to fine-scale experimental details that might vary from one run to another, even though the major elements were carefully controlled.

Five product categories had no samples exhibiting a particle production event during screening experiments. Sunscreens, the most highly populated of these five categories, included

Table 2.1: Particle Production from the Ozonolysis of Personal Care Products

Product category	Number screened	Number quantified	Mixed results, <math><10^9</math> particles	Emitted <math><10^9</math> particles	Emitted $>10^9$ particles
Aftershave	3	2	1	1	
Antiwrinkle cream	3	1	1		
Body and face lotion	19	1			1
Body spray	6	4	1		
Cleanser	3	0			
Cream / moisturizer	5	1	.	1	
Deodorant	27	7	1	1	
Facial scrub / mask	7	3	1	2	
Hair styling	3	0			
Perfume	2	0			
Scalp / hair treatment	3	1			1
Sunscreen	9	0			
Whitening cream	1	0			
Total	91	20	5	5	2

nine specific PCPs. Deodorants and body sprays had the highest number of products exhibiting particle emissions in the screening survey, but with very few detectable signals in the quantification experiments. Propellants used in the body sprays may be responsible for the initial signal, which, when heated by the sample holder in the quantification experiments, may have been lost by volatilization prior to ozone injection.

Nine sunscreens covering most common formulations were tested: sprays, tanning oils, creams, sports preparations, and fragrance-free children’s sunscreens. Sunscreen products have been previously linked to some environmental health concerns, in particular, associated with paraben exposure. (Rudel and Perovich, 2009) A survey of common sunscreens at a major drug store indicates that fragrance is not normally reported on the labels, so it is not known how the tested products relate to the full range of marketed formulations with respect to fragrances. None of the nine samples showed any detectable particle emissions in the screening experiments. The lack of any sunscreen product that reacts with ozone at 25 ppb to produce particles suggests that UFP particle production may not be an important issue for sunscreens at normal indoor ozone concentrations.

The category with the largest number of products tested in the screening experiments was deodorants. Four different formulations of deodorants were tested: white solids, invisible solids, clear gels and liquid roll-ons. Spray deodorants were also tested, categorized here as body sprays. During the screening survey, seven deodorants, about a quarter of the deodorants tested, exhibited some particle production. Under further investigation in the quantification experiments, only two of these seven deodorants exhibited a detectable particle generation event. Both samples emitted a small number of particles, less than 10^5 per event, and one sample had mixed results in the quantification experiments. There is evidence from other studies that deodorants in particular are a source of particle mass in the near field. Conner and Williams (Conner and Williams, 2004) analyzed the composition of particles collected in the human personal cloud and found particles with an Al–Zr–Cl composition, which they suspected to be originating from applied deodorants. The present study shows that deodorants are capable of producing secondary particles in response to ozone exposure, but do not do so consistently or in large quantities.

In our quantification experiments, only two products had emission events with more than 10^9 total emitted particles. For context, note that prior studies have reported that the use of a gas stove and the heating of a steel pan can produce 10^{12} – 10^{13} particles per event; cooking popcorn in a microwave oven was reported to produce 10^{10} – 10^{11} particles (Bhangar *et al.*, 2011; Wallace *et al.*, 2015; Zhang *et al.*, 2014). Liu *et al.* (Liu *et al.*, 2014) measured the particle production from natural mosquito repellents with similar ozone exposures as in the present study and found total particle production in the range 10^9 – 10^{11} particles, depending on the amount of product applied. Both of the products in this study with more than

10^9 total emitted particles are formulated or fragranced with a known secondary aerosol precursor, tea tree oil or lavender scent. However, other tested products that appeared to contain such precursors either did not exhibit particle production, or emitted a total number of particles that is orders of magnitude smaller. The relative rarity of personal care products in this survey with strong particle emissions when exposed to ozone suggests that only certain specific products have the potential of significantly increasing a users' ultrafine particle exposure.

For all product categories, some of the products emitted no particles in screening tests. This finding suggests that the basic product formulations do not inherently produce particles upon ozonolysis. The experiments reported here support an inference that fragrances are the main secondary aerosol precursors. The amount of fragrance mixed into each personal care product is unknown, so it is not possible to differentiate which products have higher concentrations of terpene-based fragrances, or to estimate an effective emission factor for fragrances mixed into products. The product emission factors we can calculate are also subject to differences in the amounts of fragrances used among brands, or even among product batches within a given brand.

Table 2.2: Results of the Quantification Survey, by Product^a

ID	Product category	Fragrance / formulation	Total particle production	Duration (min)	Avg. particle production rate (min^{-1})	Peak particle production rate (min^{-1})
P1	Scalp / hair treatment	Tea tree oil	$5.5 \pm 2.6 \times 10^9$	89	$6.2 \pm 2.8 \times 10^7$	$2.3 \pm 0.5 \times 10^8$
P2	Body and face lotion	White lavender	$1.1 \pm 1.2 \times 10^9$	57	$2.0 \pm 1.4 \times 10^7$	$9.2 \pm 5.3 \times 10^7$
P3	Facial scrub / mask	Apricot	$1.5 \pm 0.9 \times 10^7$	25	$5.7 \pm 3.1 \times 10^5$	$3.8 \pm 0.5 \times 10^6$
P4 ^b	Antiwrinkle cream	Grape seed	$1.4 \pm 0.6 \times 10^7$	27	$5.0 \pm 2.4 \times 10^5$	$3.4 \pm 0.5 \times 10^6$
P5	Aftershave	Astringent	$2.0 \pm 2.3 \times 10^7$	53	$3.6 \pm 4.0 \times 10^5$	$1.4 \pm 1.5 \times 10^6$
P6 ^b	Aftershave	Balm	$6.5 \pm 2.8 \times 10^5$	21	$3.0 \pm 1.3 \times 10^4$	$1.6 \pm 0.3 \times 10^5$
P7 ^b	Body spray	Fragrance	$5.8 \pm 2.9 \times 10^5$	28	$2.1 \pm 1.0 \times 10^4$	$1.1 \pm 0.2 \times 10^5$
P8 ^b	Facial scrub / mask	Lemon and mandarin	$8.4 \pm 3.7 \times 10^5$	92	$9.2 \pm 4.0 \times 10^3$	$3.1 \pm 0.4 \times 10^4$
P9 ^b	Cream and moisturizer	Dry skin cream	$3.4 \pm 2.9 \times 10^5$	89	$3.9 \pm 4.0 \times 10^3$	$2.7 \pm 1.4 \times 10^4$
P10	Facial scrub / mask	Green tea scrub	$8.3 \pm 3.5 \times 10^4$	18	$4.6 \pm 1.9 \times 10^3$	$2.6 \pm 0.4 \times 10^4$
P11	Deodorant	White solid	$4.0 \pm 3.2 \times 10^4$	17	$2.3 \pm 1.9 \times 10^3$	$1.4 \pm 1.1 \times 10^4$
P12 ^b	Deodorant	White solid	$2.5 \pm 1.1 \times 10^4$	17	$1.5 \pm 0.6 \times 10^3$	$9.1 \pm 1.1 \times 10^3$

^aEach product was tested twice except for P1 and P2, which were tested three times. ^bThe indicated PCP had mixed results, with one of the two experimental runs not exhibiting any particle production. In these cases, the total production, duration and rate were calculated from the experimental run with particle production.

2.3.1. Quantifying Particle Emissions from Specific Products

Table 2.2 summarizes the quantification experiment results. For cases where replicate experiments produced measurable particle events, the total particle production, duration, average particle production rate, and peak particle production rate are reported as the averages of the quantification experiment results (see Appendix Table A.1.1 for full results). There was no significant correlation between source strength and event duration in the quantification experiments. However, source strength was correlated with peak particle production rate. Personal care products P1 (a tea tree oil scalp treatment) and P2 (white lavender body lotion) exhibited the highest total particle emission and peak particle production rate, by at least a few orders of magnitude. P1 and P2 had event durations that were longer than most other samples, but were not the longest. Most emission events were of duration less than 30 min. Two samples, including P2, had event durations around 50 min, and three samples, including P1, had event durations that lasted approximately 90 min. All of the samples tested revealed emission rates that peaked in the first third of the respective emission event, indicating that the maximum user exposure rate would occur soon after initial application.

When applying these results to estimates of real-world exposure, the differences between a heated aluminum sample plate and human skin should be taken into account. For example, skin oil contains squalene, which also is reactive with ozone and which has exhibited particle production events in laboratory experiments (Wang and Waring, 2014). The application method used in this study ensures at least a monolayer of PCP, whereas real-life application methods for some products, like sprays, are likely to yield thinner coverage. Work by Waring and Siegel (Waring and Siegel, 2013) suggests that, under normal indoor conditions, ozone reaction with D-limonene is reaction rate limited, and not transport limited. Thus, both the fractional coverage of a PCP on the skin and the presence of other ozone-reactive species may influence particle formation in a manner that differs from these laboratory experiments.

2.3.2. UFP Emissions from Selected Personal Care Products

The personal care products with the highest particle production rates and total particle emissions, P1 and P2, were a tea tree oil scalp treatment, and a white lavender body lotion. Both P1 and P2 had other products in the same product line with different fragrances that did not produce detectable particle emissions. Tea tree oil and lavender are commonly used for their fragrance, and have been shown to emit terpenoids, including eucalyptol, linalool, terpinene-4-ol, and γ -terpinene (Su *et al.*, 2007; Hsu *et al.*, 2012). Tea tree oil and lavender oil have also been shown directly to react with ozone at common indoor concentrations to produce secondary organic aerosol (Hsu *et al.*, 2012; Weschler, 2006).

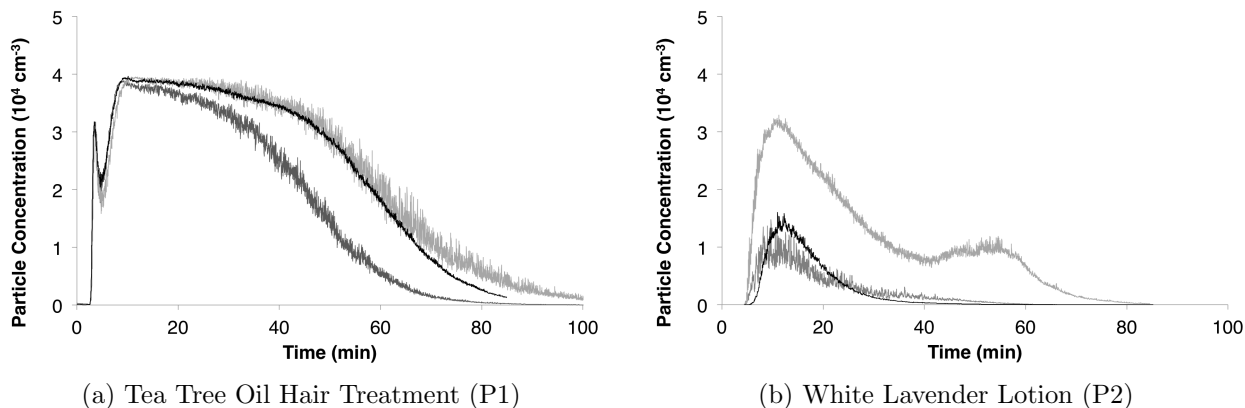


Figure 2.2: Particle concentration versus time for the two highest particle-producing samples: (a) tea-tree-oil scalp treatment (P1), and (b) white lavender body lotion (P2). Note that the maximum measured concentrations are below the WCPC’s upper quantification limit of $6 \times 10^4 \text{ cm}^{-3}$.

Time-dependent particle number concentrations in chamber air are shown for three quantification runs for P1 in Figure 2.2a. Each experimental run for P1 exhibited the same shape, which is distinct from the sharp single peak seen with most other samples. After ozone was introduced, the particle concentration quickly rose to a steady peak level for ~ 30 min before decaying over the next hour or so. The single or multiple peak profile that characterized the other samples, and is absent in P1, might be indicative of ozone being the limiting reactant for the tea tree oil hair product. Also noteworthy is that P1 was the tested product with the strongest and longest lasting particle emission event.

The white lavender body lotion P2 (Figure 2.2b) yielded interesting results in the quantification experiments. Of the three reported experimental runs, two had a single peak shape similar to the majority of sampled products. These runs produced approximately equal total particle emissions. The third run was distinct in shape and had a higher total number of particles emitted. The third run showed a $5\times$ increase in total particle emissions and a $4\times$ increase in average particle emission rate compared with the other two runs. Moreover, the high emitting run for P2 also exhibited a second emission peak about 50 min after ozone introduction. Extensive testing was done with this PCP to investigate the variability of these results. The appearance of the second peak was correlated with experimental runs that had higher total particle emissions, but the significant variability between runs, as noted above, could not be resolved. The experimental runs that are presented here are those performed concurrently with the rest of the quantification experiments.

Significant variability of total particle emissions, spanning an order of magnitude between experimental runs for a single personal care product, was observed while developing the test-

ing procedure for these quantification experiments. Extensive testing was done with a small selection of products to develop a more reliable procedure; however, the particle nucleation process seems to be too sensitive to subtle experimental details within this chamber system to obtain a greater degree of reproducibility. Particle emissions exhibited variability in two different ways: magnitude of the total particle emissions, and the appearance/disappearance of particle emission peaks. To illustrate, particle number concentration profiles from an alcohol-based aftershave, P5, are presented in Figure 2.3a. These showed the greatest variability between total particle emission events during the quantification experiments, with one experimental run producing only 14% the total particle count produced in a second run.

The antiwrinkle cream, P4, presented in Figure 2.3b illustrates a sample that had particle emissions in one quantification event. However, in a second run, the particle concentration remained at the background level the whole time, and, at the plotted scale, the null result run cannot be distinguished from the horizontal axis. It is possible that the concentration of condensable VOCs emitted from the PCP is near the lower limit necessary for nucleation. PCP that had mixed results such as this case had low overall particle emissions; maximum particle concentrations for these products were in the range 4–600 cm^{-3} , a few orders of magnitude lower than common ambient and indoor concentrations.

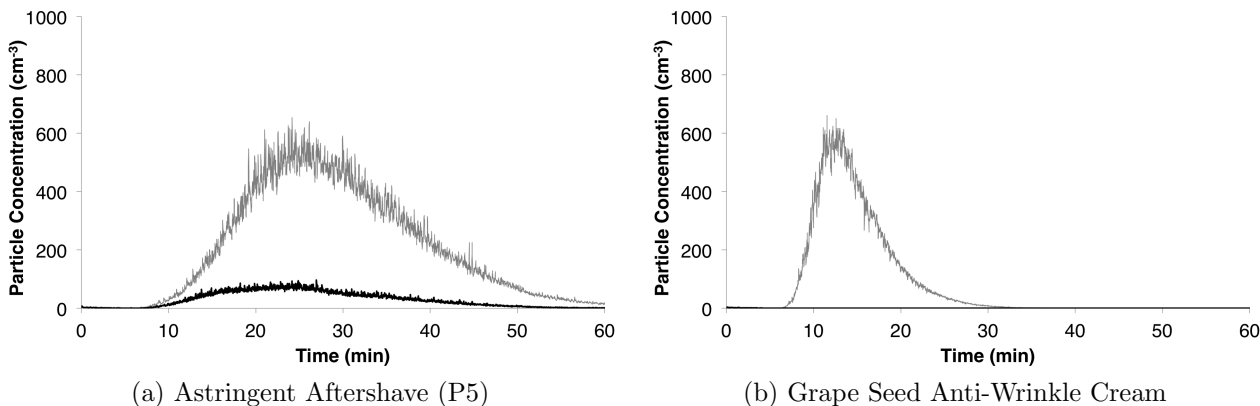


Figure 2.3: Example time-dependent particle concentration profiles, illustrating the variability of total particle emissions from different PCP: (a) an alcohol-based aftershave (P5) with one experimental run having a total particle emission a factor of 7 higher than the other; and (b) an eye cream (P4), showing examples of mixed results where one experimental run exhibited no particle emission whereas a second run did.

2.3.3. Estimating Exposure Consequences

Reaction chamber testing has the advantage of precisely measuring the emission profile from a specific source, but does not immediately provide contextual understanding of the source’s

Table 2.3: UFP Exposure Examples by the Ozonolysis of Selected Products

Scenario	Room vol (m ³)	AER (h ⁻¹)	Ventilation rate (L/s)	Occupants (#)	Background [PN] (cm ⁻¹)
Bathroom	14	2.6	12.5 ^b	1	14500 ^d
Classroom	610 ^a	5 ^a	850	80 ^a	2400 ^c

Scenario	P1		P2	
	Room Conc. Increase (cm ⁻³)	BZ ^e Conc. Increase (cm ⁻³)	Room Conc. Increase (cm ⁻³)	BZ ^e Conc. Increase (cm ⁻³)
Bathroom	101	190	33	77
Classroom	96	190	31	77

^aClassroom dimensions, ventilation rate and occupancy from Bhangar *et al.* (2014). ^bFrom ASHRAE (2016b) Table 6.5. ^cFrom Mullen *et al.* (2011) Table 2, site S5. ^dFrom Bhangar *et al.* (2011). ^eBZ = breathing zone.

effect on indoor air the parameters and results of these modeled examples. The bathroom is assumed to have a volume of 14 m³ (2.4m×2.4m×2.4m). The classroom parameters are based on the university classroom studied by Bhangar et al. (Bhangar *et al.*, 2014) Ventilation rates were chosen based on ASHRAE standards for the bathroom (ASHRAE, 2016b) and on classroom air-exchange rate (AER) measurements. The increment in breathing zone PN concentration attributable to ozonolysis was estimated by assuming a well-mixed thermal plume, an emission rate equal to the peak emission rate for the sample, and an airflow rate through the thermal plume of 20 L/ s (Craven and Settles, 2006). The increase in room concentration was estimated using an emission rate equal to the average emission rate multiplied by the number of occupants. For both P1 and P2, the increases in breathing zone concentration and room concentration were 2–3 orders of magnitude less than the background PN concentration. Even under more severe conditions, it is unlikely that particle concentration increases from this particular reaction would result in significantly increased UFP exposure. For significantly lower ventilation rates other indoor air quality issues will become serious before UFP from these products becomes significant. These exposure estimates suggest that particles produced by the ozonolysis of personal care products examined in this study do not pose a direct health hazard.

Though there is some degree of variability between experimental runs and among different PCPs, that feature is secondary to the primary observations from this study. UFP production by the ozonolysis of personal care products under normal indoor conditions is uncommon and, when present, it is generally weak. For the screening tests, the product selection process emphasized those PCP suspected of exhibiting reactivity with ozone. Of the 91 samples originally surveyed for UFP production, only two samples produced enough UFP to reasonably be considered as a sizable potential source of particle exposure by themselves.

Our findings support previous work suggesting that deodorants,(Conner and Williams, 2004) terpene-based fragrances, (Weschler and Shields, 1999; Morawska *et al.*, 2001; Rohr, 2013; Hallquist *et al.*, 2009) and some essential oils (Hsu *et al.*, 2012) can produce condensable species in the form of secondary airborne particulate matter. However, we find that only in a few select cases does ozonolysis of personal care products cause significant particle production when used in quantities typical of a single application. Particle exposure from this mechanism alone is likely to not be a cause for concern, unless it is demonstrated that the chemical species produced by ozonolysis are harmful, rather than the overall secondary particulate matter, as assessed here in terms of newly nucleated particles.

Chapter 3

Pollutant Mixing Time in a Thermally Stratified Chamber

3.1. Introduction

When estimating pollutant exposure in indoor environments it is often assumed that the space is well-mixed. IAQ studies most commonly place a single sensor in a central location between 1.0–1.2 m (Mahyuddin and Awbi, 2012), which is consistent the fact that many indoor spaces can be characterized reasonably well using the well-mixed assumption. These spaces are also easily modeled, as a well-mixed space can be described by ordinary differential equations instead of much more computationally complex partial differential equations that are necessary when considering three spatial dimensions. The exposure for some pollutant emission sources may be reasonably estimated by a model made up of well-mixed compartments that are nested with each other. When a microenvironment is caused by an occupant’s direct actions, such as particles that are resuspended by walking (Licina *et al.*, 2017), or comes from the human surface itself (Vannucci and Nazaroff, 2017), then the microenvironment is a result of the occupant’s thermal plume, and a well-mixed compartment model may be appropriate (Furtaw *et al.*, 1996). In such a case the actual mixing may occur quickly once the pollutants are transported into the bulk air of the room.

There are combinations of emission sources and ventilation conditions where the pollutants are inherently not well-mixed, and no use of nested compartments can capture the effect. Some pollutant emissions form microplumes, which meander and create quickly fluctuating zones of high exposure next to zones of low exposure. Known as the proximity effect, it is difficult to estimate occupant exposure when they are subject to these types of pollutant sources (Acevedo-Bolton *et al.*, 2012). There are also ventilation conditions, such as naturally ventilated rooms under thermal stratification, that can cause stable patterns of low and high exposure zones which can be difficult to predict *a priori*, and will shift over time, especially when the pollutants of concern are bioeffluents emitted by the occupants themselves (Mahyuddin *et al.*, 2014). It is possible to recreate these systems in controlled chambers, and the effect on exposure can be significant (Mahyuddin and Awbi, 2010; Suzuki *et al.*, 2007; Rim and Novoselac, 2009).

For systems that experience some periods of unmixed conditions, the exposure significance of the unmixed periods can be estimated by looking at the time frames involved. Mage and Ott (1996) propose a conceptual model to describe the mixing of episodic pollutant emissions using three time periods: t_α is the time when the pollutant source is actively emitting; t_β is when the emission stops, but the pollutant is still not well-mixed; t_γ is time from when the pollutant concentration is uniform until the concentration below measurable quantities from ventilation. For a room in which $t_\gamma \gg (t_\alpha + t_\beta)$ the pollutant concentration is uniform for the majority of the period of exposure, and it is reasonable to model the system using the well-mixed assumption. This conceptual model allows us to find characteristic times for mixing, and understand under what conditions the well-mixed assumption is insufficient.

The mixing time of a chamber is a more practical way to quantify mixing than trying to specifically measure t_β , which requires measuring every point in the room to identify the slowest mixing position. The mixing time for a room is the period of time it takes for the relative standard deviation of a spread of sensors to go below 10% after a pulse release of a pollutant Baughman *et al.* (1994); Drescher *et al.* (1995). There have not been many studies that specifically measure mixing time; Baughman *et al.* (1994) measured the mixing time for an unventilated room under quiescent conditions and with some two different heat sources. Drescher *et al.* (1995) used the same room as Baughman *et al.*, and measured the mixing time as a function of mechanical mixing power from fans oriented to create turbulent mixing. These studies have been the basis for some computational fluid dynamic models (Gadgil *et al.*, 2003). This study seeks to further the experimental work begun by these studies by measuring the mixing time as a function of vertical thermal stratification, and the presence of a heated object.

3.2. Methods

3.2.1. Apparatus

Mixing experiments were conducted in a $1.22\text{ m} \times 1.22\text{ m} \times 1.22\text{ m}$ chamber originally created for a previous study, see Thatcher *et al.* (1996) for construction details. The chamber is roughly 1/3 height scale, which is large enough for air flow characteristics that lead to spatial heterogeneities in normal indoor environments. The front and back walls were insulated to approximately adiabatic condition; the ceiling, floor, and opposing walls were made of aluminum backed with insulation, and are thermally controlled. The temperature control for the surfaces was either an electric heating pad, or tubing for cooling fluid placed against the back of the aluminum panel and insulation on the outside. The floor was chilled by a refrigerated/heating circulator (VWR), and was controlled by a RTD temperature probe attached to the inside of the surface with thermal paste. The air and surface temperatures inside of the chamber were measured by an OctRTD data logger (MadgeTech), which has 8 RTD temperature probes. Four sensors were placed in a vertical line in the center of the chamber at 0.24, 0.49, 0.73, and 0.98 m; the four other sensors were attached to the center of the temperature controlled walls/ceiling/floor with thermal paste. To ensure that the probe placement was representative and that walls heated/cooled homogeneously, a separate logging thermometer (OMEGA Engineering) was used in a 5×5 grid to spot check the surfaces in heating/cooling mode, and the ceiling/floor were measured to have a standard deviation of 1.2 and 1.3 °C, respectively, see Figure A.2.1 in the Appendix.

The tracer gas used in this study was a neutrally buoyant mixture of 37.5% He and 62.5% CO₂ (Praxair Distribution, Inc.). CO₂ was measured in this study using six HOB0 MX-1102 sensors, which had a reported accuracy of ± 50 ppm or 5% of reading, and had a response time of 1 min to 90% of the final reading. The sensors were validated in a series of preliminary tests, which are reported in the Appendix. The sensor response time to a step change in concentration was measured to be 1-2 min to reach 90% of the final reading, see Figure A.2.4. The accuracy of the sensors was measured between 400-3000 ppm by collocating the sensors in a small chamber, and comparing the sensor results to the average of two LI-820 (LI-COR, Inc.), which were recently calibrated. The uncorrected precision of these sensors, here defined as the average deviation of the sensors from the average of the sensors, was 100 ppm + 6.9% of the measurement, see Figure A.2.2. The accuracy of the sensors before correction, found by comparing the average of the MX1102 sensors to the LI-820 sensors, was 5 ppm + 9.2% of the measurement. On each experiment day a correction factor is calculated for each MX-1102 sensor using the LI-820 via the procedure is detailed below. Using the correction procedure in the validation experiments, the precision became 15 ppm + 0.6%, and the accuracy became .5 ppm + 0.03% of the measurement, see Figure A.2.3.

Before each CO₂ injection and after the chamber has become well-mixed, three LI-820 measurements are taken to calculate the daily correction factor for each sensor. The LI-820 sensors did not directly sample from the chamber, instead a 60 cm³ syringe was used to draw air from small tubes that extended into the chamber and were collocated with each of the MX-1102 sensors. This technique was validated by using calibrated syringe samples of 1000 ppm CO₂ gas, and zero gas to flush the LI-820's in between. The measured concentration from the syringe delivery was compared to delivering the 1000 ppm gas through constant flow, see Figure A.2.5. The syringe delivery method was shown to be equivalent to the constant flow method, and a 60 cm³ syringe sample measured at 99.3% of the calibrated concentration. At the end of each day a correction factor for each sensor is calculated by taking a linear regression of the MX-1102 readings to the LI-820 readings. After the sensor readings have been corrected, the measurement concentrations are normalized for comparison between tests.

3.2.2. Experimental procedure

Three sets of experiments were conducted in this study: sensor placement tests to determine optimal CO₂ sensor placement to measure the relative standard deviation; stratification experiments to measure the mixing time as a function of the vertical air temperature gradient; and heated object experiments to measure the effect of additional heat sources on the mixing time in a stratified environment. For each set of conditions, three replicate experiments were performed. The night before a test day the ceiling, floor, and heated object were turned on to achieve steady-state conditions. On the morning of the experiment three syringe samples of air were taken via tubes that extended to each of the CO₂ sensors, and the well-mixed concentration was obtained for the first correction factor point. The first mixing time test was initiated by a burst release of the neutrally buoyant CO₂ tracer gas from a brass tube fitted with a piece of foam to ensure a low-velocity injection that extended from the front wall to the source position, see Figures 3.1 and 3.2. A pump attached to the injection tube was used to quickly flush the tube with air. The burst release designed to release a total displaced volume of 2 liters of gas, and with roughly half of the volume as flushing air. The observed increase in well-mixed CO₂ concentration for 25% of the tests was greater than 520 ppm, and for 75% of the tests was less than 690 ppm. The system was allowed to collect data for an hour before three syringe samples were extracted to ensure that the system had become well-mixed, and obtain the next correction factor point. On each experiment day three tests were conducted without opening the chamber, so the well-mixed concentration at the end of the day was 2200-3100 ppm. After the last test the chamber was opened to allow for ventilation, the data was collected from the MX-1102 sensors, and the system reset for the next day's temperature conditions.

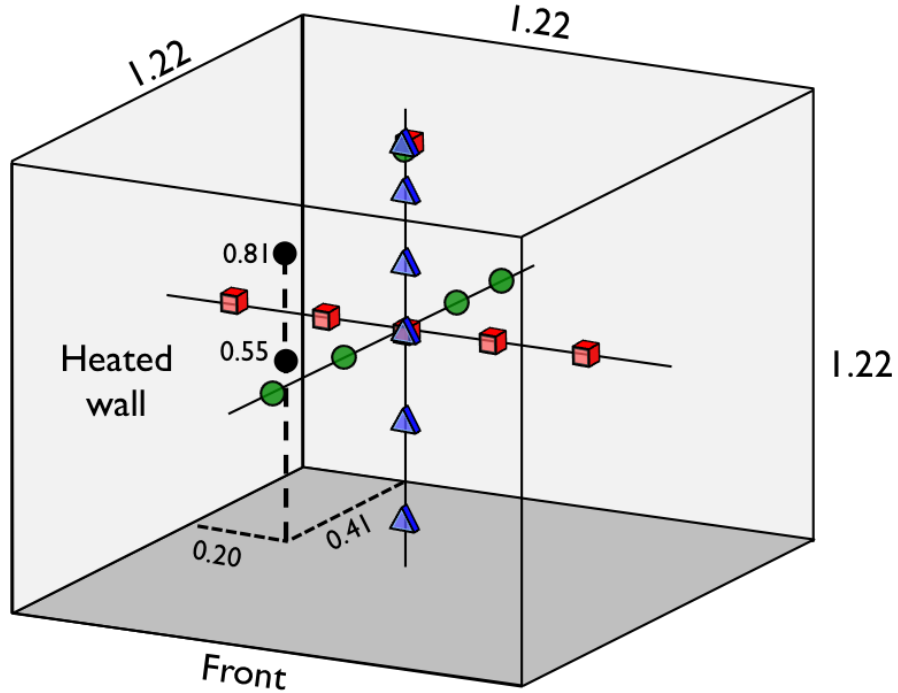


Figure 3.1: Diagram of chamber and sensor position during sensor placement tests, all lengths are given in meters. The red squares, blue triangles and green spheres indicate the sensor placement in tests using left–right, vertical, and front–back orientation. The black circles indicate the upper and lower source positions, and the center and top sensor positions are kept throughout all the tests to ensure similar conditions.

The sensor placement experiments consisted of measuring the mixing time at a stratification of $1.2\text{ }^{\circ}\text{C}/\text{m}$ for six different combinations of sensor and source positions, see Figure 3.1. Two release locations, both off center and corresponding roughly to an equivalent height for a standing or sitting occupant, were tested three times for three different configurations of the six sensors. For all placement tests one sensor was left near the ceiling in the center, and the other five were placed in a line crossing the center; the chamber center being a second consistent position. The results from these tests were used to determine which areas of the chamber were most important to capture the bulk of the spatial variation of tracer concentration. For the stratification and heated object experiments the sensors were placed with an emphasis on vertical spread, a secondary emphasis on having sensors horizontally across from the source, and one sensor was placed closer to the front, see Figure 3.2. There are some additional implications about the role of microplumes during mixing that are addressed in the Results and Discussion.

The stratification and heated object experiments were conducted similarly. The stratifica-

tion experiments consisted of symmetrically changing the ceiling and floor temperature to maintain an average air temperature between 23–25 °C. The stratification level reported in this study is calculated from the air temperature sensor at heights of 0.24 m and 0.98 m. The heated object experiments used the ceiling and floor conditions that were equivalent for 2.4 °C/m stratification. The heated object was either the heated wall, which is close to the source and noted in Figure 3.2, or a 10.2 × 25.4 cm heat sheet curled into a 10.2 cm high cylinder. The heated sheet was placed on a small wooden block 5 cm high to stop conduction to the floor, except for a few tests when it was placed directly on the ground. The temperature gradient in the heated wall/object experiments would not end up being 2.4 °C/m, as the heated object increased the overall temperature of the chamber. The floor chiller used a control loop that maintained the same surface temperature, so the cooling power increased with the presence of the heated object, but the heating element for the ceiling was controlled by maintaining a consistent power output, so the surface temperature increased with the presence of the heated object. This is somewhat analogous to a non-ventilated residence with a basement at a constant temperature and a roof being heated by the sun.

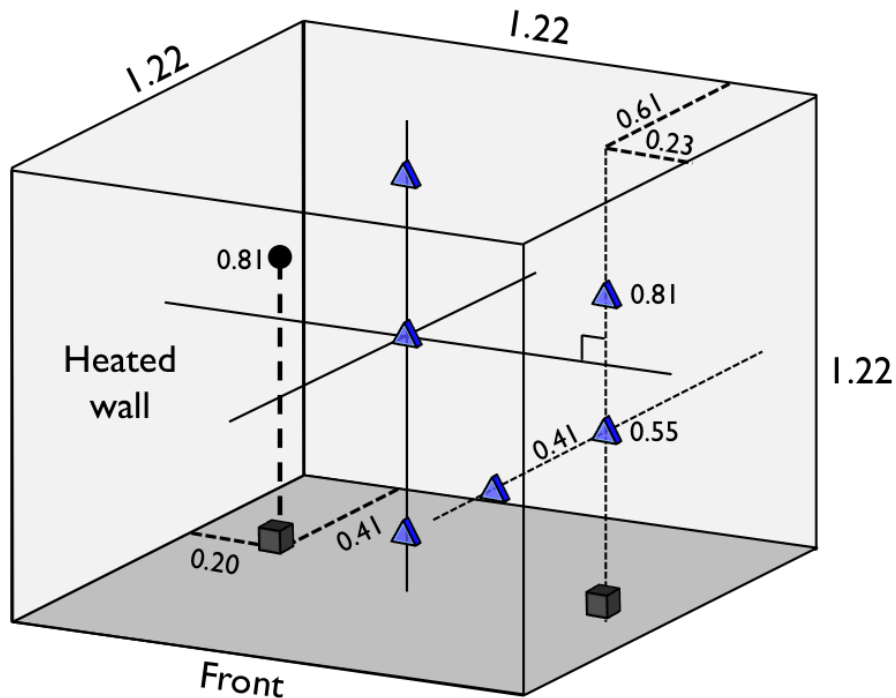


Figure 3.2: Diagram of sensor position during stratification and heated object experiments, all lengths are given in meters. The black circle indicates the source location, the black squares the heated object location, and the blue triangles the sensor locations.

3.3. Results and Discussion

Figure 3.3 shows the mixing time as a function of temperature stratification. There is clearly different behavior when the stratification is near zero, isothermal conditions, than when there is an established thermal gradient, stratified conditions. From 0–0.16 °C/m the mixing time quickly drops from 100 min to 40 min. As the stratified conditions are established and the thermal gradient increases, from 0.16 °C/m to 3 °C/m, the mixing time increases from 38 min to 50 min. The most significant effect shown seems to be the transition from isothermal conditions to stratified conditions, and a correlation of 4.2 min (°C/m) is present.

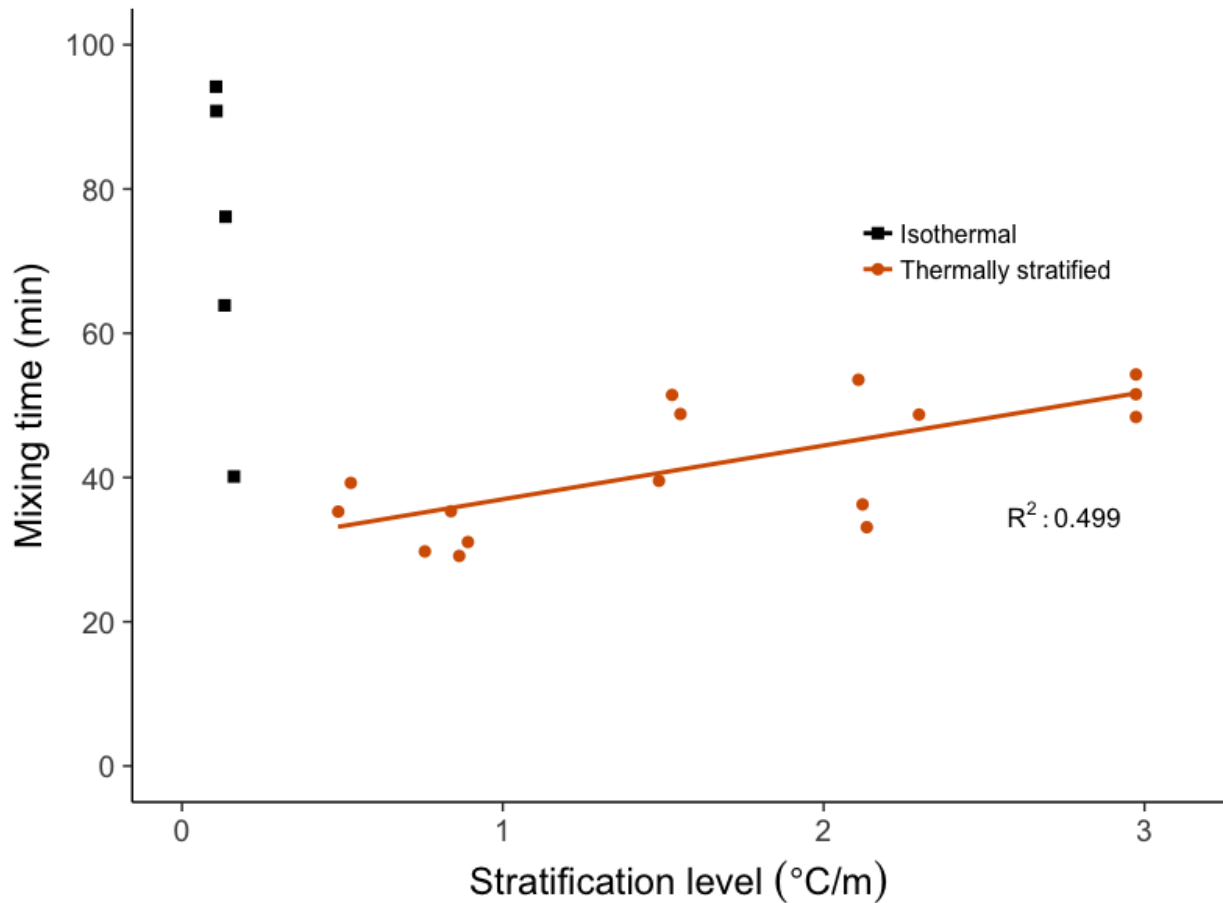


Figure 3.3: Chamber mixing time under various stratification levels for a burst release of CO₂. Temperature gradient is created by symmetrically heating the ceiling and cooling the floor. Mixing time is rounded to the nearest two minutes, and identical results have been shifted slightly for visual differentiation.

The spread of the mixing times may also give insight into the stability of the air motion during these conditions. While the mixing time is monotonically decreasing in the isothermal conditions, all of the heating/cooling was turned off so thermal gradient at those levels is coincidental. The variation in mixing time during isothermal conditions is likely a natural variability arising from changes in initial conditions that are too small to be captured. Once stratification has been established the mixing time is lower, but there is also less variability. The variability in mixing time under isothermal conditions suggests unstable quiescent conditions that can be easily disturbed. The lower variability in mixing time under all stratified conditions indicates stable quiescent conditions, where disturbances are dampened. The main source of air mixing in this system is turbulent diffusion, if molecular diffusion is considered, then the characteristic time for mixing in a volume can be estimated by $L^2 D^{-1}$, where L is the characteristic length for the space, and D is the diffusivity coefficient. For the pollutant front to reach the opposite wall L is 1 m, and at a common diffusivity coefficient of $0.16 \text{ cm}^2 \text{ s}^{-1}$ the characteristic time would be 62500 seconds, or 17 hours.

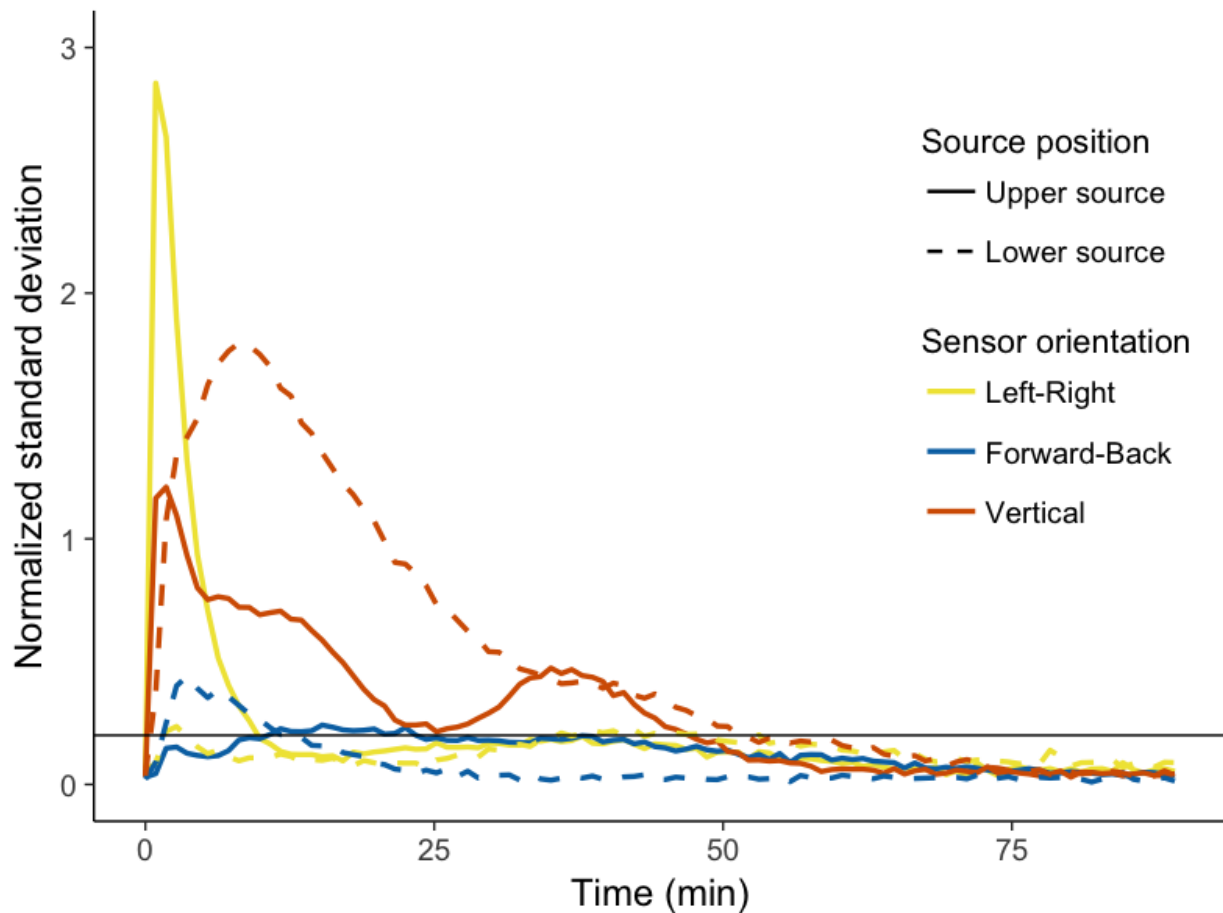


Figure 3.4: Standard deviation of sensors in a line during the placement experiments, at a stratification level of $1.2 \text{ }^\circ\text{C/m}$. The standard deviation was averaged between the 3 replicate tests, the line of sensors was oriented in one of three directions, and the tracer gas released in one of two different source positions, as shown in Figure 3.1.

The isothermal mixing time found in this study can be compared to other pollutant mixing studies, once the difference in mixing time definition (the common 10% threshold used in other studies versus the 20% in this study) and chamber size have been accounted for. Based on the theoretical work by Corrsin (1957), Drescher *et al.* (1995) proposed a relationship between mixing time and forced convection mechanical power for a cubic room:

$$\tau_{mix} \sim \frac{\rho^{1/3} V^{5/9}}{P^{1/3}} \quad (3.1)$$

where ρ is the density of the air, V is the volume of the room, and P is the mechanical mixing power. Scaling the quiescent mixing time of 35 minutes found in Drescher *et al.* (1995), and 80 minutes found in Baughman *et al.* (1994), to the volume of the chamber in this study, the equivalent 10% threshold mixing times would be 170 and 390 minutes, respectively. The equivalent quiescent mixing time in this study, 40-100 minutes, is between a factor of 2 to an order of magnitude faster, and is likely due to the higher threshold that had to be used due to sensor accuracy in this study. An additional difference in this study was the relative volume of the tracer gas to the chamber. In this study 2 l of gas were released, Baughman *et al.* (1994) used SF₆ so the release volume was on the order of milliliters, and Drescher *et al.* (1995) released 1.5 liters of CO mixture. The tracer gas pulse in this study represents a little more than 0.1 % of the total chamber volume, which is 20 times larger than in Drescher *et al.* (1995), and 3 orders of magnitude larger than in Baughman *et al.* (1994). Even a small differences like that in the tracer gas release may cause significant air mixing under quiescent conditions if the conditions are unstable.

The sensor placement tests can provide insight into the dominant motion of the pollutant microplume under increasing stratification. Figure 3.4 shows the standard deviation of the sensors placed in a straight line in three orientations during the sensor placement tests, which were done at a stratification level of 1.2 °C/m. The standard deviation of the sensors is a proxy for how much horizontal variation occurs along each axis, and was primarily used to determine where sensors should be positioned to characterized the chamber. The vertical axis is clearly the most significant dimension, and is indicative that the tracer gas is not exactly neutrally buoyant, so it must have a temperature difference to the rest of the air. It can be deduced that the tracer gas is negatively buoyant, as the left-right line for the upper source shows a strong initial peak from the microplume crossing the center plane, and the lower source line has no such peak. As the stratification level increases, the mean air temperature remains the same, so the negative buoyancy of the tracer gas should be the same in all cases. Since the mixing time increases with increasing stratification, this indicates that the thermal stratification does dampen air motion, and supports the idea that the mixing process is more stable under stratification.

In real-world scenarios the stability of the mixing may be more indicative of how well-mixed the space becomes than the actual mixing time measured in this study. An isothermal condition that behaves similarly to those in this experiment may act as a well-mixed space

when there are even small disturbances, such as being occupied. The 38–50 minute mixing times of the stratified conditions may be more stable, and the observations made in this lab study may be representative of real-world conditions. The higher stability of the stratified conditions that lead to slow mixing may also lead the mixing conditions to be more resilient to small disturbances that occur with occupancy. For emission sources that are also associated with heat sources, like cooking or other sources of combustion, there will be additional effects on the mixing conditions from the thermal plume of the heat sources.

The heated object and heated wall experiments, see Figure 3.5, showed that the addition of a heated object drastically decreased the mixing time of the chamber. Using the relationship in Equation 3.1, assuming the heating power is linearly correlated with mechanical mixing power, and that the chamber is half-height, a 20 W heated object is roughly representative of a single occupant. Due to the sensor responsiveness, mixing times below 10 minutes are assumed to represent well-mixed conditions. All of the heated object tests at 28 W, and most of the source-located 10 W heated object tests show a nearly well-mixed system. Given the limitations of scaling the results of a chamber study to a full-scale system, these results show the general concept that the addition of heated objects to thermally stratified, non-ventilated system have a drastic effect to reduce the overall mixing time. These experiments were also done at steady state conditions, and given that it can take hours to achieve steady state, it is reasonable to assume that most occupied spaces are to some degree in a state of transition.

Figure 3.5 also shows that the reduction in mixing time is smaller when a wall is heated, as opposed to a free-standing object. Additionally there is some effect due to the position of the heated object, but it is less significant than the effect seen for the heated wall versus the object. Gadgil *et al.* (2003) support the that the mixing time has a larger dependence on the air motion within the room than on source position, so it is reasonable that the amount of air flow from the thermal plume is more significant than the exact flow pattern. In real scenarios these results highlight the fact that the occupancy of a room has a significant effect on the pollutant dispersal, and that the occupant activity does not need to always be accounted for.

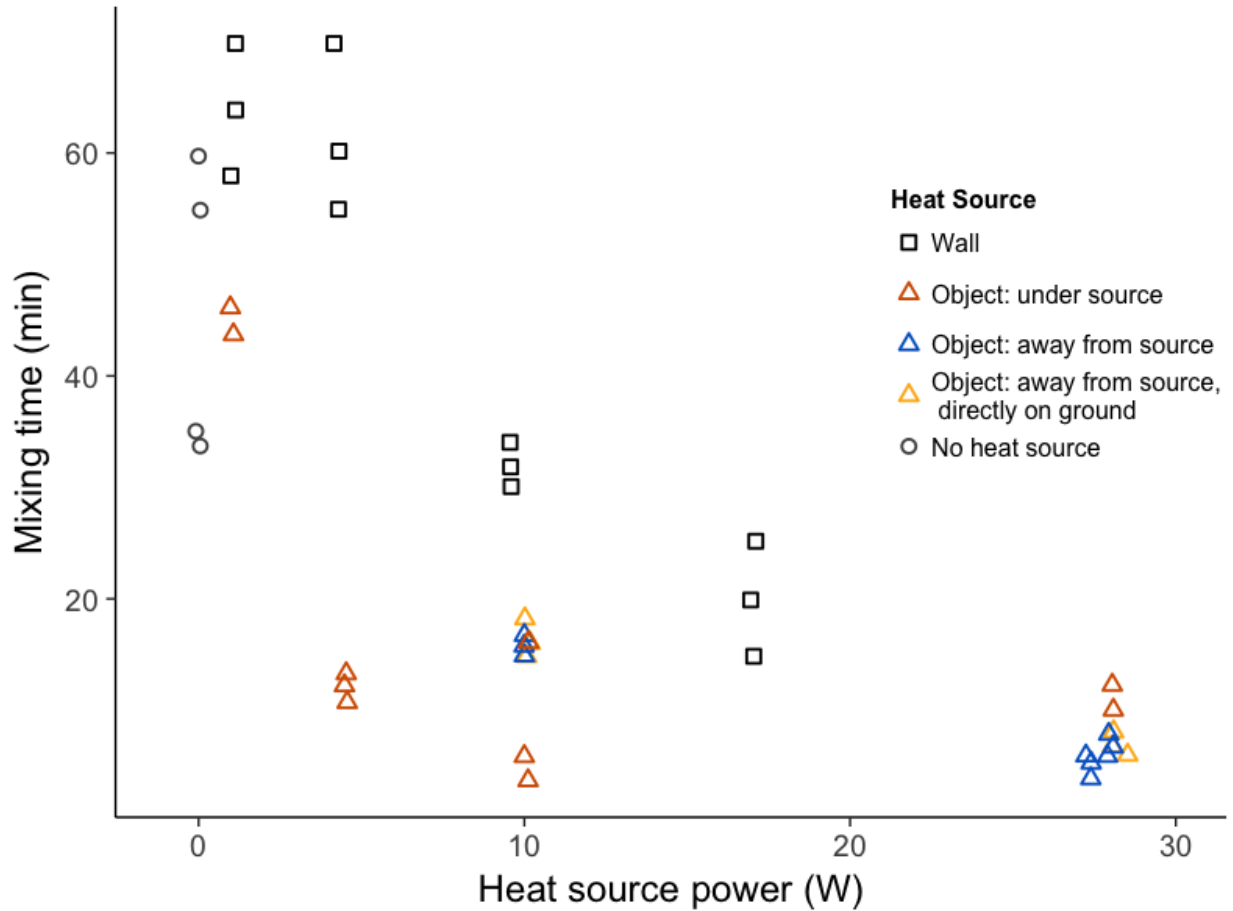


Figure 3.5: Mixing time under ceiling-floor conditions equivalent $2.4\text{ }^{\circ}\text{C} / \text{m}$ stratification. The zero power conditions are those presented in the stratification only figure, the heated wall entries have the wall closest to the source heated at various powers, and the heated object refers to a heat pad curled into a cylinder. The heated object was placed on a wooden block underneath the CO_2 source, on the opposite side of the chamber to the CO_2 source, and on the opposite side of the chamber while not using the wooden block.

3.4. Conclusion

The results of the experiments performed in this study suggest that mixing in quiescent rooms that are either isothermal or have a high thermal stratification is significantly slower than mixing at low thermal stratification. Isothermal conditions may have a longer mixing time than stratified conditions. Once stratification has been achieved, increasing the level of stratification increases the mixing time, due to a dampening effect on air motion. The effect on the mixing time from small disturbances is more significant in isothermal conditions than

in stratified conditions, indicating that the results from this study may be more representative of real rooms with thermally stratified conditions, as a real room under isothermal conditions is likely to have some small sources of disturbances. The increased mixing effect from stratification is also highly affected by the presence of additional heat sources, free-standing objects more so than a heated wall. This study also illustrates the importance of occupancy to mixing, and suggests that mixing results in an unoccupied room may be significantly different than the mixing conditions in an occupied space.

Researchers that are studying isothermal spaces that are occupied and utilize the well-mixed assumption are supported by the results of this study. Studies that take place in quiescent, isothermal spaces and in thermally stratified spaces are encouraged to be cautious about using the well-mixed assumption in such a space. For such spaces, if the mixing time is similar to or greater than either the air exchange rate or the time that occupants are exposed, then the well-mixed assumption may not be valid. Researcher can mitigate for a potentially unmixed space by either careful placement of sensors in specific locations that they show to be representative of the desired value. For instance, in a thermally stratified space with mechanical ventilation where a researcher wishes to quantify the total emission of a non-reactive pollutant from a short-term source, placing the sensor near the return grille and integrating the pollutant flux until the concentration goes to zero will provide a good estimation of the total emission regardless of how well-mixed the pollutant is in the space. Researchers should be aware of what types of spaces potentially are not well-mixed, and take it into account either in their study procedure.

Chapter 4

Optimal Placement of CO₂ Sensors for a Displacement Ventilation System

4.1. Introduction

CO₂ based demand controlled displacement ventilation (DCDV) is a desirable ventilation strategy for optimizing energy savings while maintaining acceptable IAQ (Emmerich and Persily, 2001; Chenari *et al.*, 2016; Schäfer *et al.*, 2013). CO₂ demand control ventilation refers to a system by which the ventilation rate is controlled based on the current occupancy indirectly determined by CO₂ concentration. Using CO₂ concentration as a control condition has the benefits of being related to IAQ (Persily, 1997), and is a proxy for both the number and the activity level of the occupants. CO₂ demand control has also been shown to have significant benefits: up to 34% energy savings in some studies (Lu *et al.*, 2011); and reduced headaches, tiredness, and improved IAQ (Norbäck *et al.*, 2013). ASHRAE standard 62.1-2010 ASHRAE (2016b) indicates the CO₂ demand control systems should use a setpoint of around 700 ppm higher than ambient levels, and the approach put forth in the standard has been shown to produce an energy savings (Ng *et al.*, 2011). In real demand control situations there may be issues with CO₂ sensors that are not sufficiently accurate due to lack of calibration or shifting during time (Fisk *et al.*, 2010). These demand control systems also need to be able to deal with the delay between changes in occupancy and changes in

CO₂ concentration, which is a subject of current research (Cali *et al.*, 2015; Jin *et al.*, 2015; Weekly *et al.*, 2015).

Displacement ventilation (DV) systems are designed to provide fresh air to occupants more efficiently than a mixing ventilation system (Stymne *et al.*, 1991). In a DV system cold, fresh air is supplied near the ground level at a low velocity so that it creates a layer that covers the floor, is drawn up to occupants' breathing zone by their thermal plume and has a lower level of concentrations associated with heat sources than air at the same height in the center of the room (Chenari *et al.*, 2016; Brohus and Nielsen, 1996). Exhalations and bioeffluents from the occupants are in part entrained by the thermal plume and transported towards the ceiling exhaust, though movement can reduce this effect (Bjørn and Nielsen, 2002) and breaths from one occupant can penetrate another's thermal plume (Olmedo *et al.*, 2012). These systems intentionally create a vertical thermal and pollutant concentration gradient in the room, which can be challenging to model accurately (Xing *et al.*, 2001), especially for transient conditions (Yang *et al.*, 2014). Originally DV systems were conceptually modeled as a lower transition zone where temperature and pollutant concentration linearly increase until a neutral height is reached, and then an upper well-mixed zone above that (Mundt, 1994). The neutral height is defined as the height at which the net airflow through the thermal plumes is equal to the room ventilation rate, though calculating this height is not straightforward (Xing and Awbi, 2002). A more nuanced 3-zone model predicts a lower clean zone where air from the breathing zone is entrained, a transition zone of larger error around 0.6–1.2m (Xu *et al.*, 2001), and an upper-well mixed zone that still has the neutral height as the lower boundary (Mateus and da Graça, 2015).

The variability of CO₂ concentration within a space ventilated by a DV system, especially the larger error found within the transition zone (Xu *et al.*, 2001), has implications on the effectiveness of a combined DCDV system where the CO₂ sensors are placed at the breathing height. Combined DCDV systems have been shown to be mutually beneficial in reducing energy use and supplying fresh air to occupant breathing zones (Wachenfeldt *et al.*, 2007; Schäfer *et al.*, 2013). There are no specific guidelines in current ASHRAE standards for DC in specifically DV systems (ASHRAE, 2016b), though it is noted that typical CO₂ DC placement is at the breathing zone height (page 151, **Indoor Concentration** section). In this study we explore how much horizontal variability there exists in CO₂ concentration for a full sized chamber with heated manikins that have a constant release of pure CO₂ from the breathing zone, after the entire system has been allowed to reach steady state conditions. Since it has been noted that even in mixed ventilation rooms with occupants there are fast fluctuations as large as 200 ppm (Fisk *et al.*, 2010), it is hypothesized that wall-mounted CO₂ DC sensors at breathing level, typically 1.0-1.8 m, will experience large error that is inherent to their placement. We will explore if placing the sensors near the return grille will give more predictable results, as this placement has been suggested for DC mixed ventilation systems (Fisk *et al.*, 2010).

4.2. Methods

4.2.1. Experimental setup

All tests were performed in a 4.27 m x 4.27 m x 3.0 m chamber at Price Industries in Winnipeg, Canada. Figure 4.1 has the details of the chamber setup, sensor locations, and power usage of the all the heat sources. The chamber is well-sealed and insulated: it was constructed with insulation on the inner wall, then a water-based radiant panel attached to the insulation, an air void, and an insulated outer wall. All of the radiant panels to control the wall temperatures were left off, so the chamber was nearly adiabatic. The ventilation system was single pass provided from a supply room with an outdoor access door to a 121.5 cm × 33 cm × 61.5 cm tall, low face velocity diffuser (Price DF1 48×24×13 model with 10" inlet) placed on the ground, in the corner of the room (see Figure 3.2 for orientation). The indoor door to the supply room was left closed so that some air from the rest of the laboratory was present, but not enough to cause changes in supply air CO₂ concentration. Air was exhausted from the chamber through a return grille made up of 4 holes of diameter 6.35 cm cut over the door into a plenum between the radiant wall panels and the outer insulation. An exhaust fan ensured that the chamber stayed at neutral or a slight over-pressure, the chamber was never at negative pressure, and always less than 30 Pa difference.

All of the heat sources within the chamber had their power usage measured during testing, see Appendix A.3.1. All of the sensors and instruments used 13 W, and the only other heat sources were the manikins, computer setups, and lights. Lighting was provided by 4 linear fluorescent fixtures for a total power of 190 W. Five heated manikins, four at 85 W and one at 65 W, were positioned around the room seated at desks, with head heights ranging from 1.25 to 1.4 m and an average of 1.34 m from the floor. A desktop computer was placed in front of each manikin with both the computer tower and monitor placed on top of the table. All of the computers were set to remain active, and the power output of the computer and monitor setup ranged from 60 W to 134 W. The total heat load for the 1, 3, and 5 manikin conditions were, respectively, 1076, 765, and 422 W. The load per unit area for the 1, 3, and 5 manikin conditions were, respectively, 59, 42, and 23 W/m². The manikin and computer setups not currently being used were left in place. The climatic chamber meets the requirements stated in DIN EN 14240-2004 (CEN, 2004).

The CO₂ flow rate from each manikin was determined to be 7.5 m³/s (0.45 lpm) via chamber mass balance in each test, and confirmed with water displacement tests. This CO₂ release rate was roughly 1.5× higher than would normally be found in a normal office environment, and corresponds to about 2 MET (metabolic equivalent of task) in males (Persily and Jonge, 2017). The higher release rate was used due to equipment considerations, but was not

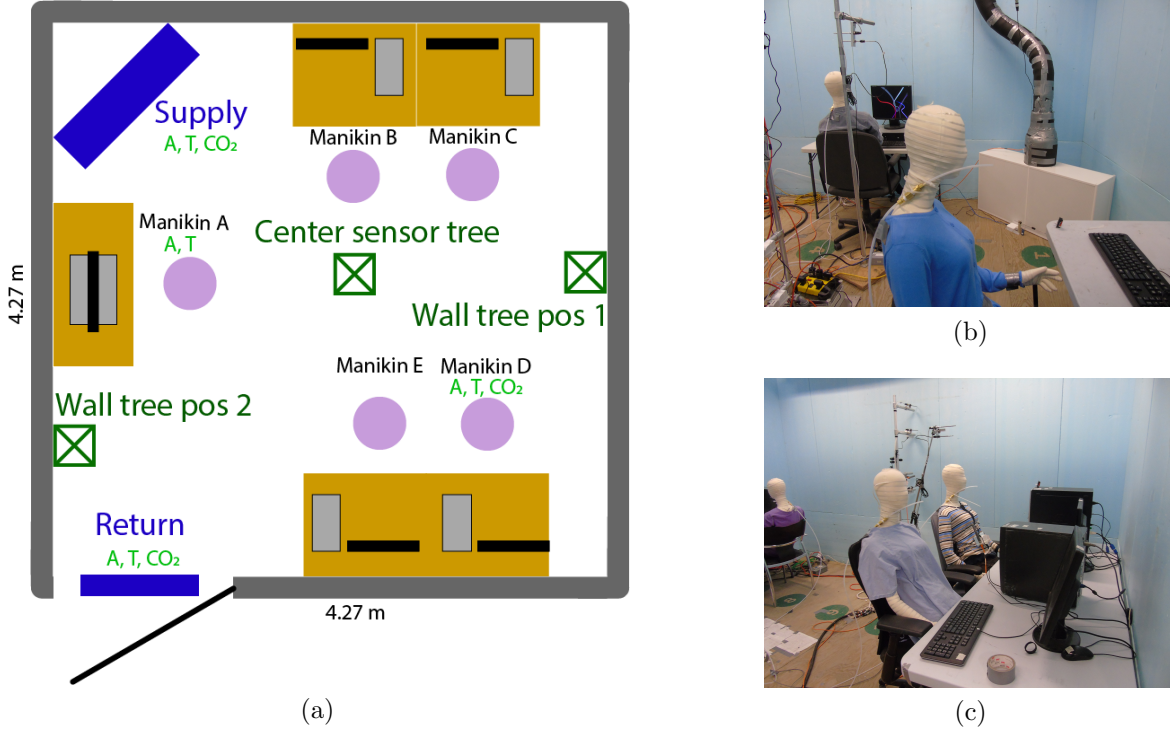


Figure 4.1: (a) Diagram of experimental chamber at Price Industries along with power consumption and sensor placement. Green indicates sensors (A: air velocity sensor, T: temperature sensor, CO₂: CO₂ sensor), lavender indicates manikins, blue indicates ventilation supply and return, brown indicates tables, black indicate monitors, and grey indicates computer towers. (b) Picture of Manikin A, B, the diffuser and the center sensor tree. (c) Picture of Manikin C, D, E, and the wall sensor tree in position 1.

considered problematic as it was within a reasonable range and the results were normalized. The manikins were non-breathing, and CO₂ was released continuously from a tube extending 10 cm in front and slightly below the nose of each manikin. Pure CO₂ was delivered to the manikins via common manifold, the flow rate was controlled by adjusting the line pressure and placing a 0.10 mm (0.004 inch) critical orifice (O’Keefe Controls) at the end of tube. The water displacement tests consisted of attaching balloons to the end of each line, allowing the balloons to fill for 10 minutes, measuring the volume of each of the balloons using water displacement, and using that to calculate the CO₂ flow rate from each manikin line. For two manikins, Manikin A & D, an air velocity sensor was placed 0.2 m above its head, and a temperature sensor was placed 0.25 m above its head.

A stationary sensor tree in the center of the room had temperature sensors at heights of 0.1, 0.3, 0.6, 1.1, 1.4, 1.7, 2.2, 2.6 m; and CO₂ sensors at heights of 0.3, 0.6, 1.1, 1.7, 2.2, 2.6 m. A wall tree positioned at either wall tree pos 1 or wall tree pos 2 (see Figure 3.2), had temperature sensors at heights of 0.1, 0.25, 0.6, 1.1, 1.7, 1.9, m; and CO₂ sensors at

0.6, 1.1, and 1.7 m from the ground. Supply air temperature was measured within the duct immediately before the diffuser, while a velocity sensor, and CO₂ sensor were co-located directly in front of the supply diffuser, 0.1 m off of the ground. Exhaust air temperature was measured both in front of the exhaust ports, with a co-located CO₂ sensor, and in the plenum, though the difference was never more than 0.001 °C apart. All temperature probes were RTD 1/10 DIN Accuracy Class, with an expanded uncertainty of 0.1 K and were calibrated just before the experiment began. The velocity probes, hot sphere anemometers (TSI 8475) were calibrated just before the experiments, and have an accuracy of 3% of reading + 1% of full scale (0.05- 2.5 m/s). The CO₂ sensors were from leased from Senseware in 2017, and had a reported accuracy of 25 ppm ± 3% of the reading.

4.2.2. Experimental procedure

The night before a test the thermal manikins, desktop computers, lights, and ventilation conditions were set and the chamber allowed to reach thermal steady state. The next morning the CO₂ emission was initiated, and the chamber allowed to reach steady state CO₂ concentration conditions. Steady state conditions were determined to have been reached when all of the CO₂ sensors readings were stable for at least an hour, determined when the 30 minute CO₂ concentration average and the previous 30 minute average were within twice the instrument's uncertainty, roughly 50 ppm. Once steady state has been reached, an hour of data was collected. All of the experiments had two data collection runs with the exception of Day 1. After the first experiment was completed, a researcher briefly entered the chamber, and moved the wall tree to the second position. The adjustment took less than 1 minute, and care was taken not to open the door wide. The chamber was left to return to steady state, defined as above, and the second data collection run was performed. Table 4.1 below contains the conditions for all of the experiments, including the label, stratification level, number of manikins used, supply air flow rate, and which day the experiment was performed. The supply air temperature was 18 °C for all conditions. The average stratification level for the 'High' conditions is 6.9 °C/m, and the average stratification level for the 'Medium' condition is 4.1 °C/m. Table A.3.2 in the Appendix further lists all of the conditions for each individual data collection run.

For each data collection run the time-series data was averaged, and the CO₂ sensors the average supply concentration was subtracted from the average sensor concentration to obtain the increase in CO₂ concentration, which is used in the rest of this study. The standard deviation of the time-series data was compared to the reported accuracy of each sensor, and as they were comparable the sensor accuracy used in the uncertainty analysis was the standard deviation. The uncertainty from the supply sensor was propagated by adding in quadrature the standard deviation of the supply sensor and the other target sensor. For each experimental condition that had two data collection runs the co-located sensors were

Table 4.1: Experimental conditions and labels

Day	Label	Stratification level [T(1.1m) - T(0.1m)] (°C / m)	Stratification label	Number of manikins	Supply air flow (l/s)	Air exchange rate (hr ⁻¹)
1	5Ha	7.21	High	5	101	6.6
2	5Hb	7.26	High	5	101	6.6
3	3Ha	7.03	High	3	63	4.1
4	3M	3.78	Med	3	123	8.1
5	1M	4.68	Med	1	38	2.5
6	5M	3.78	Med	5	172	11.3
7	3Hb	6.25	High	5	62	4.1

Supply temperature was 18 °C for all conditions

averaged together, and that average is used as the steady state measurement. Since the two data collection runs are done under near identical conditions, the uncertainty of each measurement is reduced: the standard deviations of the two measurements were added in quadrature and the result divided by two. The only sensors that were not co-located in the two data collection runs were those on the wall sensor tree.

The co-located measurements between the first and second data collection run on any given day were nearly identical. The maximum difference in temperature readings for any of the co-located sensors was 0.3 °C, and the average difference 0.1 °C. The maximum difference in CO₂ concentration measurements between any of the colocated sensors was 20 ppm, and the mean difference was 5 ppm. Two conditions were repeated on different days to test the reproducibility of the system. The 5 occupant, high stratification condition, and 3 occupant, high stratification condition experiments were conducted twice, though the 5 occupant condition on Day 1 had only one data collection run. In the 3 occupant case, the difference between temperature measurements on the two days had a maximum variation of 1.49 °C, and a mean variation of 0.65 °C; the difference between CO₂ measurements had a max of 36.7 ppm, and an average difference of 17.2 ppm. In the 5 occupant cases, the difference between temperature measurement between each day had a maximum variation of 1.18 °C, and a mean variation of 0.21 °C; the difference between CO₂ measurements had a max of 39.8 ppm, and an average difference of 20.6 ppm. The uncertainty of the CO₂ measurements for all sensor positions, after the treatment described above, was no more than 37.7 ppm, and the uncertainty in temperature was no more than 0.377 °C. The difference in measurements between tests runs performed within one experiment on the same day, and test runs performed in repeat experiments on separate days was comparable to the measured uncertainty of the sensors themselves.

4.3. Results and Discussion

The CO₂ profiles for all the conditions, see Table 4.1 for details, show significant horizontal spatial variability within occupant breathing heights, where CO₂ demand control sensors are typically placed. Figure 4.2 show the increase in CO₂ above supply concentration for several vertical profiles, for all experimental conditions. The average increase in CO₂ concentration from the supply to the return is 388 ppm for the high stratification conditions, and 204 ppm for the medium stratification conditions. All of the concentration increase profiles have three distinct zones: a base zone below 1.1 m that is nearly at supply concentration levels; a transition zone from 1.1 m to 1.7 m where the concentration rapidly increases; and a top layer above 1.7 m where the concentration is nearly at return concentration levels. This is similar to some models of bioeffluent pollutant concentrations in a displacement ventilation system (Mateus and da Graça, 2015). The existence of a well-mixed top layer is clearly visible, though the neutral height and the thickness of the transition zone cannot be estimated from the CO₂ concentration measurements, as both the vertical density of sensors is too thin for reasonable resolution, and because the horizontal variability makes defining a single neutral height from pollutant concentration ambiguous.

In contrast with the CO₂ vertical profiles, the vertical temperature profiles do not have significant horizontal variability. Figure 4.3 has the vertical dimensionless temperature profiles for all of the tests, the profiles of the temperatures is located in the Appendix, A.3.1. The temperature measurements closest to the ground, 0.1 m, show significant horizontal variability, but none of the sensors at the other heights do. The temperature above the heads of manikin D has a slight temperature elevation, but that is to be expected while in the occupant thermal plume. Otherwise all of the temperature measurements follow the same vertical profile. The variation near the ground is expected by the idealized displacement ventilation models. The supply air spreads horizontally across the ground in a thin, well-mixed layer, and the temperature is expected to increase to half of the total increase between return and supply air in the room. Above the thin ground layer, the temperature is expected to linearly increase until the neutral height is reached, and then to be constant in the top well-mixed layer. Previous experiments (Mundt, 1994; Brohus and Nielsen, 1996) using furniture and manikin heat sources tend to show a sharper transition than experiments using cylindrical or ground level heat sources. The neutral height is clearly visible in the profiles, but there is not a sharp transition. In the high stratification conditions the transition occurs somewhere between the 1.1, 1.4, and 1.7 m sensors. In the medium stratification conditions the neutral height is slightly higher, somewhere between the 1.4, 1.7 and 1.9 m sensors. The higher neutral height is to be expected in the lower stratification conditions, as there is more ventilation air per watt of total heat source.

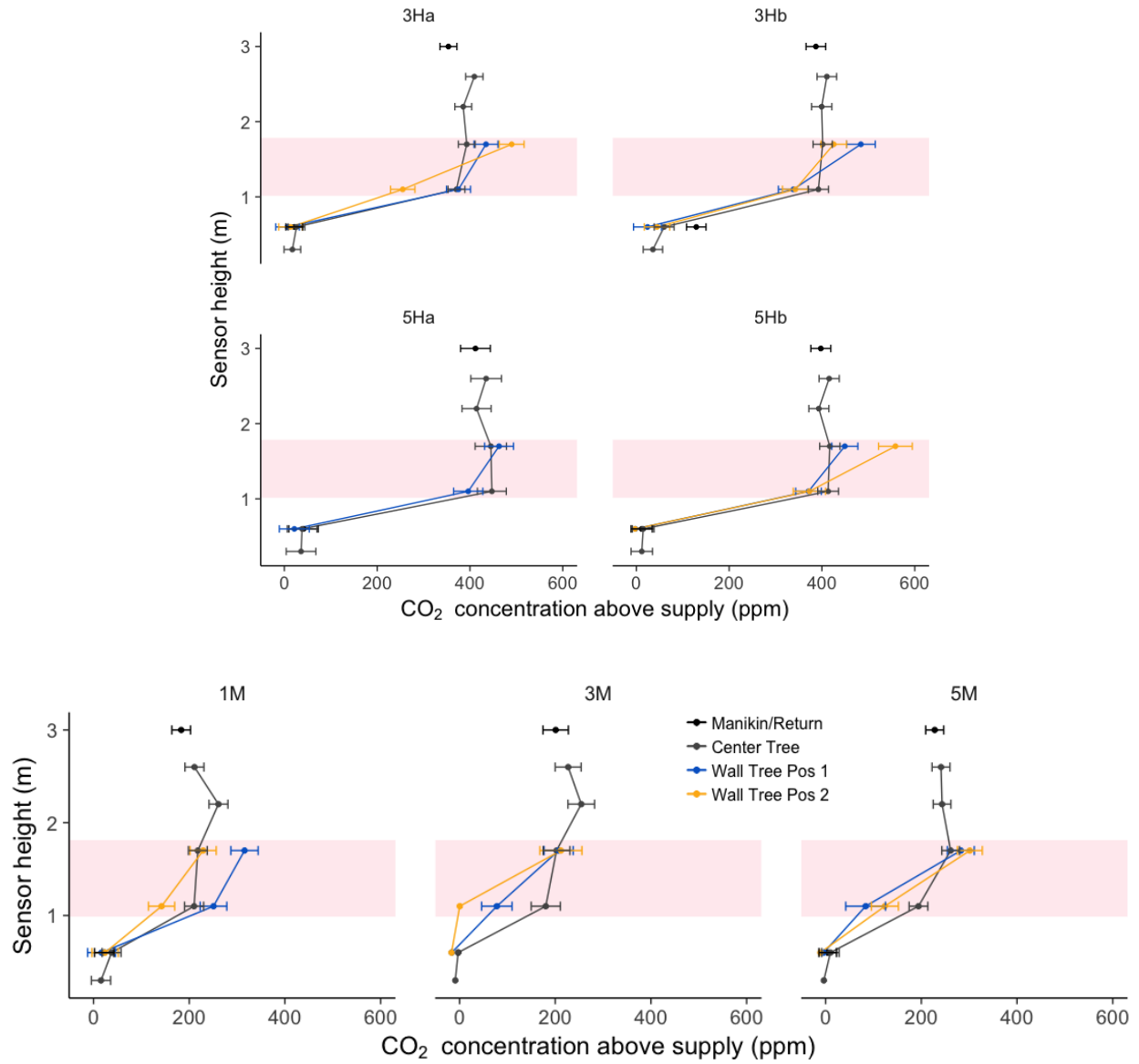


Figure 4.2: CO₂ concentration profiles for 3 occupant (top) and 5 occupant (middle) high stratification conditions, and all medium stratification conditions (bottom). Shaded region represents typical breathing heights for seated and standing occupants, 0.8–1.8 m.

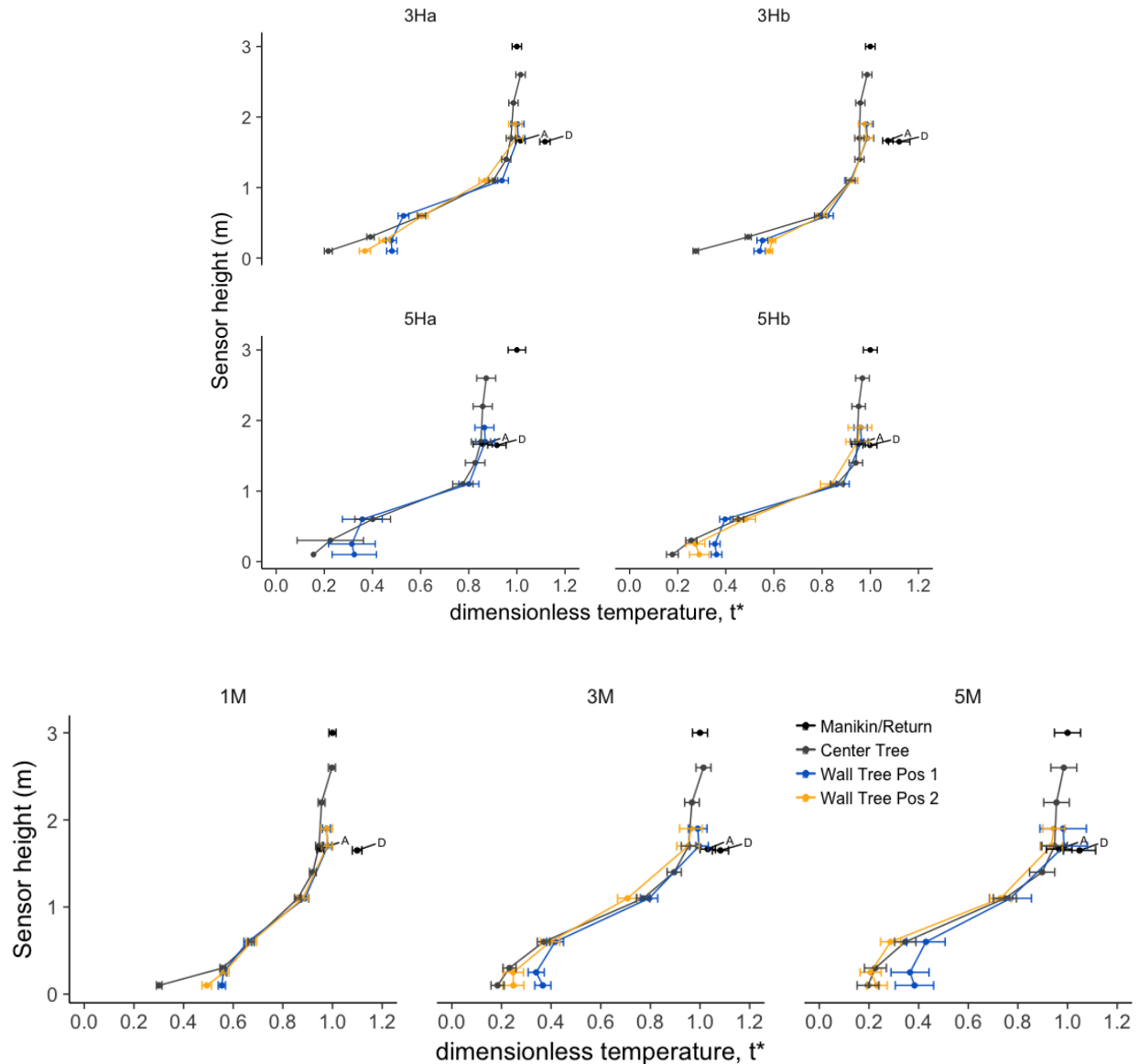


Figure 4.3: Vertical dimensionless temperature profiles for 3 occupant (top) and 5 occupant (middle) high stratification conditions, and all medium stratification conditions (bottom). 'A' and 'D' represent the temperature measurements 25 cm above the labeled manikin's head.

Across all tests the difference between the wall sensor measurements and the center tree sensor measurements at 1.1 m and 1.7 m was greater on average than at 0.6 m by, respectively, a factor of 4.0 and 2.7, suggesting that CO₂ concentration is less horizontally homogeneous at the breathing height than below it. Table 4.2 summarizes the difference between wall and center CO₂ and temperature measurements by height, Figure 4.4 visually shows the

comparison between wall sensor and center sensor measurements. All of the temperature measurements had less than 0.5 °C difference between wall and ambient temperature measurements, suggesting that overall horizontal variability is also less than 0.5 °C. Between 1.1 m and 1.7 m, the observed variability in CO₂ rise is similar in magnitude for all tests. Wall CO₂ sensor readings are typically lower than center room readings at 1.1 m, while typically higher than center room readings by a similar amount at 1.7 m. There is no trend based on number of occupants, but there is a significant difference at those two heights between the medium and high stratification conditions. During the high stratification conditions the average wall to center concentration difference is roughly 50 ppm, and is the same at 1.1 m and at 1.7 m. Under medium stratification conditions the average difference at 1.1 m is 95 ppm, and the average difference at 1.7 m is only a third of that, 31 ppm. Compared to the CO₂ concentration difference between the supply and return, 200-400 ppm, a 50 to 150 ppm variation represents a significant possible misrepresentation of room conditions. Only the center tree and the return grille had CO₂ sensors located above 1.7 m, however it is reasonable to assume that the concentration at the walls will be at equivalent concentrations.

The relative horizontal homogeneity in the vertical temperature profile versus the CO₂ profile suggests that horizontal thermal transport is faster than horizontal mass transport. Since the CO₂ is generated within the thermal plume of an occupant, the gas is transported vertically to the upper well-mixed layer by convection, and is transported horizontally predominantly through turbulent diffusion. Heat generated by the occupants that warms the air surrounding their body also is transported vertically by convection, and horizontally predominantly by turbulent diffusivity. Note that a significant portion of the heat generated by the occupants does not directly heat the surrounding air, and is transported instead by radiation to surrounding surfaces. The turbulent diffusivity for mass and heat can be quantified by the eddy mass diffusivity, and the eddy thermal diffusivity, respectively. In indoor environments there are only a few studies that directly measure the eddy mass diffusivity coefficient, (Cheng *et al.*, 2011; Shao *et al.*, 2017), and none for the eddy thermal diffusivity coefficient; both of those coefficients can be found using certain CFD models. The turbulent Lewis number is the ratio of the eddy thermal diffusivity to the mass diffusivity, $Le_t = \frac{\alpha_t}{D_t}$, where α_t is the eddy thermal diffusivity coefficient, and D_t is the eddy mass diffusivity coefficient. These results suggest that for a thermally stratified system, the turbulent Lewis number is greater than 1, which would result in a less horizontal variability in temperature than in pollutant concentration.

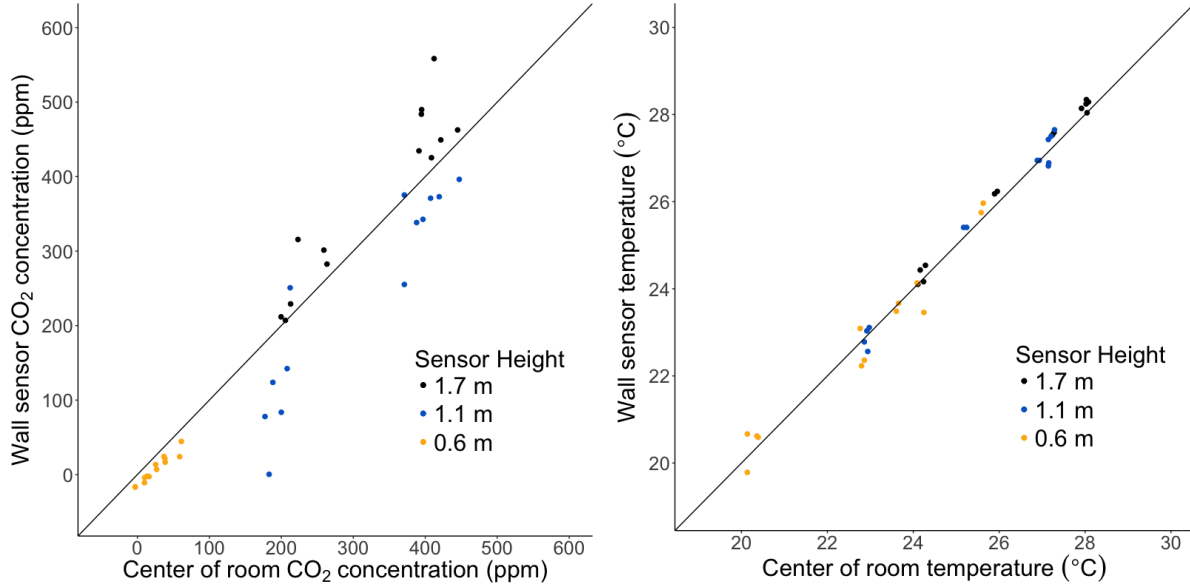


Figure 4.4: Difference between wall sensor measurements center of room sensor measurements at the same height within the same data collection run. The reference line is 1:1.

The stratification levels in this study are much larger than those suggested by ASHRAE standards, which specify there should be less than 3 °C temperature difference between seated head level (1.1 m), and ankle level (0.1 m), or 4 °C temperature difference between standing head (1.7 m) and ankle height (0.1 m) in an office environment (ASHRAE, 2016a). The stratifications levels used in this study, by that definition, are all above what is prescribed. The high levels of stratification were a consequence of restricting ventilation flow rate so that ventilation conditions were restricted by CO₂ concentration. Supplying air at a temperature less than 18 °C would be abnormally cold, and creating conditions with a smaller stratification level would require supplying a higher ventilation rate, and decrease return CO₂ concentration. The current return CO₂ concentration in this study for the high stratification conditions is similar to those found in the example designs in the ASHRAE (2016b) appendix on displacement ventilation. In the high stratification conditions the return temperature is near 28 °C, and in the medium stratification conditions it is near 25 °C. Using the 50 % rule commonly found in ideal displacement models, half of the temperature gain should occur at the ground, between the temperature found at the diffuser, and that found at the ankles (0.1 m). The 50 % rule would imply that 0.1 m temperature measurements should be at 23 °C, and 21.5 °C, respectively. There is nearly 1 °C discrepancy, which would change the stratification level of the medium stratification condition to about 3 °C per m. However, even at these high levels, temperature gradients are not necessarily uncomfortable. Studies identifying the relative importance to thermal comfort of difference displacement ventilation characteristics have shown that temperature gradient has almost no effect on thermal comfort, even up until stratification levels of 8 °C between ankles (0.1 m) and head (1.1 m) (Liu *et al.*, 2017).

At lower levels of stratification than those found in this study, we expect that there is less horizontal variability in CO₂ concentration. As supply air flow increases to virtually eliminate thermal stratification, it is reasonable to expect that the room acts as if it has mixing ventilation instead of displacement ventilation, and the horizontal variability effect observed in this study should disappear as well. While there is still a thermal stratification, the neutral height will increase with decreasing stratification. This can be seen in Figure 4.2 in the center room CO₂ concentration at 1.1 m for both the 3 and 5 manikin conditions. For example, at 1.1 m, the increase in CO₂ concentration over the supply for the 3 manikin case is 180 ppm at 3.8 °C/m, and 380 at 7 °C / m. Since the neutral height represents that start of the upper well-mixed layer that has high CO₂ concentration, a higher neutral height will decrease the potential of gas from the highly concentrated layer mixing into the breathing height air. Additionally at and below the breathing height exhaled CO₂ will experience a buoyancy force that is proportional to the temperature difference between the exhaled breathe, and the surrounding air. A high temperature gradient then creates a high buoyancy force gradient, which reduces the ability of exhaled breathe to transport against the gradient. As the thermal stratification decreases, CO₂ from exhalations should be more able to mix within the breathing zone, leading to less horizontal variability.

The conditions tested in these experiments are with manikins that are not breathing or moving, and the chamber is allowed to sit overnight to achieve thermal steady-state. The additional factors of an occupied room with a displacement system will be significant in both creating microenvironments, as well as increasing mixing. Exhaled breath has been shown to travel further in a DV system than a mixing system, penetrating into the pollutant transition layer more than the steady release in this study (Olmedo *et al.*, 2012). Occupant motion will be a source of mixing, and also cause short-term emissions scattered around the room as the occupant breathes while in motion. If occupant activities and breathing pattern could reasonably exacerbate the horizontal variability found in this study, or diminish it. If mixing due to occupant motion primarily causes additional horizontal mixing, then there will be less of a difference between wall and center CO₂ concentration. If occupant motion causes vertical mixing that transports high CO₂ concentration air from the upper well-mixed layer to the breathing height, then it is possible that this increases the difference between wall and center room CO₂ concentration. More studies should be done to determine if the horizontal variability observed in this study is exacerbated by human occupancy, or if the variability decreases.

To measure condition unambiguously, a CO₂ sensor near the top of the room or at the return grille is preferable to placement at the breathing height in order to assure that the sensor placement is not subject to the significant horizontal variability in CO₂ concentration observed in this study. Temperature sensors, which did not have an observable horizontal variation at the breathing height, can be placed on the wall at the breathing height where they typically are now. A horizontal variation in sensor readings at the breathing height is

Table 4.2: Average and maximum difference between wall and center CO₂ and temperature measurements

	Average CO ₂ difference (ppm)			Average temperature difference (°C)		
	0.6 m	1.1 m	1.7 m	0.6 m	1.1 m	1.7 m
All tests	18	71	48	0.32	0.21	0.21
High stratification	19	51	62	0.39	0.23	0.22
Low stratification	16	88	29	0.25	0.20	0.20
1 occupant tests	17	52	42	0.14	0.23	0.26
3 occupant tests	18	80	39	0.30	0.22	0.23
5 occupant tests	17	63	51	0.45	0.21	0.15
	Maximum CO ₂ difference (ppm)			Maximum temperature difference (°C)		
	0.6 m	1.1 m	1.7 m	0.6 m	1.1 m	1.7 m
All tests	35	183	146	0.79	0.38	0.31
High stratification	35	116	146	0.79	0.36	0.31
Low stratification	22	183	92	0.53	0.38	0.29
1 occupant tests	22	66	92	0.12	0.29	0.29
3 occupant tests	35	183	95	0.79	0.38	0.31
5 occupant tests	21	116	146	0.56	0.29	0.26

significant if it affects DCDV functioning. In Appendix A of ASHRAE (2016b) they report that typically DCDV CO₂ sensors have an accuracy of ± 75 ppm. With only two different wall sensor positions, it is reasonable to use the maximum difference between the wall and the center of the room to decide on significance. The maximum difference between the wall and center positions, see Table 4.4, at 0.6 m was 35 ppm, at 1.1 m it was 183 ppm and at 1.7 m it was 146 ppm, indicating that wall sensors located between 1.1 and 1.7 m in a space analogous to the chamber in this study may lead to a DCDV system not functioning as intended.

Perhaps more significant than risk of under-ventilation is that assuming a 1-to-1 ratio in breathing height wall sensor to occupant exposure will lead to underestimating the true ventilation efficiency of a properly functioning displacement ventilation system. Besides the direct 150 ppm variability measured for all breathing height, a CO₂ sensor that is placed in a location without horizontal variability still needs to be corrected to estimate the concentration within the breathing zone. The entrainment of air into the thermal plume of the occupant means that the CO₂ concentration within the breathing zone will be less than the ambient concentration at the breathing height. It may be possible to achieve greater energy efficiencies by allowing more recirculation to occur if the breathing zone concentration can be estimated while taking into account the effect of entrainment into the thermal plume.

In order to estimate the occupant exposure from a sensor measurement, a correction factor must be used. This can be broken into two different relationships: the relationship between the concentration at the sensor location to the ambient, vertical concentration gradient; and the relationship between vertical concentration gradient to the breathing zone concentration. The relationship between breathing zone concentration levels and ambient concentration at the breathing height was attempted in this experiment, but the results were inconclusive. As CO₂ sensor was placed on the belly of Manikin D, as there was too much self-exposure closer to the breathing zone, in an attempt to measure the actual occupant exposure, but this technique was insufficient. This has been presented in previous studies, and one model is to assume breathing zone concentration is a weighted average between the lower zone concentration and the transition zone concentration (Brohus and Nielsen, 1996). As seen in this study, the concentration in the transition zone is highly variable, so it may be more practical to find a weighted average using the lower and the upper well-mixed zones. However, in either model the value of coefficients for the weights is unknown, and there is no current study that adequately describes a procedure to find them in a real space. Figure 4.5 shows the ratio of CO₂ concentration measured at the ceiling vs the concentration measured in the center of the room at 0.6 m, and 1.1m. There is a slight trend with stratification level, as the lowest amounts of stratification also have the lowest ratios, but overall the relationship is weak. There is a very strong difference between the ratio at 0.6 m, and at 1.1 m, which can be explained by referring back to Figure 4.2. In Figure 4.2 it is clear that between 0.6 m and 1.7 m is where there is the steepest concentration gradient. Further work should be conducted on this issue.

With this data it is not possible to adequately estimate occupant exposure. The inconclusive results from the ratio of ceiling concentration to center of room concentration makes it difficult to estimate the ambient concentration at the breathing height, and estimating the true breathing zone concentration impossible. More data is required to understand how the concentration profile changes with stratification level, and the steep vertical concentration gradient that occurs right at the breathing height ensures that high levels of precision is necessary. The uncertainty in the ambient to breathing zone relationship significantly affects any efforts made to estimate occupant exposure. Accurately measuring the ventilation flow rate into the room in tandem with the return grille concentration should be sufficient to measure occupancy, and along with a breathing height temperature for thermal control may a preferable demand control system.

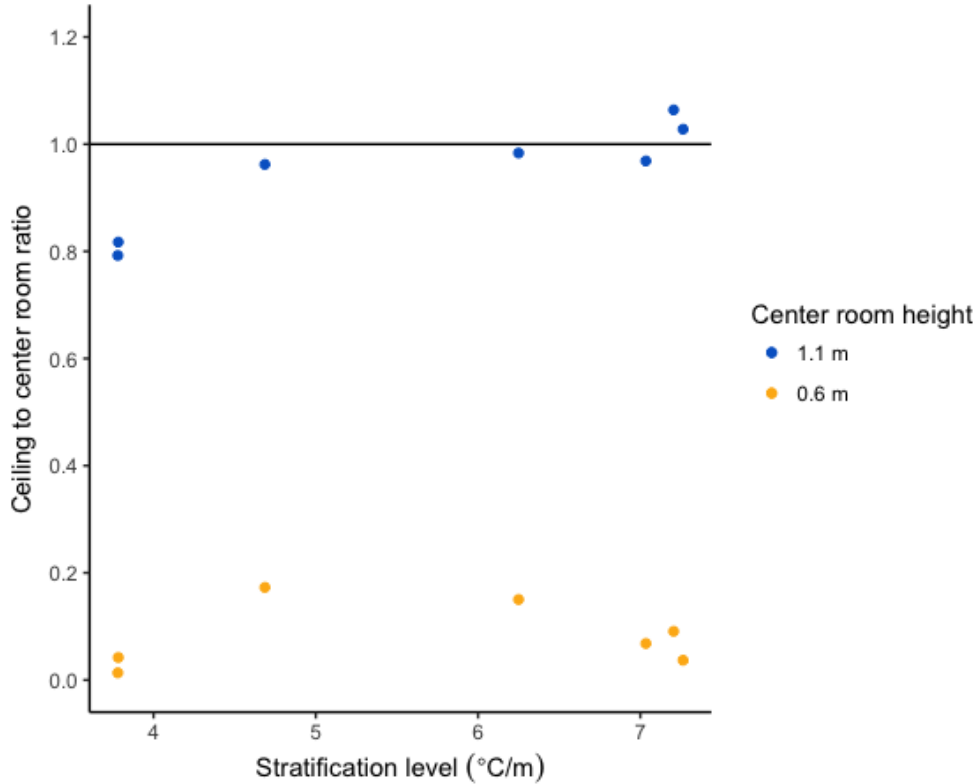


Figure 4.5: Ratio of ceiling level CO₂ concentration increase over supply concentration to center ambient concentration increase, $\frac{C_{ceiling} - C_{supply}}{C_{center} - C_{supply}}$, where C is the CO₂ concentration at various points in the chambers.

4.4. Conclusion

The results of this study suggest that CO₂ demand control sensors in a room with displacement ventilation should be placed by the ceiling, or near the return grille as there are horizontal variations in CO₂ concentration at the breathing height that can lead to misrepresentation of room conditions. A set of chamber experiments were conducted with 1, 3, and 5 heated manikins seated in front of computer stations with a steady release of CO₂ in their breathing zones. A spread of vertical temperature and CO₂ sensor trees measured the vertical temperature and pollutant concentration profiles, and the amount of horizontal spatial variation in measurements as a function of height was observed. Temperature was shown to be horizontally homogeneous, suggesting that placing temperature sensors at the breathing height anywhere along the walls will be representative of occupant thermal exposure. CO₂ concentration was shown to have up to 150 ppm of horizontal variability for sensors between 1.1–1.7 m high. It is suggested that CO₂ DC sensors be placed near the top of the room

so that there is a less ambiguous relationship between occupancy, room ventilation rate, and measured CO₂ concentration. A correction factor to relate concentration measured by a ceiling-mounted CO₂ DC sensor to exposed would be necessary, or at least suggested set point that ensures adequate fresh air delivery. The relationship between a ceiling mounted sensor and occupant exposure consists of the relationship between ceiling concentration and the vertical ambient profile, as well as the relationship between the vertical ambient profile and breathing zone concentration. The former relationship was estimated as a ratio, but additional work is needed.

Chapter 5

Conclusion

5.1. Summary of Major Findings

The goal of this dissertation was to model the interactions between humans and the indoor environment to incorporate knowledge of microenvironments into optimal sensor positioning for exposure estimates. A process is proposed to provide a conceptual model for determining which microenvironments are important for estimating exposure, exploring the pollutant transport mechanisms that lead to exposure within these microenvironments, exploring the implications for current sensor usage in indoor environments, and using laboratory studies to quantify these insights. Given that indoor air quality is a multifaceted public health issue, there is no simple approach to diagnosing and improving the conditions in a given building. It is necessary for researchers and practitioners interested in IAQ diagnostics to approach a given site with an open-ended mindset that allows one to determine the simplest possible conceptual model that leads to accurately relating measurements to exposure estimates.

In Chapter 2 a potential near-person emission source of ultrafine particles is explored experimentally. The specific conditions of the perihuman zone are simulated in a flow-through chamber, and the particle production from the ozonolysis of personal care products is measured. 92 personal care products in 13 different product categories were exposed to ozone

at a reasonable indoor concentration of 23 ppb in a small, flow-through reactor. The total particle production, particle emission event duration, and particle production rate were measured.

- None of the 92 personal care products were expected to significantly increase occupant exposure, based on the observed particle production. 2 personal care products were found to have significant particle emissions of greater than 10^9 particles, a tea tree oil hair treatment and a white lavender lotion, but in typical scenarios it is expected that they would have a mild effect on total particle exposure.
- The magnified exposure deriving from these products being used in the perihuman zone was not shown to be a significant factor. The modeled scenarios showed that for these particular products in a typical bathroom and classroom environment the exposure from the initial emission that preferentially increased the perihuman particle concentration was not significantly more than would be modeled by a well-mixed environment. For these emission sources modeling the microenvironment is not necessary.
- The duration of the particle production even never lasted more than 120 minutes, indicating that particle production from the ozonolysis of these products is limited to the soon after application. For a typical user applying these products in the morning, there does not seem to be any exposure effects later on in the day.

Chapter 3 is an extension of the pollutant mixing time previously performed by Baughman *et al.* (1994); Drescher *et al.* (1995). A vertical thermal gradient was created in an unventilated, half-height chamber, and a pulse of neutrally buoyant CO₂/He mixture was released as a tracer gas. Six CO₂ sensors were spread out in the chamber to measure the relative standard deviation. The mixing time was measured as a function of the level of stratification, and as a function of heating power supplied to either a small heated object, or one of the walls. The placement of the CO₂ sensors was determined by a series of placement tests to compare the importance of different axes to capturing the total amount of variation occurring in the chamber.

- Mixing time increases with increasing levels of stratification, but the more important differential occurs when the chamber transitions from isothermal to stratified conditions. While there are isothermal conditions there is a high level of variability in the mixing time, indicating that the slow mixing condition is unstable. When there were stratified conditions the mixing time was shorter than the isothermal conditions, but there was also less variability in results, which points to a condition that is more stable to small disruptions.
- The presence of a heated object was a highly significant source of mixing. The mixing time quickly fell with increasing heating power, and the effect was larger for the free-standing heated object than the heated wall. This effect highlights the importance of room occupancy, and not automatically assuming that pollutant transport dynamics in an unoccupied room are representative of those in an occupied space.

- The sensor placement tests illustrate the microplume motion during mixing. These tests clearly indicate that random sensor placement is not guaranteed to accurately capture the state of mixing, and highlight the importance of carefully selecting sensor locations in indoor spaces.
- Studies that are performed in isothermal spaces likely can assume that the space is well-mixed if it is occupied, while thermally stratified spaces cannot automatically be assumed to be well-mixed. If the mixing time is measured to be similar or greater than either the air exchange rate, or the amount of time occupants are exposed to a pollutant from a periodic emission source, researchers should ensure enough sensors are used to sufficiently characterize the space.

Chapter 4 presents an experiment examining the spatial heterogeneities of CO₂ in a full-scale chamber with displacement ventilation, heated manikins, and pure CO₂ emissions from the breathing zones. CO₂ sensors were spread out in vertical line in the center of the room, and at two wall positions. The main objective of this study was to determine if demand control sensors placed on the walls at the breathing height produced consistent results that were representative of the breathing zone CO₂ concentrations. Occupancy was varied between 1, 3, and 5 manikins, and two levels of stratification were tested.

- Supporting an effect noticed in an other study (Xu *et al.*, 2001), around the breathing height there exists a zone of high horizontal variability. In steady state conditions where CO₂ is released in a steady flow, a 50–150 ppm variability existed between CO₂ sensors at the same height, but at different wall positions. This represents a significant mischaracterization of room conditions.
- In a real room occupant activity and breathing will have an effect on horizontal and vertical mixing. Horizontal mixing will likely decrease the amount of horizontal variation we measured, while vertical mixing will likely increase it. Further work is necessary to discern whether real conditions exacerbate or mitigate potential for breathing height sensor mischaracterization observed in this study.
- The CO₂ sensors above the neutral height all agree, and suggest that demand control sensors placed against the ceiling or the return grille will have less variability than one placed at breathing height, leading to less ambiguity in determining room conditions. The consistency of a sensor in a return grille placement is highly significant for a demand control sensor, as it will lead to more consistent ventilation outcomes.
- Regardless of what height the sensor is placed at, some type of correction algorithm will be necessary to estimate the breathing zone concentration from these measurements. The most attractive benefit of a displacement ventilation system is that the occupant thermal plume transports preferentially cleaner air from the lower level of the room, meaning that room conditions at the breathing height are inherently different than the breathing zone.

5.2. Recommendations for Future Research

5.2.1. Contextualizing indoor sources by their microenvironmental conditions

Emissions that occur within the perihuman zone will be subject to unique conditions and lead to a higher exposure than would be predicted by assuming well-mixed conditions. It is important to differentiate between indoor emission sources that occur within the perihuman zone, and to report the exposure effect they will have in context to their source position. Emission sources that might have otherwise been dismissed as insignificant could gain significance if they are positioned within the perihuman zone.

5.2.2. Improving control in a DCDV system

The end of Chapter 4 leaves an open question of how to relate the CO₂ concentration measured at the return grille of a DV system to the breathing zone concentration. Further study using CFD models may help illuminate what this relationship may be, and could lead to improving current practices. At a minimum it would be helpful to calculate what are appropriate CO₂ setpoints for a DC sensor in such a placement to ensure adequate ventilation. It would also be helpful to recalculate the setpoint for a DC sensor placed on a wall at the breathing height while taking into account the variability measured in this study so that current building owners can take action based on these results.

Another possible solution to DC control in a CO₂ DCDV system could be to incorporate a measurement of supply air flow into a room, and use that in conjunction with a return grille CO₂ sensor. An orifice and pressure sensor in the supply duct could inexpensively measure the supply air flow. In combination with a return vent CO₂ sensor, measuring the occupancy with such a system would be straightforward and robust. An additional temperature sensor would allow a DCDV control system to separately determine the thermal needs and the current occupancy for a room.

5.2.3. Implications for IAQ engineers

The process proposed in the introduction of this dissertation is meant to be general enough to be applicable for both researchers characterizing a field site, as well as professional engineers interested in performing indoor air diagnostics for clients. Below is an example of utilizing the principles of this process to assess a privately owned space, and consult on design parameters for IAQ improvements. This was part of a larger project, and only the specific IAQ portions are included. A brief description of the space and the diagnostic process using the proposed steps is provided, as well as a summary of the results for the non-expert clients. A technical report that was included for the clients to provide to designers should they need the specifics is provided in the appendix of this chapter.

1. **Describe** the space as a function of room characteristics, ventilation conditions, occupancy, and activity.

The building is a large workshop (roughly 26 m × 40 m × 6.7 m high) with a small classroom (8.6 m × 5.5 m × 2.3 m high) built in the space that has a mezzanine area above it. Small classes of 10–20 students learn green construction techniques in the classroom, and practice on tiny house constructions in the workshop area. Staff and student surveys revealed significant complaints of very high temperatures in the summer, and very cold temperatures in the winter. IAQ concerns in the workshop centered around significant emissions of dust within the workshop that settled on many surfaces, and potentially a large forced convection, natural gas heater that was used constantly when it is cold. Classroom IAQ concerns centered on bioeffluents from the students, as there was no mechanical ventilation and the doors were kept closed during the winter to conserve heat.

2. **Identify** relevant microenvironments, and any occupant IAQ complaints.

The classroom was assumed to be its own compartment during the winter when the doors were closed. During the summer the classroom doors were kept open and a fan was used to increase air movement for thermal comfort, so it was assumed likely that it was well-mixed with the workshop during that period.

3. **Estimate** exposure to pollutant sources to determine the simplest appropriate model

There are no other pollutant sources in the classroom except for the occupants. In the workshop the saws in the construction area were suspected to be the main source for dust. There were also VOC concerns from the use of paints and other construction material.

4. **Describe** the pollutant transport within and between the compartments

The bay doors were poorly sealed, leading to high levels of natural ventilation and a noticeable draft near the floor during the summer staff reported that there was a large temperature gradient, the mezzanine and students on ladders were significantly hotter than at the ground level. The classroom had no designed ventilation system, so it was likely fairly well isolated when the doors were closed.

5. **Parameterize** the system variables to a set of measurable conditions

CO₂ and temperature as a function of height in the workshop and classroom were used to determine air motion and bioeffluent accumulation. Air exchange rate, measured differently in the two spaces, was also measured to determine ventilation conditions.

6. **Experiment** with field measurements and laboratory studies

A two week study was conducted to characterize the summer CO₂ and temperature conditions within the building. Vertical temperature and CO₂ concentration gradients were measured by a string of small sensors suspended in the classroom and workshop. The air exchange rate for the building was measured with a tracer gas decay test in the classroom, and a blower door depressurization test in the workshop.

7. **Summarize** the knowledge gained by the process to obtain the maximum impact with the intended audience

The results of the tests were summarized in a technical report (see the Appendix), and were presented visually in the three diagrams presented below.

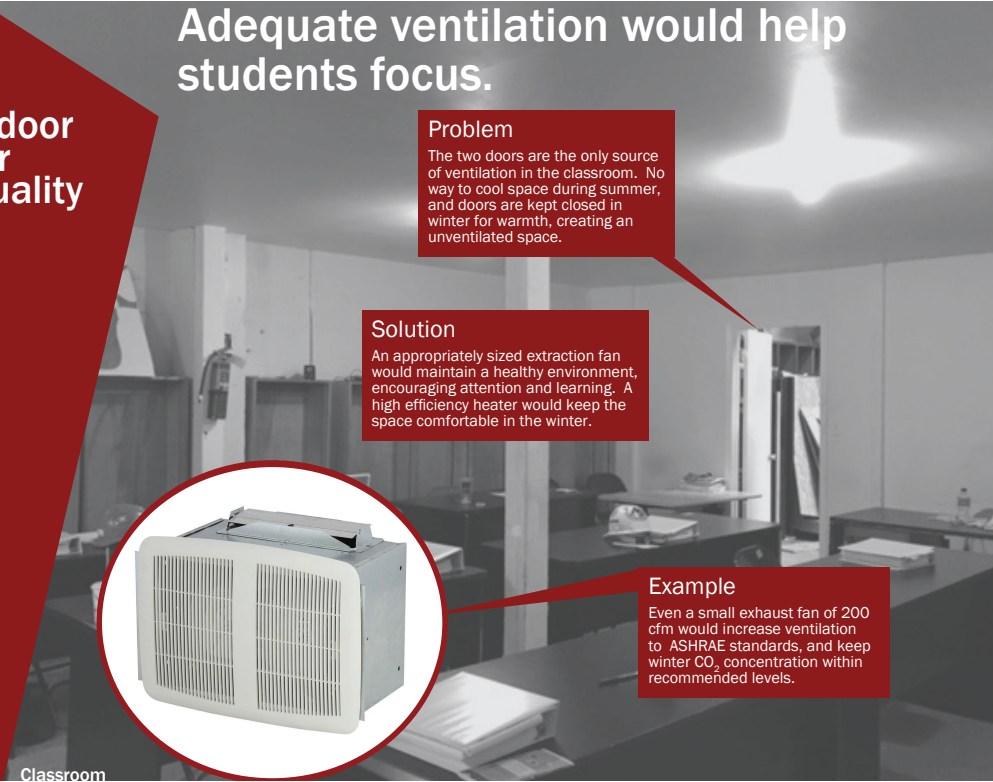
Indoor Air Quality

Adequate ventilation would help students focus.

Problem
The two doors are the only source of ventilation in the classroom. No way to cool space during summer, and doors are kept closed in winter for warmth, creating an unventilated space.

Solution
An appropriately sized extraction fan would maintain a healthy environment, encouraging attention and learning. A high efficiency heater would keep the space comfortable in the winter.

Example
Even a small exhaust fan of 200 cfm would increase ventilation to ASHRAE standards, and keep winter CO₂ concentration within recommended levels.



Classroom


Indoor Air Quality

Better air quality will ensure good student health.

Problem
Indoor woodworking creates copious amounts of dust, which spreads throughout the workshop. This creates an unhealthy environment, and dirties many of the surfaces. Paint and glue use indoors also creates volatile organic compounds, which are linked to adverse health effects.

Solution
Isolating the construction projects with curtains, separately ventilating the area, and using dust collectors during carpentry tasks will remove pollutants before they can spread throughout the building.

Example
The ramp area near the unused bay door (currently used for trash) could be actively used for building the student-built structures. The bay doors are normally permeable to air, which would effectively increase ventilation rates near the work that has the most impact on air quality. Also the adjacent door could be opened during high emission tasks to protect occupant health.



Workshop

Better thermal comfort in the workshop will encourage better concentration.

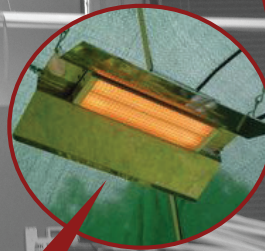
Thermal Comfort

Problem

During the summer the temperature in the upper half of the building is regularly 20 °F above the comfort zone, and even at the floor it is still uncomfortably warm.

Solution

An extractor fan in the back window with a short piece of ducting to pull air directly from the peak of the ceiling would efficiently cool the entire building.



Problem

The building envelop is not well sealed, making the workshop and classroom difficult to keep comfortably warm in the winter

Solution

Radiant heaters warm using infrared light, directly heating occupants within close proximity, and line-of-sight. Forced air heaters warm the bulk air, which is quickly ventilated outdoors in this workshop.

Workshop

References

- Acevedo-Bolton, V.; Cheng, K.-C.; Jiang, R.-T.; Ott, W. R.; Klepeis, N. E.; Hildemann, L. M. 2012. Measurement of the proximity effect for indoor air pollutant sources in two homes. *Journal of Environmental Monitoring*, 14 (1) 94–104.
- Allen, J. G.; MacNaughton, P.; Satish, U.; Santanam, S.; Vallarino, J.; Spengler, J. D. 2016. Associations of cognitive function scores with carbon dioxide, ventilation, and volatile organic compound exposures in office workers: a controlled exposure study of green and conventional office environments. *Environmental health perspectives*, 124 (6) 805.
- Allen, J. G.; McClean, M. D.; Stapleton, H. M.; Nelson, J. W.; Webster, T. F. 2007. Personal exposure to polybrominated diphenyl ethers (PBDEs) in residential indoor air. *Environmental Science & Technology*, 41 (13) 4574–4579.
- ASHRAE. 2016a. ANSI / ASHRAE Standard 55 - 2017: Thermal environmental conditions for human occupancy. *American Society of Heating, Refrigeration, and Air-Conditioning Engineers: Atlanta, GA, 2016*.
- ASHRAE. 2016b. ANSI / ASHRAE Standard 62.1-2016: Ventilation for Acceptable Indoor Air Quality. *American Society of Heating, Refrigeration, and Air-Conditioning Engineers: Atlanta, GA, 2016*.
- Baughman, A.; Gadgil, A.; Nazaroff, W. W. 1994. Mixing of a point source pollutant by natural convection flow within a room. *Indoor Air*, 4 (2) 114–122.
- Bhangar, S.; Huffman, J.; Nazaroff, W. W. 2014. Size-resolved fluorescent biological aerosol particle concentrations and occupant emissions in a university classroom. *Indoor Air*, 24 (6) 604–617.
- Bhangar, S.; Mullen, N.; Hering, S.; Kreisberg, N.; Nazaroff, W. W. 2011. Ultrafine particle concentrations and exposures in seven residences in northern California. *Indoor Air*, 21 (2) 132–144.

- Bjørn, E.; Nielsen, P. V. 2002. Dispersal of exhaled air and personal exposure in displacement ventilated rooms. *Indoor Air*, 12 (3) 147–164.
- Brohus, H.; Nielsen, P. V. 1996. Personal exposure in displacement ventilated rooms. *Indoor Air*, 6 (3) 157–167.
- Cali, D.; Matthes, P.; Huchtemann, K.; Streblow, R.; Müller, D. 2015. CO₂ based occupancy detection algorithm: experimental analysis and validation for office and residential buildings. *Building and Environment*, 86 39–49.
- CEN, E. 2004. 14240-2004. *Ventilation for Buildings—Chilled Ceilings—Testing and Rating.*, European Committee for Standardization, Brussels, Belgium.
- Chenari, B.; Carrilho, J. D.; da Silva, M. G. 2016. Towards sustainable, energy-efficient and healthy ventilation strategies in buildings: a review. *Renewable and Sustainable Energy Reviews*, 59 1426–1447.
- Cheng, K.-C.; Acevedo-Bolton, V.; Jiang, R.-T.; Klepeis, N. E.; Ott, W. R.; Fringer, O. B.; Hildemann, L. M. 2011. Modeling exposure close to air pollution sources in naturally ventilated residences: Association of turbulent diffusion coefficient with air change rate. *Environmental science & technology*, 45 (9) 4016–4022.
- Coleman, B. K.; Lunden, M. M.; Destailats, H.; Nazaroff, W. W. 2008. Secondary organic aerosol from ozone-initiated reactions with terpene-rich household products. *Atmospheric Environment*, 42 (35) 8234–8245.
- Conner, T. L.; Williams, R. W. 2004. Identification of possible sources of particulate matter in the personal cloud using SEM/EDX. *Atmospheric Environment*, 38 (31) 5305–5310.
- Corrsin, S. 1957. Simple theory of an idealized turbulent mixer. *AIChE Journal*, 3 (3) 329–330.
- Corsi, R.; Siegel, J.; Karamalegos, A.; Simon, H.; Morrison, G. 2007. Personal reactive clouds: Introducing the concept of near-head chemistry. *Atmospheric Environment*, 41 (15) 3161–3165.
- Craven, B. A.; Settles, G. S. 2006. A computational and experimental investigation of the human thermal plume. *Journal of Fluids Engineering*, 128 (6) 1251–1258.
- Drescher, A.; Lobascio, C.; Gadgil, A.; Nazaroff, W. W. 1995. Mixing of a Point-Source Indoor Pollutant by Forced Convection. *Indoor Air*, 5 (3) 204–214.
- Emmerich, S. J.; Persily, A. K. 2001. *State-of-the-art review of CO₂ demand controlled ventilation technology and application*, in: *NISTIR 6729*. Technical report.
- Evans, W. C. 1996. Linear systems, compartmental modeling, and estimability issues in IAQ studies. In: *Characterizing Sources of Indoor Air Pollution and Related Sink Effects*, ASTM International.

- Ezzati, M.; Kammen, D. M. 2002. The health impacts of exposure to indoor air pollution from solid fuels in developing countries: knowledge, gaps, and data needs. *Environmental Health Perspectives*, 110 (11) 1057.
- Ezzati, M.; Saleh, H.; Kammen, D. M. 2000. The contributions of emissions and spatial microenvironments to exposure to indoor air pollution from biomass combustion in Kenya. *Environmental Health Perspectives*, 108 (9) 833.
- Ferro, A. R.; Kopperud, R. J.; Hildemann, L. M. 2004. Elevated personal exposure to particulate matter from human activities in a residence. *Journal of Exposure Science and Environmental Epidemiology*, 14 S34–S40.
- Fisk, W. J.; Sullivan, D.; Faulkner, D.; Eliseeva, E. 2010. CO₂ monitoring for demand controlled ventilation in commercial buildings. *Lawrence Berkeley National Laboratory, LBNL-3279E*.
- Fung, C.-C.; Shu, S.; Zhu, Y. 2014. Ultrafine particles generated from coloring with scented markers in the presence of ozone. *Indoor Air*, 24 (5) 503–510.
- Furtaw, E. J. J.; Pandian, M. D.; Nelson, D. R.; Behar, J. V. 1996. Modeling indoor air concentrations near emission sources in imperfectly mixed rooms. *Journal of the Air & Waste Management Association*, 46 (9) 861–868.
- Gadgil, A.; Lobscheid, C.; Abadie, M.; Finlayson, E. 2003. Indoor pollutant mixing time in an isothermal closed room: an investigation using CFD. *Atmospheric Environment*, 37 (39) 5577–5586.
- Godwin, C.; Batterman, S. 2007. Indoor Air quality in Michigan schools. *Indoor Air*, 17 (2) 109–121.
- Hallquist, M.; Wenger, J.; Baltensperger, U.; Rudich, Y.; Simpson, D.; Claeys, M.; Dommen, J.; Donahue, N.; George, C.; Goldstein, A.; *et al.* 2009. The formation, properties and impact of secondary organic aerosol: current and emerging issues. *Atmospheric Chemistry and Physics*, 9 (14) 5155–5236.
- He, C.; Morawska, L.; Hitchins, J.; Gilbert, D. 2004. Contribution from indoor sources to particle number and mass concentrations in residential houses. *Atmospheric Environment*, 38 (21) 3405–3415.
- He, G.; Yang, X.; Srebric, J. 2005. Removal of contaminants released from room surfaces by displacement and mixing ventilation: modeling and validation. *Indoor Air*, 15 (5) 367–380.
- Hsu, D.-J.; Huang, H.-L.; Sheu, S.-C. 2012. Characteristics of air pollutants and assessment of potential exposure in spa centers during aromatherapy. *Environmental Engineering Science*, 29 (2) 79–85.

- Huang, H.-L.; Tsai, T.-J.; Hsu, N.-Y.; Lee, C.-C.; Wu, P.-C.; Su, H.-J. 2012. Effects of essential oils on the formation of formaldehyde and secondary organic aerosols in an aromatherapy environment. *Building and Environment*, 57 120–125.
- Huang, Y.; Ho, K. F.; Ho, S. S. H.; Lee, S. C.; Yau, P.; Cheng, Y. 2011. Physical parameters effect on ozone-initiated formation of indoor secondary organic aerosols with emissions from cleaning products. *Journal of Hazardous Materials*, 192 (3) 1787–1794.
- Jin, M.; Bekiaris-Liberis, N.; Weekly, K.; Spanos, C.; Bayen, A. 2015. Sensing by proxy: Occupancy detection based on indoor CO₂ concentration. *UBICOMM 2015*, 14.
- Jonsson, Å.; Hallquist, M.; Ljungström, E. 2008. The effect of temperature and water on secondary organic aerosol formation from ozonolysis of limonene, Δ 3-carene and α -pinene. *Atmospheric Chemistry and Physics*, 8 (21) 6541–6549.
- Klepeis, N. E.; Nelson, W. C.; Ott, W. R.; Robinson, J. P.; Tsang, A. M.; Switzer, P.; Behar, J. V.; Hern, S. C.; Engelmann, W. H. 2001. The National Human Activity Pattern Survey (NHAPS): a resource for assessing exposure to environmental pollutants. *Journal of Exposure Science and Environmental Epidemiology*, 11 (3) 231.
- Knol, A. B.; de Hartog, J. J.; Boogaard, H.; Slottje, P.; van der Sluijs, J. P.; Lebet, E.; Cassee, F. R.; Wardekker, J. A.; Ayres, J. G.; Borm, P. J.; *et al.* 2009. Expert elicitation on ultrafine particles: likelihood of health effects and causal pathways. *Particle and Fibre Toxicology*, 6 (1) 19.
- Lai, A. C.; Nazaroff, W. W. 2000. Modeling indoor particle deposition from turbulent flow onto smooth surfaces. *Journal of Aerosol Science*, 31 (4) 463–476.
- Leech, J. A.; Nelson, W. C.; Burnett, R. T.; Aaron, S.; Raizenne, M. E. 2002. It's about time: a comparison of Canadian and American time-activity patterns. *Journal of Exposure Science and Environmental Epidemiology*, 12 (6) 427.
- Lelieveld, J.; Evans, J. S.; Fnais, M.; Giannadaki, D.; Pozzer, A. 2015. The contribution of outdoor air pollution sources to premature mortality on a global scale. *Nature*, 525 (7569) 367.
- Li, X.; Inthavong, K.; Ge, Q.; Tu, J. 2013. Numerical investigation of particle transport and inhalation using standing thermal manikins. *Building and Environment*, 60 116–125.
- Licina, D.; Melikov, A.; Sekhar, C.; Tham, K. W. 2015. Transport of gaseous pollutants by convective boundary layer around a human body. *Science and Technology for the Built Environment*, 21 (8) 1175–1186.
- Licina, D.; Tian, Y.; Nazaroff, W. W. 2017. Emission rates and the personal cloud effect associated with particle release from the perihuman environment. *Indoor Air*, 27 (4) 791–802.

- Lim, S. S.; Vos, T.; Flaxman, A. D.; Danaei, G.; Shibuya, K.; Adair-Rohani, H.; AlMazroa, M. A.; Amann, M.; Anderson, H. R.; Andrews, K. G.; *et al.* 2013. A comparative risk assessment of burden of disease and injury attributable to 67 risk factors and risk factor clusters in 21 regions, 1990–2010: a systematic analysis for the Global Burden of Disease Study 2010. *The lancet*, 380 (9859) 2224–2260.
- Lioy, P. J. 2010. Exposure science: a view of the past and milestones for the future. *Environmental Health Perspectives*, 118 (8) 1081.
- Liu, J.; Fung, D.; Jiang, J.; Zhu, Y. 2014. Ultrafine particle emissions from essential-oil-based mosquito repellent products. *Indoor Air*, 24 (3) 327–335.
- Liu, S.; Schiavon, S.; Kabanshi, A.; Nazaroff, W. W. 2017. Predicted percentage dissatisfied with ankle draft. *Indoor air*, 27 (4) 852–862.
- Loretz, L.; Api, A.; Barraji, L.; Burdick, J.; Dressler, W.; Gettings, S.; Hsu, H. H.; Pan, Y.; Re, T.; Renskers, K.; *et al.* 2005. Exposure data for cosmetic products: lipstick, body lotion, and face cream. *Food and Chemical Toxicology*, 43 (2) 279–291.
- Loretz, L.; Api, A. M.; Barraji, L.; Burdick, J.; Davis, D. A.; Dressler, W.; Gilberti, E.; Jarrett, G.; Mann, S.; Pan, Y. L.; *et al.* 2006. Exposure data for personal care products: hairspray, spray perfume, liquid foundation, shampoo, body wash, and solid antiperspirant. *Food and Chemical Toxicology*, 44 (12) 2008–2018.
- Lu, T.; Lü, X.; Viljanen, M. 2011. A novel and dynamic demand-controlled ventilation strategy for CO₂ control and energy saving in buildings. *Energy and Buildings*, 43 (9) 2499–2508.
- Mage, D. T.; Ott, W. R. 1996. Accounting for nonuniform mixing and human exposure in indoor environments. In: *Characterizing sources of indoor air pollution and related sink effects*, ASTM International.
- Mahyuddin, N.; Awbi, H. 2010. The spatial distribution of carbon dioxide in an environmental test chamber. *Building and Environment*, 45 (9) 1993–2001.
- Mahyuddin, N.; Awbi, H. 2012. A review of CO₂ measurement procedures in ventilation research. *International Journal of Ventilation*, 10 (4) 353–370.
- Mahyuddin, N.; Awbi, H. B.; Alshitawi, M. 2014. The spatial distribution of carbon dioxide in rooms with particular application to classrooms. *Indoor and Built Environment*, 23 (3) 433–448.
- Mateus, N. M.; da Graça, G. C. 2015. A validated three-node model for displacement ventilation. *Building and Environment*, 84 50–59.
- Milton, D. K.; Glencross, P. M.; Walters, M. D. 2000. Risk of sick leave associated with outdoor air supply rate, humidification, and occupant complaints. *Indoor Air*, 10 (4) 212–221.

- Morawska, L.; He, C.; Hitchins, J.; Gilbert, D.; Parappukkaran, S. 2001. The relationship between indoor and outdoor airborne particles in the residential environment. *Atmospheric Environment*, 35 (20) 3463–3473.
- Mullen, N.; Bhangar, S.; Hering, S.; Kreisberg, N.; Nazaroff, W. W. 2011. Ultrafine particle concentrations and exposures in six elementary school classrooms in northern California. *Indoor Air*, 21 (1) 77–87.
- Mundt, E. 1994. Contamination distribution in displacement ventilation—influence of disturbances. *Building and Environment*, 29 (3) 311–317.
- Nazaroff, W. W. 2008. Inhalation intake fraction of pollutants from episodic indoor emissions. *Building and Environment*, 43 (3) 269–277.
- Ng, M. O.; Qu, M.; Zheng, P.; Li, Z.; Hang, Y. 2011. CO₂-based demand controlled ventilation under new ASHRAE Standard 62.1-2010: a case study for a gymnasium of an elementary school at West Lafayette, Indiana. *Energy and Buildings*, 43 (11) 3216–3225.
- Norbäck, D.; Nordström, K. 2008. Sick building syndrome in relation to air exchange rate, CO₂, room temperature and relative air humidity in university computer classrooms: an experimental study. *International Archives of Occupational and Environmental Health*, 82 (1) 21–30.
- Norbäck, D.; Nordström, K.; Zhao, Z. 2013. Carbon dioxide (CO₂) demand-controlled ventilation in university computer classrooms and possible effects on headache, fatigue and perceived indoor environment: an intervention study. *International Archives of Occupational and Environmental Health*, 86 (2) 199–209.
- Norbäck, D.; Wieslander, G.; Zhang, X.; Zhao, Z. 2011. Respiratory symptoms, perceived air quality and physiological signs in elementary school pupils in relation to displacement and mixing ventilation system: an intervention study. *Indoor Air*, 21 (5) 427–437.
- Nørgaard, A.; Kudal, J.; Kofoed-Sørensen, V.; Koponen, I.; Wolkoff, P. 2014. Ozone-initiated VOC and particle emissions from a cleaning agent and an air freshener: Risk assessment of acute airway effects. *Environment International*, 68 209–218.
- Olmedo, I.; Nielsen, P. V.; Ruiz de Adana, M.; Jensen, R. L.; Grzelecki, P. 2012. Distribution of exhaled contaminants and personal exposure in a room using three different air distribution strategies. *Indoor Air*, 22 (1) 64–76.
- Ostro, B.; Hu, J.; Goldberg, D.; Reynolds, P.; Hertz, A.; Bernstein, L.; Kleeman, M. J. 2015. Associations of mortality with long-term exposures to fine and ultrafine particles, species and sources: results from the California Teachers Study Cohort. *Environmental Health Perspectives*, 123 (6) 549.
- Ozkaynak, H.; Xue, J.; Spengler, J.; Wallace, L.; Pellizzari, E.; Jenkins, P. 1996. Personal exposure to airborne particles and metals: results from the Particle TEAM study in

- Riverside, California. *Journal of Exposure Analysis and Environmental Epidemiology*, 6 (1) 57–78.
- Persily, A.; Jonge, L. 2017. Carbon dioxide generation rates for building occupants. *Indoor air*, 27 (5) 868–879.
- Persily, A. K. 1997. Evaluating building IAQ and ventilation with indoor carbon dioxide. *Transactions-American society of heating refrigerating and air conditioning engineers*, 103 193–204.
- Rim, D.; Novoselac, A. 2009. Transport of particulate and gaseous pollutants in the vicinity of a human body. *Building and Environment*, 44 (9) 1840–1849.
- Rim, D.; Novoselac, A. 2010. Occupational exposure to hazardous airborne pollutants: Effects of air mixing and source location. *Journal of Occupational and Environmental Hygiene*, 7 (12) 683–692.
- Rim, D.; Novoselac, A.; Morrison, G. 2009. The influence of chemical interactions at the human surface on breathing zone levels of reactants and products. *Indoor Air*, 19 (4) 324–334.
- Rodes, C. E.; Lawless, P. A.; Thornburg, J. W.; Williams, R. W.; Croghan, C. W. 2010. DEARS particulate matter relationships for personal, indoor, outdoor, and central site settings for a general population. *Atmospheric Environment*, 44 (11) 1386–1399.
- Rohr, A. C. 2013. The health significance of gas-and particle-phase terpene oxidation products: a review. *Environment International*, 60 145–162.
- Rudel, R. A.; Perovich, L. J. 2009. Endocrine disrupting chemicals in indoor and outdoor air. *Atmospheric Environment*, 43 (1) 170–181.
- Salmanzadeh, M.; Zahedi, G.; Ahmadi, G.; Marr, D.; Glauser, M. 2012. Computational modeling of effects of thermal plume adjacent to the body on the indoor airflow and particle transport. *Journal of Aerosol Science*, 53 29–39.
- Sarwar, G.; Olson, D. A.; Corsi, R. L.; Weschler, C. J. 2004. Indoor fine particles: the role of terpene emissions from consumer products. *Journal of the Air & Waste Management Association*, 54 (3) 367–377.
- Satish, U.; Mendell, M. J.; Shekhar, K.; Hotchi, T.; Sullivan, D.; Streufert, S.; Fisk, W. J. 2012. Is CO₂ an indoor pollutant? Direct effects of low-to-moderate CO₂ concentrations on human decision-making performance. *Environmental Health Perspectives*, 120 (12) 1671.
- Schäfer, M.; Detzer, R.; Hesselbach, J.; Böhm, S.; Shinde, P.; Lin, C.-X. 2013. CO₂ and thermal gradient based demand-driven stratified ventilation—Experimental and simulation study. *HVAC&R Research*, 19 (6) 676–692.

- Schlichting, H.; Gersten, K.; Krause, E.; Oertel, H. 1955. *Boundary-layer theory*, volume 7. Springer.
- Seinfeld, J. H.; Pandis, S. N. 2016. *Atmospheric chemistry and physics: from air pollution to climate change*. John Wiley & Sons.
- Seppänen, O.; Fisk, W.; Mendell, M. 1999. Association of ventilation rates and CO₂ concentrations with health and other responses in commercial and institutional buildings. *Indoor Air*, 9 (4) 226–252.
- Seppänen, O.; Fisk, W. J. 2004. Summary of human responses to ventilation. *Indoor Air*, 14 (s7) 102–118.
- Shao, Y.; Ramachandran, S.; Arnold, S.; Ramachandran, G. 2017. Turbulent eddy diffusion models in exposure assessment-Determination of the eddy diffusion coefficient. *Journal of occupational and environmental hygiene*, 14 (3) 195–206.
- Shendell, D. G.; Prill, R.; Fisk, W. J.; Apte, M. G.; Blake, D.; Faulkner, D. 2004. Associations between classroom CO₂ concentrations and student attendance in Washington and Idaho. *Indoor Air*, 14 (5) 333–341.
- Singer, B. C.; Pass, R. Z.; Delp, W. W.; Lorenzetti, D. M.; Maddalena, R. L. 2017. Pollutant concentrations and emission rates from natural gas cooking burners without and with range hood exhaust in nine California homes. *Building and Environment*, 122 215–229.
- Steinemann, A. C. 2009. Fragranced consumer products and undisclosed ingredients. *Environmental Impact Assessment Review*, 29 (1) 32–38.
- Stymne, H.; Sandberg, M.; Mattsson, M. 1991. Dispersion pattern of contaminants in a displacement ventilated room-implications for demand control. In: *Proceedings of the 12th AIVC Conference, Ottawa*, pages 173–89.
- Su, H.-J.; Chao, C.-J.; Chang, H.-Y.; Wu, P.-C. 2007. The effects of evaporating essential oils on indoor air quality. *Atmospheric Environment*, 41 (6) 1230–1236.
- Sundell, J.; Levin, H.; Nazaroff, W. W.; Cain, W. S.; Fisk, W. J.; Grimsrud, D. T.; Gynzelberg, F.; Li, Y.; Persily, A.; Pickering, A.; *et al.* 2011. Ventilation rates and health: multidisciplinary review of the scientific literature. *Indoor air*, 21 (3) 191–204.
- Suzuki, T.; Sagara, K.; Yamanaka, T.; Kotani, H.; Yamashita, T. 2007. Vertical profile of contaminant concentration in sickroom with lying person ventilated by displacement. In: *The 6th International Conference on Indoor Air Quality, Ventilation & Energy Conservation in Buildings IAQVEC*, pages 28–31.
- Thatcher, T. L.; Fairchild, W. A.; Nazaroff, W. W. 1996. Particle deposition from natural convection enclosure flow onto smooth surfaces. *Aerosol Science and Technology*, 25 (4) 359–374.

- Uhde, E.; Schulz, N. 2015. Impact of room fragrance products on indoor air quality. *Atmospheric Environment*, 106 492–502.
- Vannucci, M. P.; Nazaroff, W. W. 2017. Ultrafine particle production from the ozonolysis of personal care products. *Environmental Science & Technology*, 51 (21) 12737–12744.
- Vartiainen, E.; Kulmala, M.; Ruuskanen, T.; Taipale, R.; Rinne, J.; Vehkamäki, H. 2006. Formation and growth of indoor air aerosol particles as a result of D-limonene oxidation. *Atmospheric Environment*, 40 (40) 7882–7892.
- Wachenfeldt, B. J.; Mysen, M.; Schild, P. G. 2007. Air flow rates and energy saving potential in schools with demand-controlled displacement ventilation. *Energy and Buildings*, 39 (10) 1073–1079.
- Wallace, L.; Ott, W. 2011. Personal exposure to ultrafine particles. *Journal of Exposure Science and Environmental Epidemiology*, 21 (1) 20–30.
- Wallace, L. A.; Ott, W. R.; Weschler, C. J. 2015. Ultrafine particles from electric appliances and cooking pans: experiments suggesting desorption/nucleation of sorbed organics as the primary source. *Indoor Air*, 25 (5) 536–546.
- Wang, C.; Waring, M. S. 2014. Secondary organic aerosol formation initiated from reactions between ozone and surface-sorbed squalene. *Atmospheric Environment*, 84 222–229.
- Wargoeki, P.; Wyon, D. P.; Sundell, J.; Clausen, G.; Fanger, P. 2000. The effects of outdoor air supply rate in an office on perceived air quality, sick building syndrome (SBS) symptoms and productivity. *Indoor Air*, 10 (4) 222–236.
- Waring, M. S.; Siegel, J. A. 2013. Indoor secondary organic aerosol formation initiated from reactions between ozone and surface-sorbed d-limonene. *Environmental Science & Technology*, 47 (12) 6341–6348.
- Weekly, K.; Bekiaris-Liberis, N.; Jin, M.; Bayen, A. M. 2015. Modeling and estimation of the humans' effect on the CO₂ dynamics inside a conference room. *IEEE Transactions On Control Systems Technology*, 23 (5) 1770–1781.
- Weschler, C. J. 2006. Ozone's impact on public health: contributions from indoor exposures to ozone and products of ozone-initiated chemistry. *Environmental Health Perspectives*, 114 (10) 1489.
- Weschler, C. J.; Shields, H. C. 1999. Indoor ozone/terpene reactions as a source of indoor particles. *Atmospheric Environment*, 33 (15) 2301–2312.
- Xing, H.; Awbi, H. B. 2002. Measurement and calculation of the neutral height in a room with displacement ventilation. *Building and Environment*, 37 (10) 961–967.
- Xing, H.; Hatton, A.; Awbi, H. 2001. A study of the air quality in the breathing zone in a room with displacement ventilation. *Building and Environment*, 36 (7) 809–820.

- Xu, M.; Kotani, H.; *et al.* 2001. Vertical profiles of temperature and contaminant concentration in rooms ventilated by displacement with heat loss through room envelopes. *Indoor Air*, 11 (2) 111–119.
- Yang, X.; Zhong, K.; Zhu, H.; Kang, Y. 2014. Experimental investigation on transient natural ventilation driven by thermal buoyancy. *Building and Environment*, 77 29–39.
- Zhang, Q.; Avalos, J.; Zhu, Y. 2014. Fine and ultrafine particle emissions from microwave popcorn. *Indoor Air*, 24 (2) 190–198.
- Zhang, X.; Wargoeki, P.; Lian, Z.; Thyregod, C. 2017. Effects of exposure to carbon dioxide and bioeffluents on perceived air quality, self-assessed acute health symptoms, and cognitive performance. *Indoor air*, 27 (1) 47–64.

Appendix

A.1. Supplemental methods and results for Chapter 2

A.1.1. Supplemental methods

Emission rate calculation including loss terms

Assuming a well-mixed reaction chamber, the particle emission rate including inlet particle concentration and loss rate was determined based the following material-balance equation:

$$\frac{dC}{dt} = \frac{E}{V} - AER(C - C_{inlet}) - L_{dep} - L_{coag} \quad (\text{A.1})$$

Here C is the measured concentration in the outlet airflow, C_{inlet} is the inlet particle concentration, and L_{dep} and L_{coag} are the particle losses owing to deposition and coagulation, respectively. The emission rate, E , can be estimated by substituting for the two loss terms and rearranging Equation A.1 as follows:

$$E = V \times \left(AER(C - C_{inlet}) + \beta_{dep}C + k_{coag}C^2 + \frac{dC}{dt} \right) \quad (\text{A.2})$$

In deriving Equation A.2, L_{dep} and L_{coag} are represented as first and second-order loss processes, with rate coefficients β_{dep} and k_{coag} , respectively. To estimate the overall effect of these parameters, we assume a monodispersed aerosol at 10 nm, using the deposition model of Lai and Nazaroff (2000), and applying the Fuchs form of the Brownian coagulation coefficient in the following subsections Seinfeld and Pandis (2016). The particle diameter of 10 nm corresponds approximately to the lower size limit of the WCPC. As shown below, when assuming an airflow velocity based on the mean velocity the overall effect of the deposition and coagulation loss terms was insignificant for estimating emissions, contributing less than 1% for all samples. To estimate uncertainty, airflow velocity inside of the chamber was assumed to be equal to the inlet velocity, which is expected to be larger than the true value, and which therefore overestimates losses due to deposition.

Deposition loss rate calculations

The first-order loss rate, L_{dep} , was assumed to be a representational estimate for the chamber used in this study. For a monodispersed aerosol it can be determined by,

$$L_{dep} = \beta_{dep}(D_p) \times C \quad (\text{A.3})$$

Where C is the number concentration of particles in the chamber air. The size-dependent depositional loss coefficient, β_{dep} , is determined using the model of Lai and Nazaroff (2000). An important input parameter for the model is u^* , the friction velocity, estimated from Equation A.4:

$$u^* = \left[\nu \frac{dU}{dy} \right]^{\frac{1}{2}} \quad (\text{A.4})$$

Here, ν is the kinematic viscosity of air, and $\frac{dU}{dy}$ is the average near-wall velocity gradient within the chamber. The average velocity gradient can be estimated from the work of Schlichting *et al.* (1955), originally developed for air motion over a plate:

$$\left. \frac{dU}{dy} \right|_{y=0} = \left(\frac{0.072}{\rho_0} \right) \left(\frac{\rho_0 U_\infty^2}{2} \right) \left(\frac{U_\infty L}{\nu} \right)^{-\frac{1}{5}} \quad (\text{A.5})$$

In Equation A.5, ρ_0 is the density of air, L is the plate length, and U_∞ is the freestream air speed. For purposes of estimating the chamber loss attributable to deposition, the length of the chamber is used as L , and U_∞ is estimated from the volumetric flow rate and cross-sectional area of the chamber. For estimating uncertainty U_∞ is assumed to be the inlet velocity. These assumptions do not fully allow us to directly use the model presented in Table 2 of Lai and Nazaroff (2000), as there is no solution presented for a cylindrical chamber. Instead we modeled our chamber as a rectangular prism with the length equal to the true axis length of the chamber and the cross section represented as a square with a cross-sectional area equal to that of the actual chamber's cross-sectional area. Under the assumptions used to calculate C , and those to calculate the uncertainty, the pseudo-first order deposition rate coefficient, β_{dep} , for a monodispersed aerosol with a diameter of 10 nm was found to be $2.2 \times 10^{-5} \text{ s}^{-1}$ and $1.9 \times 10^{-3} \text{ s}^{-1}$, respectively.

Coagulation loss rate calculation

For a monodispersed aerosol, the loss rate due to coagulation, L_{coag} , can be estimated by applying Equation A.6.

$$L_{coag} = k_{coag}(D_{p1}, D_{p2}) \times C^2 \quad (\text{A.6})$$

Here k_{coag} is the size-dependent coagulation rate coefficient. We estimated k_{coag} using the Fuch's form of Brownian coagulation coefficient, (Seinfeld and Pandis, 2016) assuming that for a monodispersed aerosol $k_{coag} = k_{11}$, where $D_{p1} = D_{p2} = 10 \text{ nm}$. Under these conditions we find that for $D_{p1} = 10 \text{ nm}$, $k_{11} = 1.9 \times 10^{-9} \text{ cm}^3 \text{ s}^{-1}$.

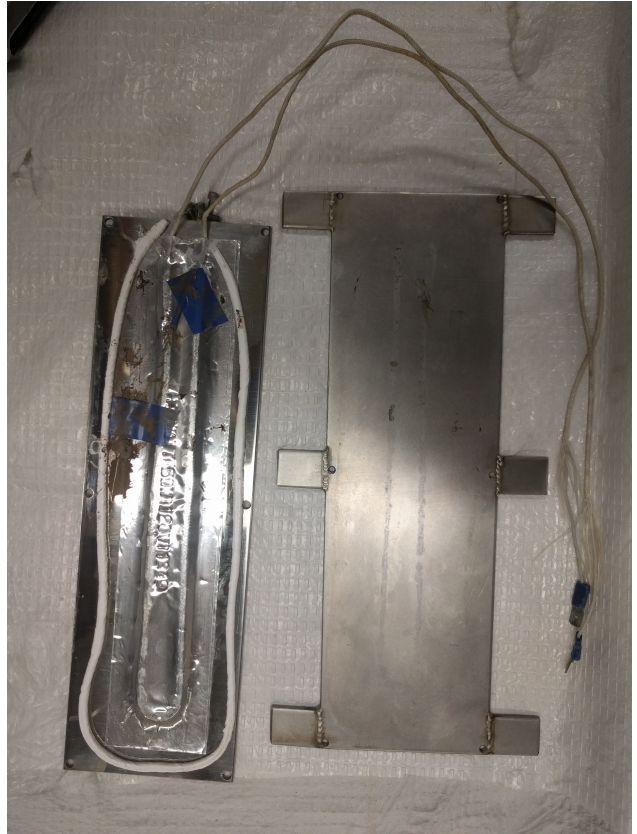
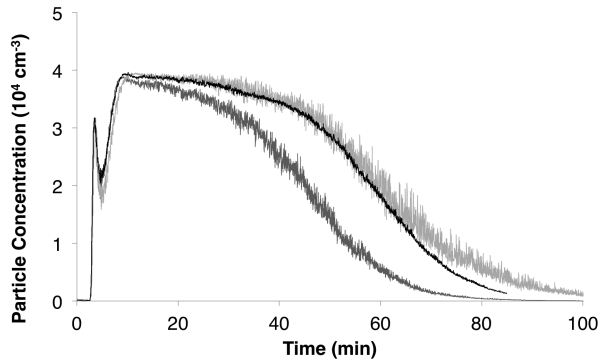


Figure A.1.1: Sample plate construction as seen from the top with an aluminum sample vessel next to it (left) and with the sample plate opened (right) to reveal the heating element, location of embedded temperature sensor, and Teflon seal.

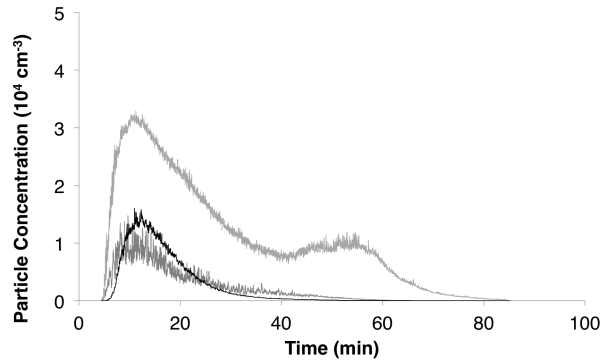
A.1.2. Results of all quantification runs

Table A.1.1: All particle production results from the quantification experiments

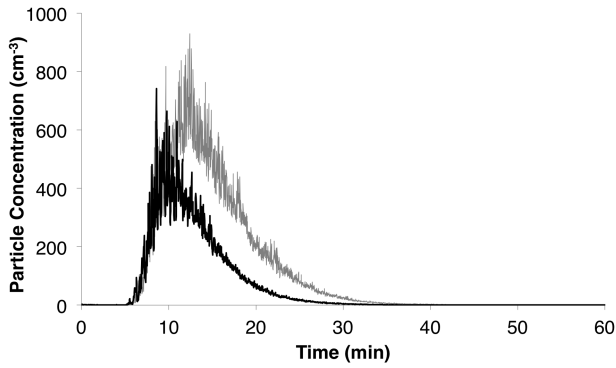
PCP #	Run #	Total particle production	Duration (min)	Avg. particle production rate (min^{-1})	Peak particle production rate (min^{-1})
P1	1	5.86×10^9	83	7.05×10^7	2.01×10^8
P1	2	6.19×10^9	106	5.84×10^7	2.12×10^8
P1	3	4.41×10^9	77	5.72×10^7	2.70×10^8
P2	1	4.99×10^8	41	1.23×10^7	6.63×10^7
P2	2	2.45×10^9	76	3.23×10^7	1.49×10^7
P2	3	4.75×10^8	54	8.79×10^6	6.00×10^7
P3	1	1.00×10^7	24	4.28×10^5	3.92×10^6
P3	2	1.90×10^7	27	7.04×10^5	3.59×10^6
P4	1	0	0	0	0
P4	2	1.35×10^7	24	5.64×10^5	3.41×10^6
P5	1	3.44×10^7	56	6.20×10^5	2.45×10^6
P5	2	4.88×10^6	53	9.20×10^4	3.11×10^5
P6	1	0	0	0	0
P6	2	6.46×10^5	21	3.04×10^4	1.58×10^5
P7	1	5.77×10^5	28	2.06×10^4	1.06×10^5
P7	2	0	0	0	0
P8	1	8.43×10^5	92	9.17×10^3	3.07×10^4
P8	2	0	0	0	0
P9	1	5.17×10^5	80	6.51×10^3	3.67×10^4
P9	2	1.73×10^5	99	1.74×10^3	1.69×10^4
P10	1	0	0	0	0
P10	2	8.35×10^4	18	4.64×10^3	2.62×10^4
P11	1	5.92×10^4	17	3.48×10^3	2.18×10^4
P11	2	2.06×10^4	18	1.18×10^3	7.10×10^3
P12	1	2.48×10^4	17	1.46×10^3	9.08×10^3
P12	2	0	0	0	0



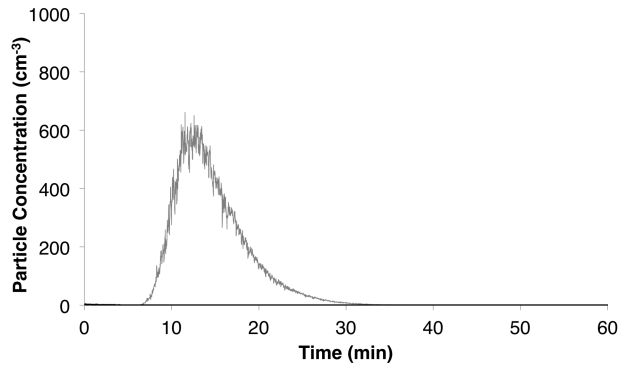
(a) Tea Tree Oil Hair Treatment (P1)



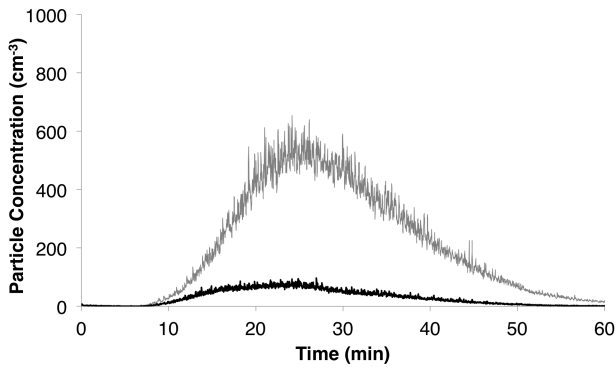
(b) White Lavender Lotion (P2)



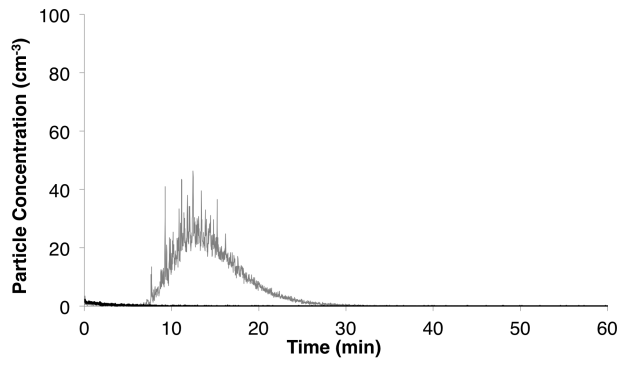
(c) Apricot Face Scrub (P3)



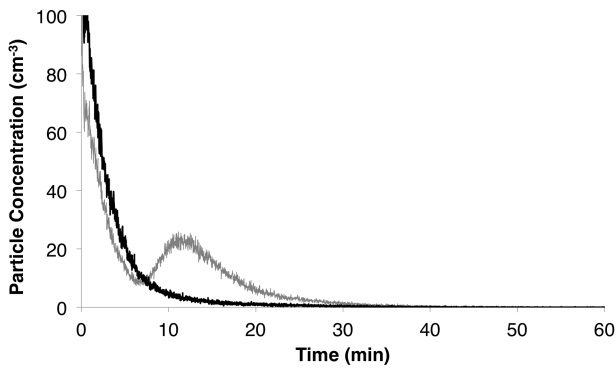
(d) Grape Seed Anti-Wrinkle Cream (P4)



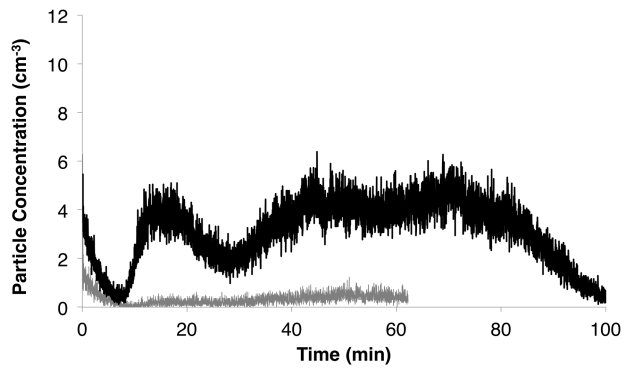
(e) Astringent Aftershave (P5)



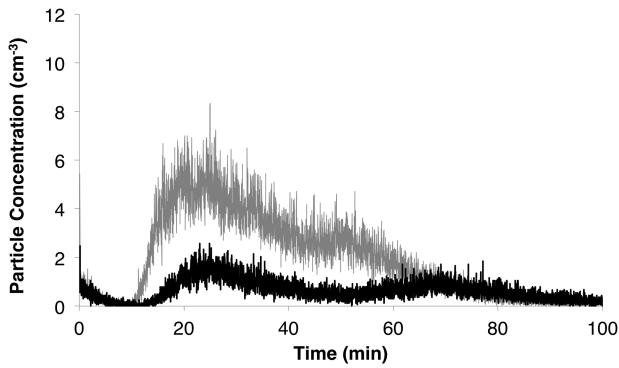
(f) Balm Aftershave (P6)



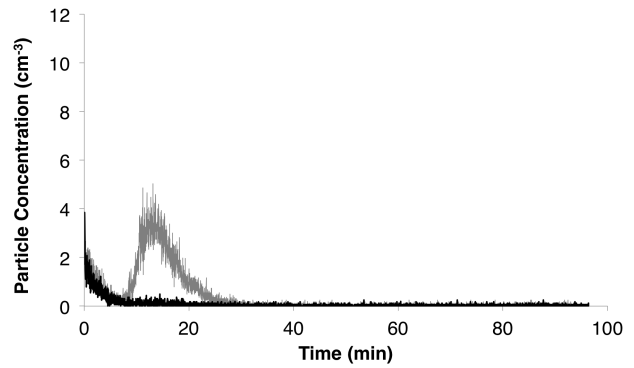
(g) Body Spray (P7)



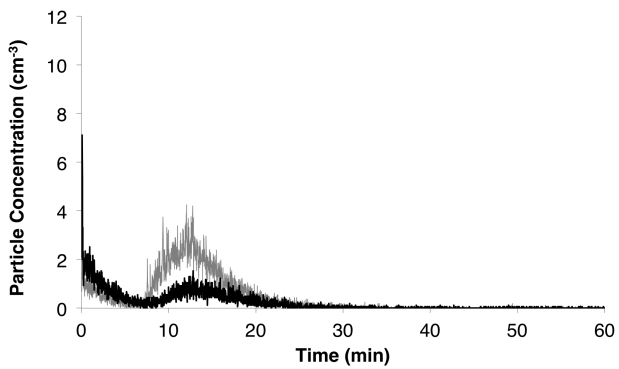
(h) Citrus Face Scrub (P8)



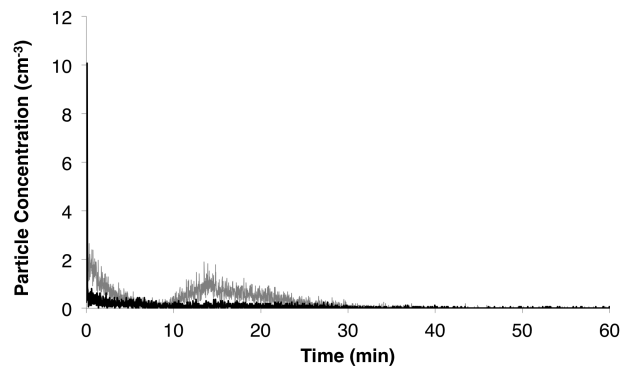
(i) Dry Skin Cream (P9)



(j) Green Tea Face Scrub (P10)



(k) White Solid Deodorant (P11)



(l) White Solid Deodorant (P12)

Figure A.1.2: Time-resolved particle concentration measurements for all quantification experiments. All figures represent the results of two test runs except for (a) and (b), for which three experimental runs were conducted.

A.2. Supplemental methods for Chapter 3

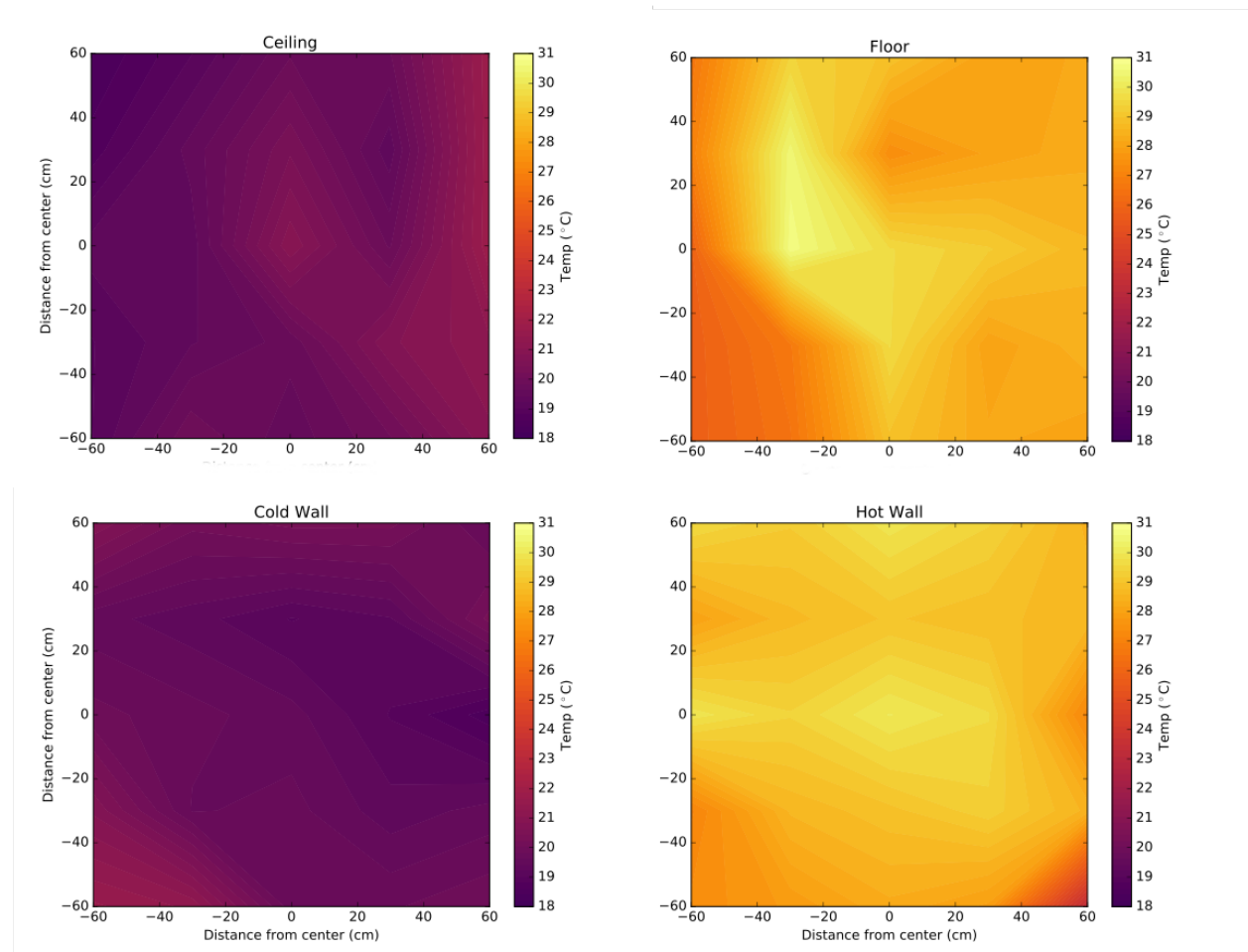


Figure A.2.1: Temperature controlled surface homogeneity while activated. Temperature measured in a 5×5 grid

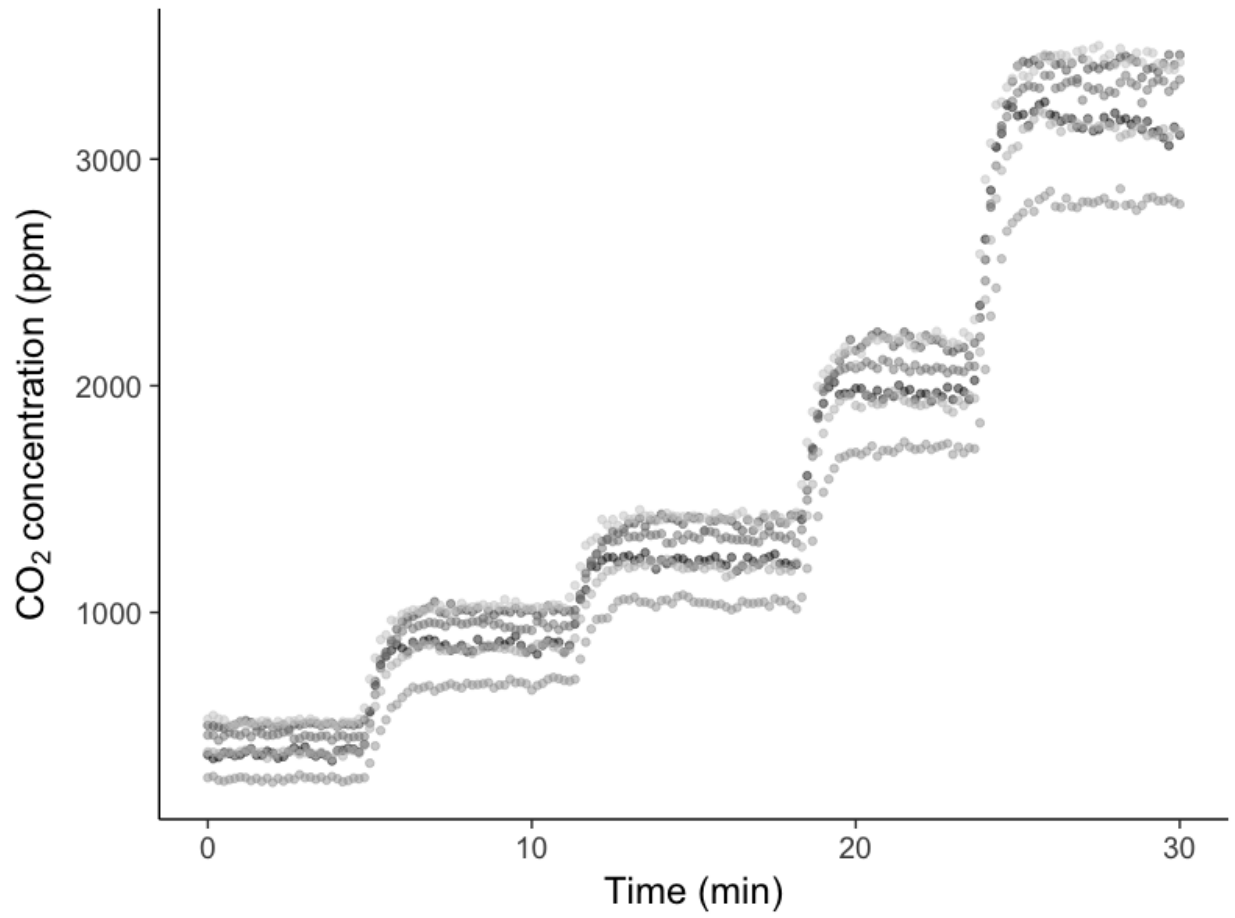


Figure A.2.2: Side-by-side comparison of CO₂ sensors at five different concentrations

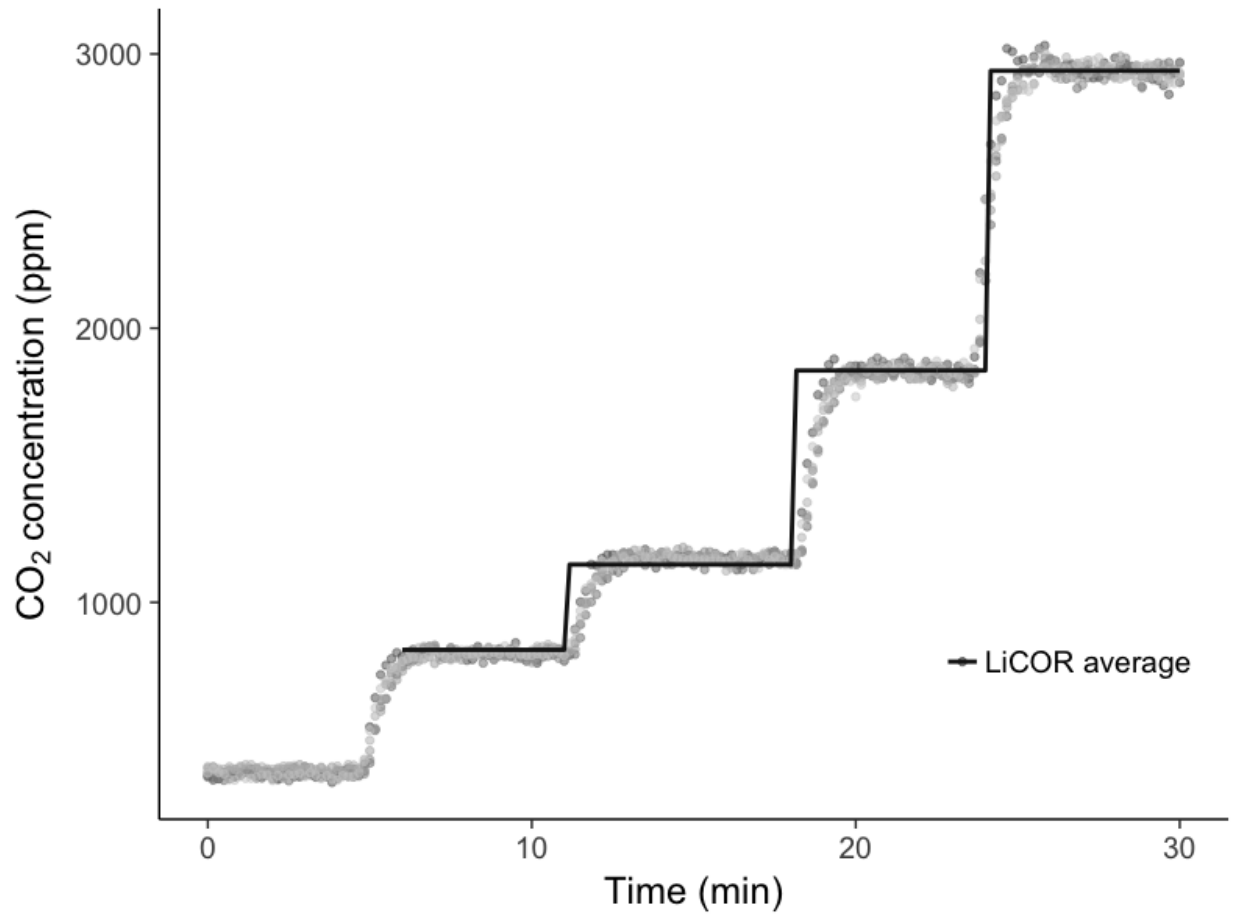
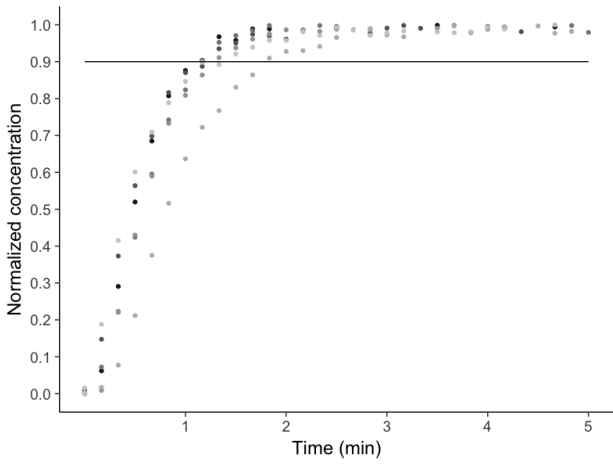
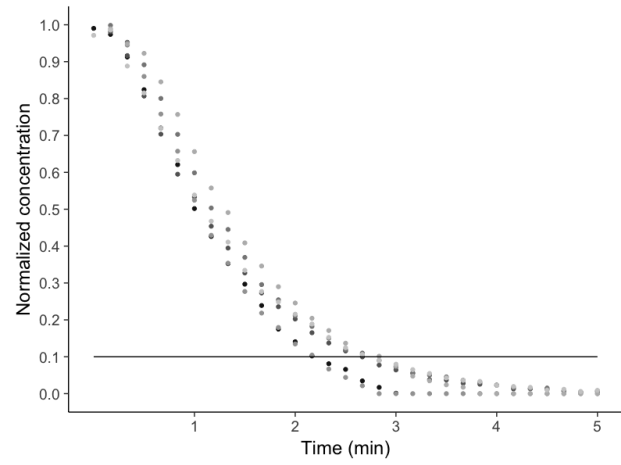


Figure A.2.3: Side-by-side comparison of CO₂ sensors after applying a linear correction factor for each sensor which is determined using concentration measurements from two LiCOR sensors.



(a)



(b)

Figure A.2.4: MX-1102 sensor response to a step increase (a) and decrease (b) in CO₂ concentration

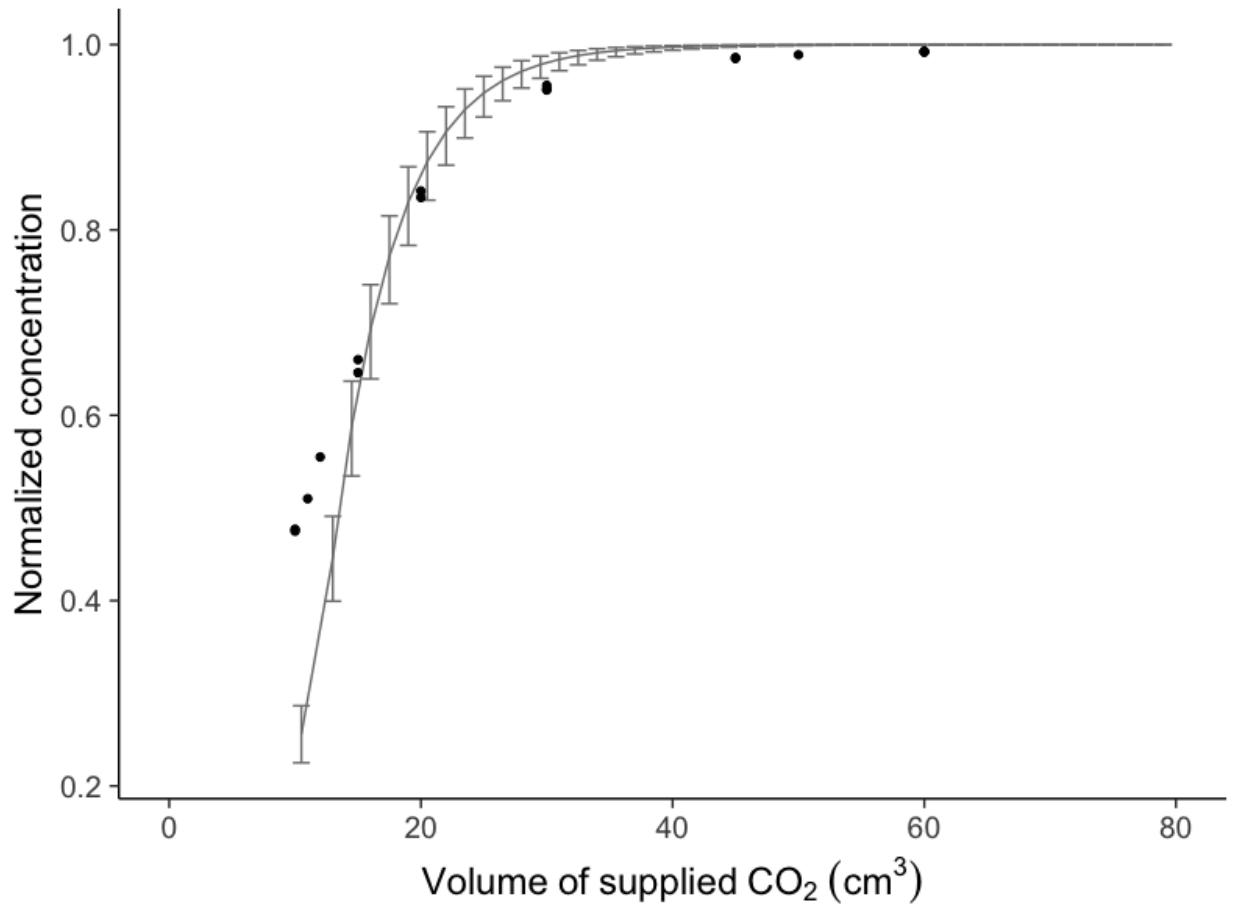


Figure A.2.5: Comparison of LiCOR measurements using a syringe to deliver the gas vs using a constant flow. 1000 ppm calibrated CO₂ gas was used, and the sensor was flushed with zero gas before syringe injection.

A.3. Supplemental methods and results for Chapter 4

A.3.1. Supplemental Methods

Table A.3.1: Heat sources present in each test condition

Heat source	Power usage (W)	Computer power (W)	Monitor power (W)	Conditions present
Manikin A	65	72	24	3, 5
Manikin B	83	40	20	5
Manikin C	83	70	29	3, 5
Manikin D	85	108	26	1, 3, 5
Manikin E	84	53	31	5
All lights	190	-	-	1, 3, 5
All instruments	13	-	-	1, 3, 5

Table A.3.2: Chamber conditions for each data collection period

Day	# of manikins	Wall sensor tree position	Supply flow rate (l/s)	Total heat load (W)	Return temperature (°C)	CO ₂ concentration at return (ppm)	CO ₂ release (lpm per manikin)
1	5	1	100.5	1100	29.80	412	0.41
2	5	1	100.7	1100	28.64	396	0.48
2	5	2	100.7	1100	28.60	399	0.48
3	3	1	63.2	778	28.29	349	0.41
3	3	2	63.2	778	28.17	358	0.42
4	3	1	122.6	776	24.46	203	0.50
4	3	2	122.2	777	24.41	199	0.49
5	1	1	38.5	428	26.34	188	0.43
5	1	2	38.2	429	26.42	178	0.41
6	5	1	172.3	1094	24.63	228	0.48
6	5	2	172.3	1098	24.61	228	0.46
7	3	1	61.4	748	27.71	381	0.47
7	3	2	62.0	747	27.69	393	0.47

A.3.2. Supplemental Results

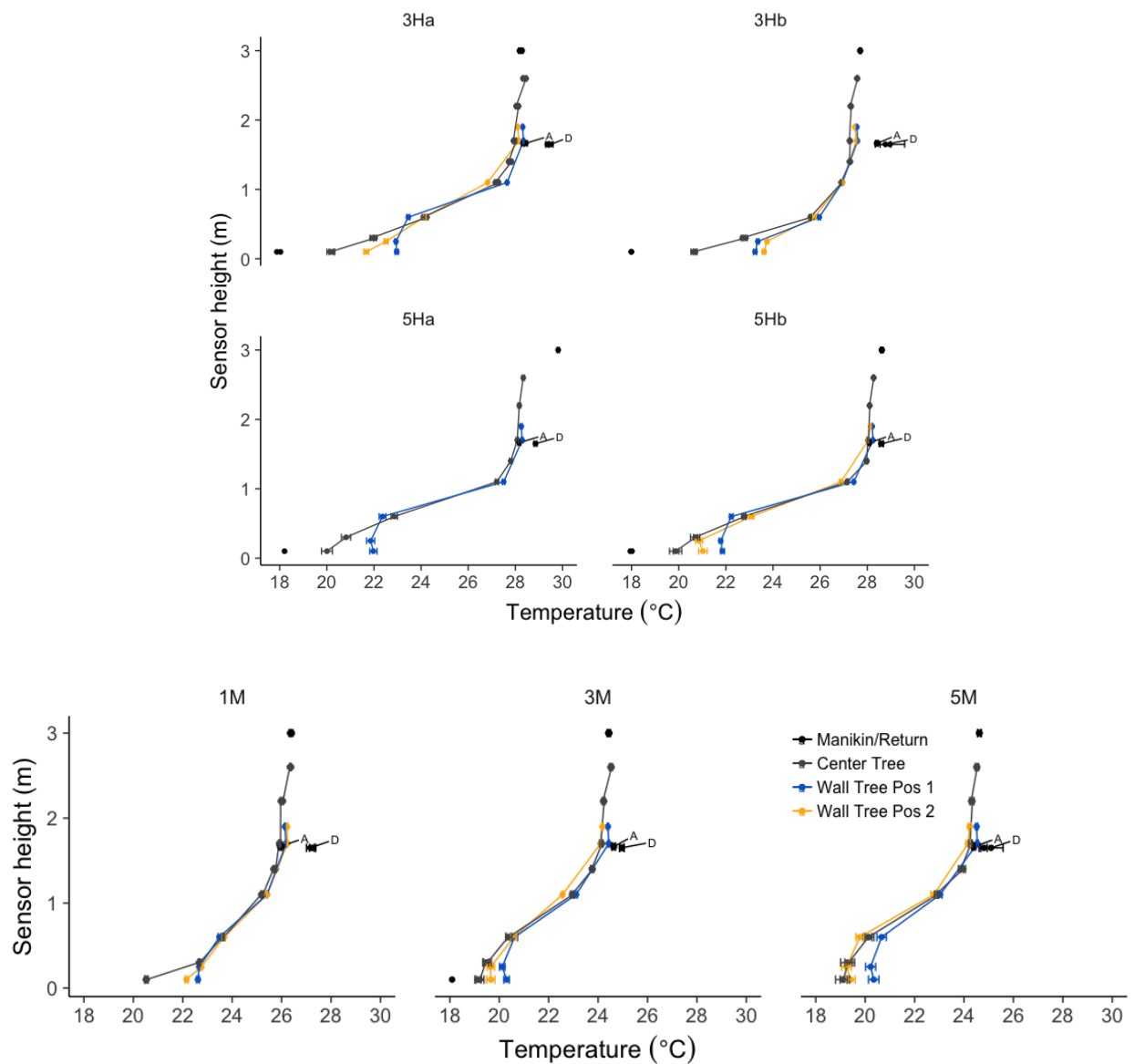


Figure A.3.1: Vertical temperature profiles for 3 occupant (top) and 5 occupant (middle) high stratification conditions, and all low stratification conditions (bottom). 'A' and 'D' represent the temperature measurements 25 cm above the labeled manikin's head.

A.4. Example technical report for IAQ diagnosis

Indoor Air Quality and Thermal Comfort

Classroom

Facts for designers

Exhaust fan specification:

- Minimum 270 cfm to ensure ventilation rates meet ASHRAE standards for a classroom of 20 people and 515 ft². However, it would be better to have 420 cfm up to 840 cfm to maximize student performance. Scale these numbers based on the expected number of occupants.
- Make sure to minimize the noise rating of the fan. Exhaust fans of 290 cfm and 2 sones exist, and are a good benchmark to judge the performance of a fan.
- Exhaust fan should be located on the ceiling, or high on a wall to preferentially ventilate the more contaminated air coming from the students. Bioeffluents, including exhaled breath, tend to rise, and in some indoor environments will collect near the ceiling.

Inlet with filter specifications:

- Inlet should be placed on opposite wall from exhaust fan to reduce the chance of "short-circuiting" air flow.
- Inlet should be placed at least a few feet above the ground on the wall to prevent cold draft from workshop during the winter.
- Inlet size should be 150 to 250 in²
- If possible, purchase a grille that allows for a filter to be used as well to improve overall classroom air quality. A filter with a MERV 5 or 6 should be sufficient.

Research Summary

Air quality in the client's classroom was determined with *in situ* measurements, and a tracer gas decay test. The pollutants of concern were human bioeffluents, characterized by the carbon dioxide concentration. The *in situ* tests directly measured the CO₂ concentration over a period of two weeks, and were measured at five different heights to determine if the air was stratified. Over the study period in the summer, both doors to the classroom remained open during the classes, and the overall CO₂ concentration remained within acceptable levels. There was a gradient, which indicated that the air near pollutants emitted by the occupants was gathering against the ceiling, and an exhaust fan placed there would perform better than one placed lower on a wall. The tracer gas decay test was used to determine the overall ventilation rate when the doors are both closed, as they are during most of the winter. We found that the ventilation rate for the classroom when closed was 27.7 cfm, which is very

low for a classroom of this size. With an occupancy of 20 people, the ventilation rate for a classroom as specified by ASHRAE 62.1 2016b (Table 6-1) should be 262 cfm. However, some studies show that students would benefit from even higher ventilation rates, 400-800 cfm (Seppänen *et al.*, 1999). We can confidently say that during the winter, when the doors are closed, the occupants of the client's classroom would benefit from an improved ventilation system.

Methods

To determine the overall air quality in the client's classroom, carbon dioxide, temperature and relative humidity were measured for two weeks in the summer from 6/27/2016 to 7/11/2016. Five sensors were placed vertically on a string in the corner of the classroom farthest away from both doors. The sensors used were Telaire System 7001 CO₂ and temperature sensors, with HOBO U12-012 dataloggers. The Telaire 7001 sensors were calibrated side-by-side along with the HOBO MX 1102 CO₂ sensors used in the workshop study using a sealed chamber. CO₂ was released in stages from 400 ppm to 3000 ppm, and the average of 2 LiCOR-820 CO₂ sensors was used as the standard for correction factors.

The air exchange rate was determined by the tracer gas decay method. Two tests were performed on 7/26/2016 in the morning and early afternoon. The CO₂ concentration was raised in the empty classroom by sublimating dry ice, and well-mixed using a large fan. When the CO₂ concentration was at least 4000 ppm the dry ice was removed, and the room vacated. Five HOBO MX 1102 CO₂ sensors were spread throughout the room to measure the empty room decay rate. The characteristic time for the decay was calculated, and the average was used to determine the overall air exchange rate. Given the volume of the classroom, the air exchange rate was used to determine the ventilation rate of the empty classroom with the doors closed. It is reasonable to assume that the calculated ventilation rate would be representative of the actual ventilation rate in the winter, when the classroom is commonly used with both doors closed.

Results

The summer observation period showed that with the doors open the CO₂ concentration never exceeded 1200 ppm, and normally stayed below 1000 ppm (see classroom CO₂ figures). Carbon dioxide is used as a proxy for all human bioeffluents, and when humans are the only source, CO₂ concentration correlates with overall sick building syndrome, sick days, and decreases in various cognitive processes (Satish *et al.*, 2012; Seppänen *et al.*, 1999). An overall maximum CO₂ concentration of 1000 ppm corresponds to ventilation that is normally sufficient to dilute body odors so that 80% of visitors into a room aren't bothered,

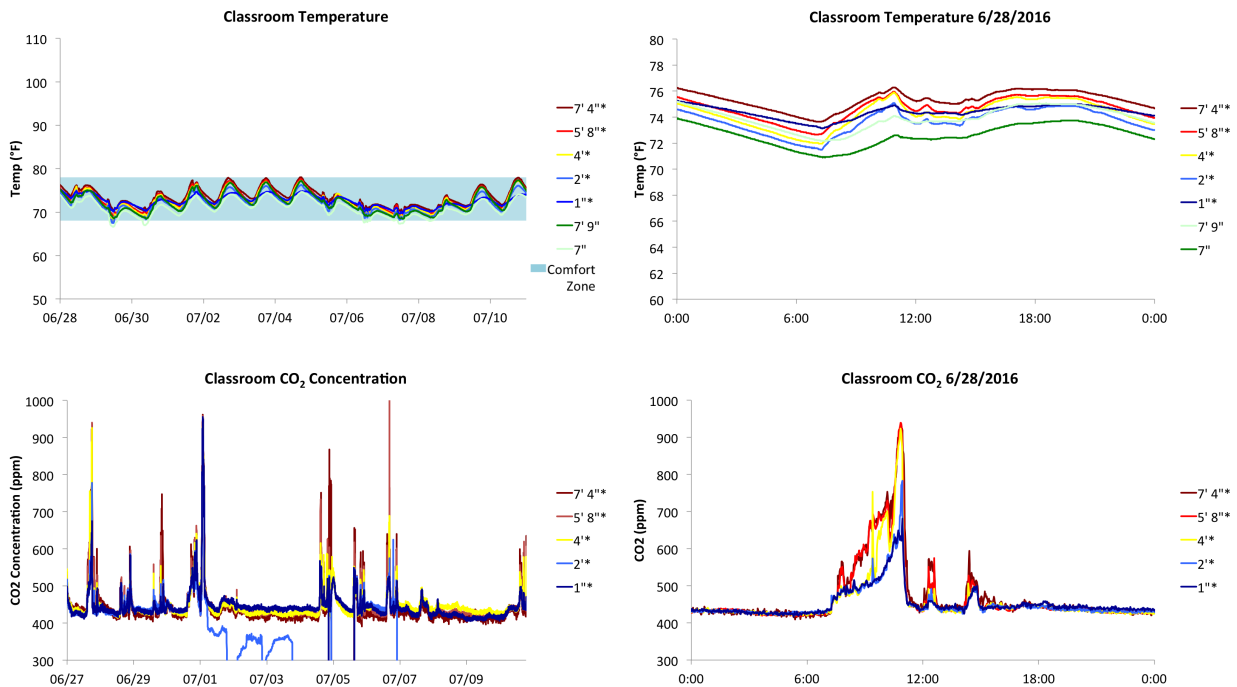
which is a commonly used standard (ASHRAE, 2016b). There have been studies suggesting that there are cognitive benefits at even lower CO₂ levels (Satish *et al.*, 2012), indicating that while the classroom air quality may be adequate while both doors are open, there is still room for improvement. The other factor to note in figures 1-3 is that the CO₂ concentration increases with height, indicating that there is some level of stratification in the classroom. Stratification is caused by heat, from the occupants in this case, reducing air mixing, increasing the concentration of bioeffluents near the ceiling, and making ceiling height exhaust ventilation more effective.

During the winter the doors to the classroom are normally kept closed, which decreases the ventilation rate and leads to different CO₂ concentration than those seen in the summer. We estimated the effect of closing the doors by a tracer gas decay test. The overall air exchange rate in the classroom, presented in the table below, was 0.4 hr⁻¹, corresponding to a ventilation rate of 27.7 cfm. This is very low for a classroom setting, ASHRAE standards suggest a minimum of 11 cfm per person, and studies have shown increases in cognitive abilities at higher airflow rates up to 21-42 cfm per person (ASHRAE, 2016b; Satish *et al.*, 2012; Seppänen *et al.*, 1999). Assuming that the client's classroom has a maximum capacity of 20 occupants, we recommend that an exhaust fan of 400-800 cfm be installed to increase ventilation. A separate inlet with a filter placed on the opposite wall will ensure that airflow within the classroom is filtered, and the classroom does not experience any depressurization.

Classroom temperatures were also measured at the same time as the CO₂ concentration. The results, presented in the classroom temperature figures below, show that during the summer the classroom temperatures vary between 70-80 °F. While this may be on the warm side, if the thermal comfort in the workshop is addressed and classroom ventilation increased, summer thermal comfort in the classroom should be sufficient. During the winter it was reported that the classroom became cold enough that the doors are normally closed, and a convection heater used. With increased ventilation, keeping the classroom warm will still be an issue, requiring a heating solution.

Literature Ventilation Rates		
ASHRAE per person ventilation rate (cfm/person)		11
Recommended per person ventilation rate (cfm/person)		21-42
Measured Classroom Ventilation Rates		
Closed door average AER (h^{-1})		0.4
Natural ventilation rate (cfm)		27.7
Estimated Closed-Door Conditions		
# of occupants	Per person ventilation rate (cfm)	Steady state CO_2 concentration (ppm)
9	3.1	3800
15	1.8	6100
20	0.65	8000

Figures



Classroom

Facts for designers

Building envelope:

- Accumulation of bioeffluents (CO₂, body odors, etc.) not an issue due to high ventilation rate.
- Building envelope not well sealed, blower door tests could not adequately depressurize to measure air tightness.

Carpentry and construction area:

- Source of sawdust, particulate matter, and volatile organic chemicals
- Best solution is to enclose in suspended/freestanding soft walls with a ceiling.
- Can place near unused bay door to allow for ventilation that is independent of the rest of the building.

Thermal comfort:

- Air above the mezzanine becomes trapped in the summer, and is heated by the ceiling into a stagnant layer.
- An extraction fan in the rear window that uses a short piece of ducting to pull hot air directly from the peak of the workshop will effectively reduce the overall temperature in the entire building.
- During the winter heating systems that use convection, like the gas heater currently used, will be inefficient as the hot air is quickly ventilated out.
- Radiant heaters that use electricity, not natural gas, in various occupied zones will give good local heating while the areas are being actively used. Radiant heaters warm surfaces within line-of-sight, not the air directly. For energy efficiency it is better to make turning the heaters on/off simple so that occupants only use when necessary.

Methods

The air quality of the workshop was measured using a string of temperature/relative humidity/CO₂ meters (HOBO MX-1102) hanging from the peak of the workshop to the floor. The sensors were calibrated as described in the Classroom IAQ – Methods appendix. Several other temperature/relative humidity meters (HOBO U12-012) were scattered around the workshop to look for any other areas of interest. The sensors were used for two weeks in the summer, from June 28, 2016 – July 11, 2016. The house prototype construction projects were examined as a pollutant source by the extrapolation of the tools, materials, and construction methods used. Additionally, the issue of sawdust dirtying surfaces was reported by staff, and observed on the mezzanine. The air tightness of the building envelope was measured using

blower door depressurization tests. Two blower doors were connected to the commonly used bay door, and the door leading to the front of house. Plastic sheets were taped to cover holes in the bay door, the "attic" area connecting the front and back of house, and other obvious holes.

Results The CO₂ measurements showed that the concentration of CO₂ mostly stayed under 600 ppm, which indicates good air quality from the point of view of bioeffluent removal. This was further supported by the results of the blower door tests. With two blower doors, we could never achieve 50 Pa of depressurization. At flow rates of 12,000 cfm and 14,300 cfm, the depressurization at the blower doors was 18 Pa and 14 Pa, respectively. This indicates that even with the obvious holes covered, the building envelope is not very air-tight. A lack of air-tightness means that natural ventilation is particularly effective, but makes achieving thermal comfort difficult.

It was reported in the survey that during the winter the workshop is particularly cold. Given the high air flow rate, it is natural that there will be a strong draft when it is cold outside. Conversely, during the summer the workshop becomes almost unbearably warm due to air becoming stagnant. While the winter over-ventilation, and summer stagnation seems contradictory, it can be due to the location of potential openings. We suspect that the bay doors are the main source of cold draft, and the lack of openings in the upper half of the building is the source of the stagnation. Referring to the workshop temperature figure below, there is a distinct jump in temperature between 15 ft and 18 ft, which corresponds to both the height of the mezzanine, and the top of the bay doors. This indicates that there may be two distinct air zones in the workshop, and consequently the building as a whole: a better mixed, high airflow zone on the ground level, and a more stratified, low airflow zone above the mezzanine. In the summer the extremely hot roof heats the stratified air zone against the ceiling, which creates hot conditions throughout the building. In the winter a draft against the ground forms, which makes the entire building colder.

Figures

